

The molecular mechanism
of outer membrane DNA transport
in bacterial transformation

- Inaugural-Dissertation -

zur

Erlangung des Doktorgrades
der Mathematisch-Naturwissenschaftlichen Fakultät
der Universität zu Köln

vorgelegt von
Christof Hepp
aus Bad Saulgau

Köln

2017

Berichterstatter: Prof. Dr. Berenike Maier
(Gutachter) Prof. Dr. Tobias Bollenbach

Tag der mündlichen Prüfung: 19.01.2017

Danksagung

Als erstes möchte ich mich bei Prof. Dr. Berenike Maier für die Möglichkeit zur Promotion in ihrer Arbeitsgruppe bedanken. Außerdem danke ich ihr für die hervorragende Betreuung. Während der Zeit in ihrer Arbeitsgruppe stand sie mir stets mit Rat und Tat zur Seite und ließ mir zahlreiche Gelegenheiten, meine Projekte selbst zu gestalten. Zudem danke ich ihr für die Möglichkeit, meine Ergebnisse auf internationalen Konferenzen zu präsentieren.

Prof. Dr. Ines Neundorf und Prof. Dr. Tobias Bollenbach danke ich für ihr Interesse an meiner Arbeit und der Bereitschaft, als Prüfungsvorsitzende und Zweitgutachter Teil meines Prüfungskomitees zu sein.

Stephanie Müller danke ich für ihre gewissenhafte und begeisternde Einführung in mein Projekt und die gute Zusammenarbeit, von der ich sehr profitiert habe.

Ebenso danke ich Dr. Enno Oldewurtel, Katja Henseler, Heike Gangel und Niklas Günther für die schöne Zusammenarbeit und die fantastischen Ergebnisse, die wir zusammen publizieren konnten. Es hat großen Spaß gemacht.

Desweiteren danke ich Thorsten Volkmann, Jan Ribbe und Dr. Lena Dewenter für unabdingbare experimentelle Unterstützung.

Ich danke auch allen jetzigen und ehemaligen Mitgliedern der AG Maier für ihre Hilfsbereitschaft, ihr Fachwissen und die äußerst hilfreichen Diskussionen. Ich habe mich bei euch immer sehr wohl gefühlt. Ihr seid ein tolles Team.

Mein ganz besonderer Dank geht an meine Familie, die immer für mich da ist und es stets schafft, mir Zuversicht zu geben.

Content

1	Introduction	10
1.1	Horizontal gene transfer by natural transformation	10
1.1.1	Bacteria exchange genetic information	10
1.1.2	The functions of natural transformation in bacteria	11
1.2	Natural genetic transformation in <i>Neisseria gonorrhoeae</i>	13
1.2.1	A life on the run – the role of genome plasticity in <i>Neisseria gonorrhoeae</i>	13
1.2.2	Genome organization.....	14
1.2.3	Repetitive sequences and mobile elements	14
1.2.4	The Gonococcal Genetic Island.....	15
1.2.5	Mechanisms of diversity generation.....	15
1.2.6	Genetic transfer.....	17
1.2.7	Barriers to genetic transfer	18
1.3	Membrane transport of biopolymers	20
1.3.1	Essentials of membrane transport.....	20
1.3.2	DNA translocation by molecular motors.....	21
1.3.3	The translocation ratchet	22
1.4	Components of the natural transformation machinery and their function	25
1.4.1	The type IV pilus machinery	25
1.4.2	Non-Tfp competence proteins	30
1.4.3	The mechanism of DNA import in Gram negative bacteria – state of the art	33
1.4.4	Structural and mechanistic differences to other bacteria.....	35
1.5	Aims of this study	37
2	Materials and Methods	39
2.1	Media and solutions	39
2.2	Molecular biological methods.....	40

2.2.1	Plasmid isolation from <i>E.coli</i>	40
2.2.2	Genomic DNA isolation from <i>N. gonorrhoeae</i>	41
2.2.3	Polymerase chain reaction	41
2.2.4	Agarose gel electrophoresis.....	42
2.2.5	DNA isolation by gel extraction	42
2.2.6	DNA restriction	42
2.2.7	Dephosphorylation.....	43
2.2.8	Ligation.....	43
2.2.9	Transformation of chemically competent <i>E.coli</i>	43
2.2.10	Transformation of <i>N. gonorrhoeae</i>	44
2.2.11	Colony PCR.....	44
2.2.12	Sequencing.....	45
2.3	Bacterial strains, growth conditions and selection conditions	45
2.4	Construction of mutant strains	47
2.4.1	Construction of $\Delta pilQ \Delta pilV, \Delta pilT \Delta pilV, \Delta comA \Delta pilV$	47
2.4.2	Construction of <i>comE</i> deletion strains.....	47
2.4.3	Construction of a <i>comE-mcherry</i> fusion strain.....	49
2.4.4	Construction of a <i>nuc</i> deletion strain	49
2.4.5	Construction of a <i>comA-mcherry</i> fusion strain.....	50
2.4.6	Construction of a <i>dprA-yfp</i> fusion strain	50
2.4.7	Construction of a <i>dprA</i> deletion strain.....	51
2.5	Preparation of fluorescently labeled DNA	53
2.5.1	Preparation of continuously labeled DNA fragments.....	53
2.5.2	DNA fragments with a single fluorophore	54
2.6	DNA uptake assays	55
2.7	Microscopy and quantitative analysis of single-cell fluorescence	55
2.7.1	Image acquisition.....	55
2.7.2	Quantification of fluorescent DNA import at the single cell level.....	56
2.8	Real-time quantification of DNA import and degradation.....	57
2.9	Duplex PCR for investigating degradation of DNA in the periplasm.....	58
2.10	Transformation assays.....	59
2.11	Preparation of biotinylated DNA fragments for optical tweezers assays.....	59

2.12	Preparation of DNA coated beads for optical tweezers assays	60
2.13	Laser tweezers setup and data analysis	60
2.14	Data acquisition of DNA uptake in the optical tweezers assay.....	61
3	Results	63
3.1	Concerted spatio-temporal dynamics of imported DNA and ComE DNA uptake protein during gonococcal transformation.....	63
3.1.1	<i>N. gonorrhoeae</i> imports Cy3-DNA in a DNase-resistant state	64
3.1.2	The periplasm of <i>N. gonorrhoeae</i> can retain ample amounts of DNA.....	66
3.1.3	Kinetics of Cy3-DNA import into the periplasm	69
3.1.4	The periplasmatic DNA binding protein ComE quantitatively increases the amount of Cy3-DNA imported into the periplasm.....	70
3.1.5	ComE-mCherry relocalizes to DNA foci	73
3.1.6	Spatio-temporal dynamics of Cy3-DNA foci and ComE-mCherry in the periplasm.	77
3.2	The kinetics of DNA uptake during transformation provide evidence for a translocation ratchet mechanism	81
3.2.1	DNA binding and uptake in the optical tweezers assay	81
3.2.2	The velocity of DNA uptake depends on ComE	85
3.2.3	Gonococcal DNA uptake is reversible at high forces.....	86
3.2.4	The velocity versus force relationship is in agreement with a translocation ratchet model	89
3.3	Single-stranded DNA uptake during gonococcal transformation	92
3.3.1	Double-stranded DNA uptake sequence (DUS) supports uptake of otherwise single-stranded DNA.....	92
3.3.2	The thermonuclease Nuc rapidly degrades imported single-stranded DNA	96
3.3.3	Uptake kinetics of ssDNA containing double-stranded DUS.....	99
3.3.4	Transformation efficiencies of dsDNA, ssDNA and dsDUS	100
4	Discussion	102
4.1	The functional roles of ComE in DNA uptake.....	102
4.1.1	ComE binds DNA in vivo and governs the DNA carrying capacity of the periplasm	102

4.1.2	Physical constraints on the molecular mechanism of DNA uptake from the uptake kinetics of ssDNA	104
4.1.3	The force-dependent velocity is consistent with a translocation ratchet driven by ComE.....	104
4.1.4	Type IV pilus retraction does not directly drive DNA import	106
4.1.5	DNA uptake is reversible for Gram negative bacteria.....	108
4.2	Power and limitations of the Cy3-DNA approach	110
4.3	Transforming DNA in the periplasm: Stability, relocalization and degradation	112
4.3.1	Spatio-temporal dynamics and maintenance within the periplasm	112
4.3.2	Nuc degrades imported DNA	114
4.4	Single stranded DNA as a substrate for natural transformation.....	116
5	Outlook.....	118
5.1	Fluorescence microscopy approaches to understand the mechanism of transport through the cytoplasmic membrane	118
5.2	Localization and quantification of ComA	119
5.3	Tracking DNA uptake by accumulation of DprA	120
5.4	Discussion of preliminary results	122
6	Abstract	124
7	Zusammenfassung	126
8	References	128
9	List of Abbreviations.....	143
	Erklärung	144
	Lebenslauf	145

Figure 1.1 Principle of a translocation ratchet. 23

Figure 1.2 Central slices of the architectural models of piliated (A) and empty (B) T4PM.... 26

Figure 1.3 A model of the DNA transport machinery..... 34

Table 2.10: *N. gonorrhoeae* strains used in this work..... 45

Table 2.11: Primers and oligonucleotides used in this work.....	51
Figure 2.1 Quantification of single cell fluorescence.	57
Figure 2.2 The DNA fragment attached to the beads.....	60
Figure 3.1 The minor pilins PilV and ComP differentially influence the amount of imported Cy3-DNA.	65
Figure 3.2 The amount of imported Cy3-DNA after 1 h is independent of fragment length. .	67
Fig. 3.3 Quantification of imported Cy3-DNA.	68
Figure 3.4 Duplex PCR of imported DNA.....	69
Figure 3.5 Dynamics of focus formation (Δ pilV) with 300 bp fragments of Cy3-DNA.	70
Figure 3.6 Fluorescence distribution of individual cells with varying comE expression.	71
Figure 3.7 Dynamics of 3 kbp Cy3-DNA import depends on ComE.	72
Figure 3.8 Dynamics of focus formation (Δ pilV) with 10 kbp fragments of Cy3-DNA.	73
Figure 3.9 Distribution of ComE-mCherry in the absence of transforming DNA.....	74
Figure 3.10 ComE-mCherry colocalizes with the spotty pattern of Cy5-DNA.	76
Figure 3.11 Dynamics of focus formation (Δ pilV) with 10 kbp fragments of Cy3-DNA.	78
Figure 3.12 Spatio-temporal dynamics of ComE-mCherry upon addition of 10 kbp transforming DNA.	79
Figure 3.13 Probability of DNA binding and uptake.	83
Figure 3.14 Velocity versus force relationship of T4P retraction.	84
Figure 3.15 The uptake velocity depends on the concentration of ComE.	86
Figure 3.16 DNA uptake is reversible upon application of force.	88
Figure 3.17 Velocity versus force relationship of DNA uptake.....	90
Figure 3.18 Velocity versus force relationship of DNA uptake for Δ comA.....	91
Figure 3.19 dsDUS supports import of ssDNA.....	94
Figure 3.20 Mid-labeling confirms that the import efficiency of ssDNA is increased by dsDUS.	95
Figure 3.21 Decay of imported dsDNA and dsDUS DNA in nuc deletion strain.....	97
Figure 3.22 Carrying capacities of various DNA fragments in a nuc deletion strain..	98
Figure 3.23 Import kinetics of dsDNA and dsDUS DNA.....	100
Figure 3.24 Transformation probability with dsDNA, ssDNA, and dsDUS.....	101
Figure 4.1 Proposed mechanism of DNA uptake into the periplasm of Gram negative bacteria.	108
Figure 4.2 Force generation by cytoplasmic and outer membrane motors.	110

Figure 4.3 The nuclease EndA in *S. pneumoniae* and Cy3-DNA in *N. gonorrhoeae* relocate at the site of cell division. 114

Figure 5.1 Localization of ComA-mCherry in comparison to imported Cy5-DNA..... 120

Figure 5.2 The cellular distribution of DprA-YFP in *N. gonorrhoeae*..... 122

1 Introduction

1.1 Horizontal gene transfer by natural transformation

1.1.1 Bacteria exchange genetic information

The simplest way for living organisms to reproduce is cell division. As the genome is copied to yield two identical daughter cells, mistakes cannot be avoided. They lead to variation among the progeny of the original ancestor, which enables evolution through natural selection. In contrast, higher eukaryotes almost exclusively propagate by sexual reproduction, a process where offspring is produced from the combined genetic makeup of two mating partners. The recombination of genetic material leads to a much higher rate in variation than mutation alone, thus speeding up a species' adaptation to the environment.

Bacteria and archaea have not evolved to reproduce sexually. However, they have evolved various mechanisms of horizontal gene transfer. In a study of 88 prokaryotic genomes the share of laterally transferred genes was estimated from 0-22% in bacterial species [1]. This result also demonstrates another remarkable property of bacterial "sex": In contrast to sexual reproduction in eukaryotes, it can cross species barriers. Gene transfer between two species is referred to as Horizontal Gene Transfer (HGT).

In nature, gene transfer between bacteria can occur in three distinct ways, namely transduction, conjugation and transformation [2, 3]. In all of these processes, DNA is transferred from a cell called the donor to another cell called the recipient, which is then able to acquire the genetic information. Transduction is mediated by bacterial viruses. DNA of an infected bacterium can end up in a virus particle and then be integrated into the genome of the

recipient after the subsequent infection. Conjugation is mediated by the DNA donor that injects genetic material e.g. a plasmid into the DNA recipient.

The third possible method of gene acquisition, natural competence for transformation, occurs throughout the bacterial domain [4]. It is different from the other methods of genetic transfer in that there are no external factors necessary for the uptake of DNA from the environment [5]. In other words, naturally competent cells take up DNA on their own initiative. Further, they can discriminate self from non-self DNA before importing it, a trait shared by several, but not all naturally transformable species [6-10]. The genes encoding for competence for natural transformation are highly conserved and have been extensively studied in *Streptococcus pneumoniae*, *Neisseria gonorrhoeae*, *Bacillus subtilis* and *Haemophilus influenzae* [4, 11-14]. Even though the parts of the competence machinery are known, the mechanism of DNA uptake and subsequent gene acquisition remains to be elucidated.

1.1.2 The functions of natural transformation in bacteria

The question how bacteria benefit from natural transformation has been discussed, but the answer is still far from clear [15-18]. Three main reasons for DNA uptake mediated by competence in bacteria have been proposed: 1. Innovation: It permits the acquisition of new genes that provide a selective advantage to the recipient and speed up adaptive evolution [19]. 2. Conservation: The imported DNA serves as a template for DNA repair, if an organisms genome is heavily damaged or mutated [20, 21]. 3. Population dynamics: According to the Fisher-Muller hypothesis, transformation combines beneficial mutations that would compete with each other in asexual populations [21]. 4. The imported DNA serves as a nutrient for the bacterial cell [17, 22].

In most naturally transformable species, the development of competence is tightly regulated [23]. This regulation has been studied most extensively in *B. subtilis*, where competence depends on the integration of signals such as nutritional stress and cell density [13]. Regulation of competence might in fact be one reason, why many bacterial strains carry a functional set of the required genes while being reported as non-competent: E.g. *Streptococcus thermophilus* can only be made competent by overexpressing the alternative sigma factor comX [24]. To date, there is no evidence that natural competence is triggered by the presence of DNA in the environment, arguing against the main purpose of imported DNA as a nutrient.

Generally, the source of transforming DNA is assumed to be lysed cells. There is debate whether DNA from the environment can provide a selective advantage, when the cells carrying it were obviously unable to adapt to their environment. However, it has been proposed that transformation by DNA of perished cells nevertheless increases fitness in naturally competent populations compared to non-competent populations [16]. Moreover, other sources of environmental DNA are known. *N. gonorrhoeae* has the ability to secrete DNA into the environment with the help of genetic element called the gonococcal genetic island (GGI) [25]. The DNA is secreted by a bacterial type IV secretion system encoded by the GGI and expected to function analogously to the VirB complex employed by *Agrobacterium tumefaciens* to transfect plant host cells [26-28]. The ability of gonococci to release donor DNA is reduced in strains not carrying the GGI [29, 30]. In *S. pneumoniae*, fratricide can serve as mechanism for gene acquisition. Under certain conditions, a fraction of the cells in a culture releases toxins that cause the remaining cells to lyse. This bacterial “murder” can serve as an active DNA acquisition mechanism [31-34]. In fact, a functional connection between competence and fratricide has been found [11, 35]. Moreover, *V. cholerae* possesses a competence-induced type VI secretion system to lyse non-immune bacteria and subsequently uses its victims’ DNA for transformation [36]. Mechanisms such as fratricide apparently strengthen the case the for DNA-as-nutrient hypothesis [17, 22]. On a closer look, several observations argue against nutrient gathering as the main purpose for DNA import in bacteria. In *S. pneumoniae*, one strand of dsDNA is degraded by an endonuclease prior to DNA import and does not enter the cell [37]. After entry into the cytoplasm of naturally transformable bacteria, the remaining strand is protected from degradation by several distinct DNA binding proteins [38-40]. In *Acinetobacter calcoaceticus*, competence is induced upon de-starvation, contrary to the expectations of the nutrient hypothesis [23].

It has been observed that the genome size of pneumococci is limited to about 2.2 Mbp. A small genome poses a selective advantage as it is easier to maintain, but limits metabolic capacities and environmental adaptability. It has been hypothesized, that natural transformation enables bacterial populations to maintain a collective gene pool, called a supragenome, that gives the members access to allelic variants and genes not present on their own chromosome [5]. It has been demonstrated that the penicillin resistance found in *S. pneumoniae* is composed from genetic building blocks found in several members of the microflora residing in the upper respiratory tract [41]. This is a remarkable example, of how natural competence in combination with external stress can lead to the solution of a survival problem by acquiring novel genes. In the next section, the genetics of *N. gonorrhoeae*, the model organism used in this study, will be

introduced. It will become clear that constant pressure by the human immune system results in high genomic plasticity. Natural transformation has the potential to increase this plasticity by gene and allele acquisition. Further, genome plasticity might create the need for extensive DNA repair which can be supported by natural transformation.

1.2 Natural genetic transformation in *Neisseria gonorrhoeae*

1.2.1 A life on the run – the role of genome plasticity in *Neisseria gonorrhoeae*

With 106 million cases worldwide, gonorrhea is a very prevalent sexually transmitted disease [42]. It is characterized by a constant inflammation of the genital tracts resulting in purulent discharge of gonococci and polymorphonuclear leukocytes [43, 44]. In the upper genital tract, gonococci can lead to serious diseases such as epididymitis in men and cervicitis, endometriosis, and pelvic inflammatory disease in women which represents a major cause of infertility. In rare cases, gonococci disseminate via the blood stream. These disseminated gonococcal infections (DGI) are associated with arthritis and endocarditis [44]. Gonococci can infect the eyes of newborns as they pass to the birth canal and the resulting conjunctivitis is one of the major causes of blindness in the developing world [45]. While being a notorious pathogen, *N. gonorrhoeae* is known for asymptomatic infections. Additionally, there are no known effective vaccine strategies for gonococci [46]. These problems in diagnosis and treatment are caused by gonococcal immune evasion strategies which involve a high level of genomic plasticity. Pathogenic *Neisseria* are reported to have a very low linkage disequilibrium, a measurement of how closely related chromosomal loci are compared to chance. This is a sign of excessive recombination within the genome [47, 48]. In combination with natural transformation, *N. gonorrhoeae* can rapidly adapt to medical treatment. Multidrug resistant strains continuously emerge [49-51].

1.2.2 Genome organization

N. gonorrhoeae has a 2.2 Mbp circular chromosome. On average, one coccal cell unit contains three chromosomes [52]. Although they are polyploid, *Neisseria* cannot carry two alleles of the same locus [53]. As the closely related but nonpathogenic *N. lactamica* strains are monoploid, polyploidy has been proposed to represent a trait associated with pathogenicity [53]. In *Deinococcus radiodurans*, a bacterium that can tolerate high doses of radiation, polyploidy is used to repair radiation induced chromosomal damage. Similarly, it could protect the genome of gonococci from the effects of vast chromosomal rearrangements. Further damage to the genome may also be caused by neutrophils of the host's immune system or lactobacilli.

1.2.3 Repetitive sequences and mobile elements

There is a great number and variety of repetitive sequences within *Neisseria* genomes. The 20-bp dRS3 repeat sequence occurs over 200 times in *N. gonorrhoeae* [54]. Inverted dRS3 sequences flank varying 50-150 bp repeat sequences (RS) which together constitute the NIME (neisserial intergenic mosaic element) [55]. Another recurring repeat sequence is the 26-bp Correia element [56-59]. Inverted repeats of the Correia element flank the CREEs (Correia repeat encoded elements). These so called minimal mobile elements (MMEs) are subject to exchange and incorporation into their conserved flanking regions [60, 61]. They have been used to define differences in gonococcal strains and to track separation of the pathogenic strains from non-pathogenic *N. lactamica* [62, 63]. CREEs are thought to function as terminators and they also contain promoter elements suggesting a role in the modulation of gene transcription [64-67]. They are often located at the sites of chromosomal inversions between different gonococcal strains, suggesting they either mediate recombination by providing homology or have an active function in genomic translocations [62].

1.2.4 The Gonococcal Genetic Island

The Gonococcal Genetic Island (GGI) might be the most remarkable mobile element in *N. gonorrhoeae*. It is a 57 kbp DNA element found in 80% of gonococcal isolates, but normally not found in commensal *Neisseria* [25, 68]. Its lower G+C content and fewer DNA uptake sequences (DUSs) suggest that it is acquired horizontally [25, 30, 69]. The GGI is integrated into the chromosome at the *dif* site, leading to a functional *difA* and a divergent *difB* [69, 70]. Importantly, the GGI encodes for a type IV secretion system (T4SS) that secretes ssDNA. Other genes encoded by the GGI include peptidoglycan binding proteins, DNA methylases, a topoisomerase, a helicase, orthologs to plasmid partitioning proteins and an ssDNA binding protein [25, 30, 71]. The mechanism of ssDNA secretion by the GGI-encoded proteins is expected to resemble the transfection of plant host cells by the *A. tumefaciens* VirB complex [26-28]. The ability of a strain to function as a DNA donor is reduced in the absence of the GGI [29, 30]. Based on these facts the GGI is considered to aid its own spread. Possible other roles associated with virulence remain to be elucidated.

1.2.5 Mechanisms of diversity generation

1.2.5.1 Phase variation

Phase variation is the reversible change of a gene products expression state between ON (expressed) and OFF (unexpressed) or a switch between two forms of a gene product [72]. *N. gonorrhoeae* possesses about 80 putative phase-regulated genes per strain; some of them have been experimentally verified to be phase-variable [73-75]. Phase variation contributes to immune evasion as the resistance to bactericidal antibodies has demonstrated [76, 77]. The genetic means of providing a phase switch include invertible DNA segments, methylation, homopolymeric nucleotide repeats or short tandem repeats. The repeats are responsible for the introduction of reading frame shifts by slipped-strand mispairing, a mechanism independent of homologous recombination [78, 79]. The frequency of phase variation has been found to increase with the number of repeats [79-81]. The homopolymeric repeats usually consist of A,C or G and are up to 17 nucleotides long [81]. Examples of phase variation mediated by homopolymeric repeats are PilC and the glycosylases for pilin and the lipooligosaccharides

(LOS) the expression of which is switched ON and OFF by shifts in their open reading frame (ORF). Due to phase switching, glycosyltransferases produce different LOS structures [82]. In *N. gonorrhoeae*, there are 12 recognizable LOS immunotypes. In other genes, polynucleotide repeats shift the spacing of -35 and -10 promoter sequences, thus affecting the expression level. Polynucleotide repeats consist of 3-5 bp elements and are less common than homopolymeric tracts [73, 75]. A repeat number change can alter the binding of transcriptional regulators. An example for this is the expression of genes mediated by the integration host factor (IHF) [83, 84]. Polynucleotide repeats consisting of multiples of three nucleotides do not lead to a reading frame shift when inside an ORF. Instead, they will have structural effects on the expressed protein [85]. Examples of genes regulated by polynucleotide repeat - mediated phase switching are the *opa* genes that encode for various binding proteins involved in pathogenicity [146]. Defects in mismatch correction lead to an increase in phase variation. In *mutS/mutL* defective mutants, phase variation is increased 10-1000-fold [86, 87]. An increase in mutations due to defective gene repair is expected to lead to a decrease in fitness. However, it might provide a selective advantage due to increased phase variation [72]. This can explain the high prevalence of strains with defective *mutL* and *mutS* genes in *N. meningitidis* isolates [81, 86].

1.2.5.2 Pilin antigenic variation

Type IV pili are cell appendages involved in natural transformation, twitching motility and adherence to epithelial cells [88-90]. They are biopolymers predominantly formed by a protein called pilin. Pilin antigenic variation (pilin Av) is an elaborate system of diversity generation to avoid immune surveillance. The effect of pilin Av is the modification of the peptide sequence: Out of many possible variants, only one is expressed.

To this end, the genome of *N. gonorrhoeae* contains one expression locus named *pilE* and several promoterless, truncated *pilS* copies [91]. In pilin Av, one of the *pilS* copies replaces the homologous stretch inside the *pilE* ORF. During this process, the *pilS* copy does not undergo a reciprocal change [92, 93]. The regions of the pilin gene affected by pilin Av are termed the variable regions. They are the surface-exposed parts of the pilus fiber and recognized by pilin antibodies [93]. The pilin sequences of meningococci and commensal species do not contain variable regions and are not subject to pilin Av [94-96]. In contrast, *N. gonorrhoeae* strains exhibit a continuous change of pilin sequences during human infection [91, 97]. The median

rate of pilin Av for gonococci is 1.7×10^{-3} events per cell per generation, which is among the highest rates of change in a prokaryotic diversity generation system.

Pilin Av depends on homologous recombination factors [98-104]. Homologous recombination has been shown to be boosted by iron loss in the medium [105]. This suggests that the iron-depleted conditions of the human body stimulate pilin Av. The mechanism of pilin Av is currently not well understood. It is mediated by the G4 motif, a 16-bp G-rich sequence upstream of *pilE*, which is predicted to form a G4 (guanine tetraplex) structure [106]. Mutation of the motif as well as specific inhibition of a G4 structure prevents pilin Av and nick formation in the G4 motif [106]. The coding sequence for an sRNA overlaps with the G4 motif and is required for its function in an orientation-dependent manner [107].

1.2.6 Genetic transfer

In contrast to most other naturally competent organisms, *N. gonorrhoeae* incorporates DNA during all growth phases [108]. As pointed out above, the versatility of mechanisms to cause genetic plasticity in *N. gonorrhoeae* is staggering. It has been proposed that natural transformation provides cells with a template for DNA repair, if their genome is too compromised from the mutational load to be repaired by itself [109]. Both double-stranded and single-stranded DNA have been reported to be taken up from the environment [110, 111]. There is considerable variation in transformation efficiency between gonococcal strains [112].

Neisseria have a strong preference for incorporating DNA of their own species. This species-specific selectivity is mediated by the recognition of a 10-bp or 12-bp DNA uptake sequence (DUS), which occurs much more frequently in the genome of *N. gonorrhoeae* than expected by chance [113]. The receptor for the DUS is the minor pilin ComP which is integrated into the type IV pilus fiber [114]. In the absence of a DUS transformation is inefficient. If the transformed DNA contains a DUS, its transformation efficiency increases by several orders of magnitude [20, 112, 113]. The location and number of DUSs are reported to have minor effects on transformation efficiency [115].

In closely related bacterial species, the DUS is slightly altered which impairs the transformation efficiency between those species [20]. These differences in sequence are referred to as DUS dialects. The 10-bp DUS occurs about 2000 times throughout the genome of *N. gonorrhoeae*. The distribution is not homogenous and genome maintenance genes contain

more DUS on average. DUSs are frequently arranged as inverted repeats and are considered to act as Rho-independent transcriptional terminators [6, 8, 116].

1.2.7 Barriers to genetic transfer

1.2.7.1 Limits to homologous recombination

To be integrated into the recipient's genome by homologous recombination, DNA needs to have flanking regions with homologies to the chromosome. For successful transformation in *N. meningitidis*, a minimum of 73 bp of homologous flanking sequences is required, while about 500 bp are required for full efficiency [115, 117, 118]. Moreover, the degree of homology within these sequences affects the efficiency of transformation. Sequence divergence is reported to prevent *B. subtilis* chromosomal transformation in a log-linear fashion [119].

1.2.7.2 Restriction-modification systems

Restriction-modification (R-M) systems serve as tools protecting prokaryotes from the harmful effects of foreign DNA. There are four general classes of R-M systems: Type I R-M systems consist of three subunits and target asymmetric bipartite sequences. Type II R-M systems consist of two separate enzymes for restriction and methylation of their targets which are mostly palindromic 4-8 bp sequences. Type III R-M systems are made from a single enzyme with two subunits for restriction and methylation. The type IV R-M systems are a rather diverse class of methyl-dependent restriction enzymes.

Type I-III R-M systems have been found in *Neisseriaceae*. During natural transformation, chromosomal DNA is converted to ssDNA before it enters the cytoplasm [120]. Thus, restriction is not considered to counteract natural transformation. While most bacterial species have 1-2 R-Ms on average, pathogenic *Neisseriaceae* possess at least 14 R-Ms [121, 122]. Given that *Neisseriaceae* are predominantly receptive for their own DNA, it is unclear why there are even more redundant, strain-specific barriers for genetic transfer [121, 122]. R-M systems have been used to determine phylogenetic clades, suggesting that they might contribute to strain stability [123]. Alternatively, R-M systems have been proposed to be selfish gene

elements that merely exist for the sake of their own propagation [124]. Interestingly, other naturally competent species like *B. subtilis*, *H. pylori* and *H. influenzae* also display an overabundance of R-M systems [121].

1.2.7.3 CRISPR-Cas mediated adaptive immunity

Clustered interspaced short palindromic repeat (CRISPR) loci provide adaptive, sequence-based immunity against incoming DNA from plasmids or phages [125]. They are made from 24-48 bp repeat sequences, separated by spacers from foreign genetic elements. CRISPR associated proteins (Cas) assist in the processing of CRISPR-RNA that hybridizes to foreign DNA and triggers its degradation. While present in *N. meningitidis* and *N. lactamica*, no CRISPR systems have been found in *N. gonorrhoeae* [126, 127]. It is important to note that CRISPR interferes with natural transformation, which is considered the major means of gene transfer in the *Neisseria* [127]. CRISPR spacers in *N. meningitidis* match sequences of other *Neisseria* indicating that there is immunity against them [127].

1.2.7.4 The thermonuclease Nuc

Another candidate for restriction of genetic transfer is the periplasmic thermonuclease Nuc. Nuc is a homolog of a secreted staphylococcal thermonuclease and both enzymes are involved in biofilm regulation [128]. It has been demonstrated that Nuc can degrade neutrophil extracellular traps (NETs) and thus promote gonococcal survival during infection [129]. Nuc carries an export signal for the bacterial Sec system, but has not been directly detected outside of the cell [128] [129]. In-vitro assays using recombinant Nuc show a certain resistance of gonococcal chromosomal DNA against degradation, in contrast to chromosomal DNA of other bacterial species [128]. A PCR fragment from gonococcal chromosomal DNA does not show resistance against degradation, suggesting that a species-specific posttranscriptional modification might protect DNA of *N. gonorrhoeae* against degradation by Nuc. Interestingly, neisserial chromosomal DNA is known to be methylated more extensively than chromosomal DNA of other bacterial strains [130].

1.3 Membrane transport of biopolymers

1.3.1 Essentials of membrane transport

Apart from apolar substances like lipids, biological membranes permit only the passive diffusion of a few low-molecular substances. Polar substances that can pass biological membranes include H₂O, ethanol, glycerol, urea and gases like O₂, NH₃, H₂ and CO₂ [131]. In passive diffusion, the transport rate of a substance is slow compared to facilitated processes and dictated by its concentration gradient over the membrane. Hence, an accumulation of the substance inside the cell is not possible. Higher-molecular substances like glucose are excluded from the membrane and cannot be transported in this manner [131].

To allow for passage of larger molecules, cells possess channel proteins. In the outer membrane of Gram negative bacteria, porins enable the diffusion of molecules on the order of 1000 kDa [131]. Moreover, the cytoplasmic membrane contains specific channel proteins for the facilitated passage of H₂O to maintain turgor pressure or the release of ions in the case of osmotic stress [131]. Like passive diffusion, channel proteins can only maintain transport along a concentration gradient and are not able to accumulate substances within the cell. To efficiently acquire and accumulate low concentration substances like nutrients from the environment, cells require active transport. This also applies in the case of some substances that can diffuse through the plasma membrane, but require active transport to be accumulated [131].

There are generally two classes of active transporters [131]. The first class uses chemical energy to drive transport against a concentration gradient. Members of this class are called primary transport systems. A prime example for primary transporters is the group of ABC-transporters, which is ubiquitous in prokaryotes. ABC transporters generally consist of two integrative membrane domains and a cytoplasmic ATP hydrolysis domain. Additionally, many bacterial ABC systems possess a substrate binding protein, which is periplasmic in gram negative bacteria and membrane-anchored in Gram positive bacteria. Upon binding to the outside of the integral membrane domains, either the substrate or the loaded substrate binding protein triggers a conformational change. This results in substrate's entry into the channel formed by the integral membrane domains. Upon hydrolysis of ATP by the cytoplasmic domains, the substrate is released into the cytoplasm [131]. The second class of active transporters are the secondary transport systems. They are characterized by low affinity for the

substrates and a higher transport rate compared to primary transport systems. In secondary transporters, the energy-dependent transport of a substrate is coupled to the energy-delivering transport of an ion, e.g. H^+ , along a concentration gradient over the plasma membrane. If H^+ is the coupling ion, transport is driven by the so-called proton motive force [131]. The underlying H^+ gradient is in turn maintained by primary transport systems. The mode of transport divides secondary transporters in three subclasses: The symporters, the antiporters and the uniporters. In symporters, the substrate and the coupling ion are transported in the same direction, while in antiporters, they are transported in the opposite direction. In uniporters, charged substrates can be transported by the membrane potential without the direct requirement of a coupling ion [131].

1.3.2 DNA translocation by molecular motors

Contrary to short molecules that can be transported via diffusion processes, the transport of biopolymers through biological membranes is always energy-dependent. If a long biopolymer is to be transported through a pore, the translocation process begins with the occasional threading of its proximal tip through the translocation pore [132]. This process is analogous to the complete translocation of a shorter substrate by diffusion. Brownian motion, the driving force of the shorter substrates diffusion through the pore, causes the polymer to fluctuate back and forth inside the pore without any net movement to either side. Hence, translocation of the entire molecule requires directed movement. One way to generate directed movement is the employment of a chemically driven, cyclic molecular motor. The motorized translocation pore would be, per definition, a primary transport system.

ATP-driven multimeric ATPases are involved in various DNA-processing tasks like cell division, chromosome segregation, DNA recombination, strand separation, conjugation and viral genome packaging. A well-described system for DNA translocation via a multimeric ATPase is the DNA packaging motor of phage $\phi 29$ [133, 134]. Its task is to package dsDNA into a preformed precursor capsid to near-crystalline density. The highly processive motor can package the $\phi 29$ genome against forces as high as 57 pN, which represents the stalling force [135]. The result is a tight confinement of DNA causing intra-capsid pressures of 60 atm that may be used to inject DNA during infection [135-137]. The translocation motor of $\phi 29$ is comprised of three components: 1. A head tail connector situated at the base of the icosahedral

prohead, which forms the DNA translocation channel [138, 139]. 2. Five or six copies of the ϕ 29 encoded prohead RNA (pRNA) that are bound to the head tail connector [138, 140-144]. 3. Multiple copies of the RNA-dependent packaging ATPase gp16 that are arranged in a ring like structure and likely form heterodimers with gp16 RNA during operation of the motor [138, 145, 146]. High processivity during translocation indicates, that the motor subunits act in a coordinated and successive fashion with multiple subunits performing at a given time [133]. To achieve its high processivity, the ϕ 29 packaging motor requires specific binding to its substrate, dsDNA. Moreover, the motor complex possesses a rigid, defined structure that puts constraints on the localization of the binding sites with respect to each other. Indeed, the motor has been revealed to depend on the secondary structure of dsDNA for efficient translocation [134]. It forms important contacts with the adjacent pairs of backbone phosphates spaced every 10 bp on one DNA strand [134].

1.3.3 The translocation ratchet

Various types of directed movement in cells do not require molecular motors that perform a mechanochemical cycle. The proximal movement of these machines arises from random thermal fluctuations caused by Brownian motion. These are rectified through a chemical potential to perform mechanical work [147, 148]. During performance, this potential steadily decreases and needs to regenerate after it is depleted. Hence, these machines are called “one-shot motors” [149]. One such machine is the translocation ratchet. It likely drives the co-translational and post-translational translocation of polypeptide chains [150]. As mentioned previously, the translocating polymer fluctuates back and forth inside a polymer in the absence of directed movement, in analogy to a reptating polymer. When the polymer chain reptates from outside, a chemical modification can occur that prevents the polymer from reptating back. Upon repetition of this process, the increasingly modified polymer is ratcheted through the translocation pore. There are several chemical asymmetries that can bias the Brownian walk of a polypeptide chain [150-153]. In post-translational protein translocation, the binding of chaperones is assumed to be the major modification contributing to the transport process [151].

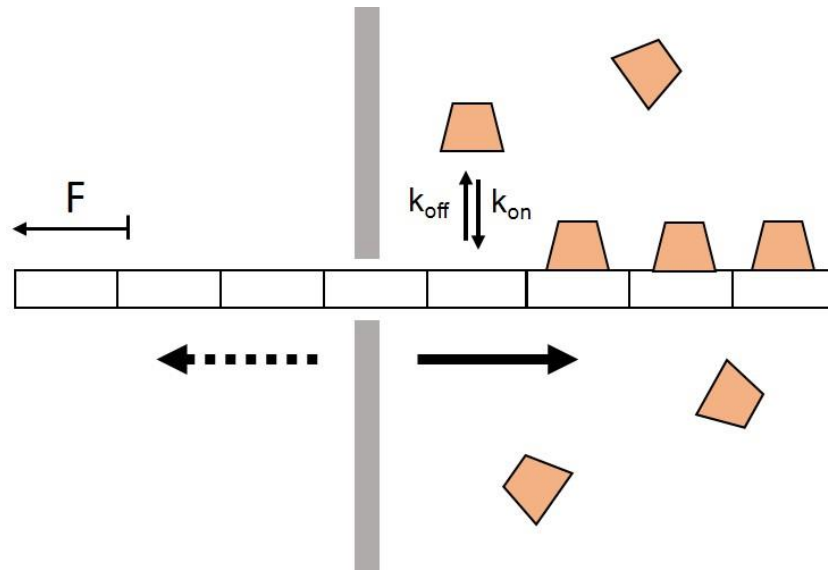


Figure 1.1 Principle of a translocation ratchet. A polymer with several segments is threaded into a membrane pore. Each segment is able to bind a chaperone (orange) in the compartment on the right. The polymer segments can freely pass through the pore from left to right (solid arrow). In contrast, the segments on the right experience an inhibition of backwards movement (dashed arrow). This inhibition is governed by the binding probability of the chaperone to a segment. The binding probability is determined by the association rate (k_{on}) and the dissociation rate (k_{off}) of chaperone binding. The resulting biased Brownian motion can perform work against an external load F .

The mechanism of a translocation ratchet has been theoretically described by Peskin and Oster [149]. In their model, a rod diffusing along the x -axis is considered with a diffusion coefficient D . The rod carries ratchet sites with a spacing a between two sites for chaperones. A ratchet site can freely cross the origin from the extracellular side to the periplasm. However, when it attempts to cross the origin from the periplasm to the extracellular space it is reflected with a probability p , provided that an intracellular chaperone is bound. The variable $x(t)$ = position of the first site within the periplasm is introduced, so that $x(t)$ is always within $(0, a)$. $c(x, t)$ is the density of the variable $x(t)$. The flux of rods at point x is

$$J = -\frac{DF}{k_B T} c - D \frac{\partial c}{\partial x}, \quad [1]$$

where F is the external force. In our experiments, F is applied by the optical tweezers at the extracellular side and therefore it always counteracts DNA uptake. The density and flux satisfy the conservation equation:

$$\frac{\partial c}{\partial t} + \frac{\partial J}{\partial x} = 0. \quad [2]$$

The boundary conditions are as follows:

$$J(0, t) = J(a, t)$$

$$c(a) = (1 - p)c(0).$$

Considering only steady states, the flux J is constant. By solving Eq. 1 with the boundary conditions, the solution is [149]

$$v(F) = \frac{2D}{a} \frac{1/2\omega^2}{\left(\frac{e^\omega - 1}{1 - K(e^\omega - 1)}\right) - \omega},$$

where $\omega = Fa/kBT$, a is the distance between two binding sites, D is the diffusion constant of DNA within the pore, and $K = k_{off}/k_{on} = (1-p)/p$ is the dissociation constant.

1.4 Components of the natural transformation machinery and their function

Natural transformation is a prevalent feature in the bacterial domain. For successful transformation, a bacterial cell is required to perform the following tasks: 1. DNA must bind to the surface of the cell. 2. The bound DNA must be transported into the cytoplasm. 3. Finally, DNA must be integrated into the genome. This process requires a multi-component machine. Its components comprise a membrane-spanning complex for DNA uptake and cytoplasmic proteins that condition the transforming DNA for recombination or formation of self-replicating plasmids. The components are well-conserved between different bacterial species. In this section, the transformation machinery in Gram negative bacteria will be introduced using *N. gonorrhoeae* as a reference organism. The proteins discussed in this section are named after their *N. gonorrhoeae* orthologs. Subsequently, established facts and proposals on the putative DNA acquisition mechanism will be presented and compared to the situation in Gram positive bacteria and *H. pylori*.

1.4.1 The type IV pilus machinery

Type IV pili (Tfp) are cell appendages essential for motility, natural transformation, biofilm formation and attachment to epithelial cells in *N. gonorrhoeae* and constitute important virulence factors in various pathogenic bacteria [88-90] [154]. Tfp mediated motility is achieved through cycles of extension, surface attachment and retraction [155, 156]. In this manner, Tfp pull the cell forward at forces of up to 150 pN [157, 158]. Tfp are related to type II secretion systems (T2SS) that export proteins into the extracellular space [159-161]. All of the studied naturally transformable bacteria rely either on Tfp or T2SS for transformation and uptake of DNA, with the exception of *H. pylori* [27, 162]. A recent study employed cryo-electron microscopy, gene deletions, and protein fusions to solve the structure of the Tfp complex in *Myxococcus xanthus* [163]. Consulting data from earlier studies on accumulation, subcellular localization and incorporation, connectivities and protein structures, a complete

picture of the Tfp architecture has been generated [164-185]. In this subsection, Tfp architecture and function will be outlined based on this body of work (Figure 1.2).

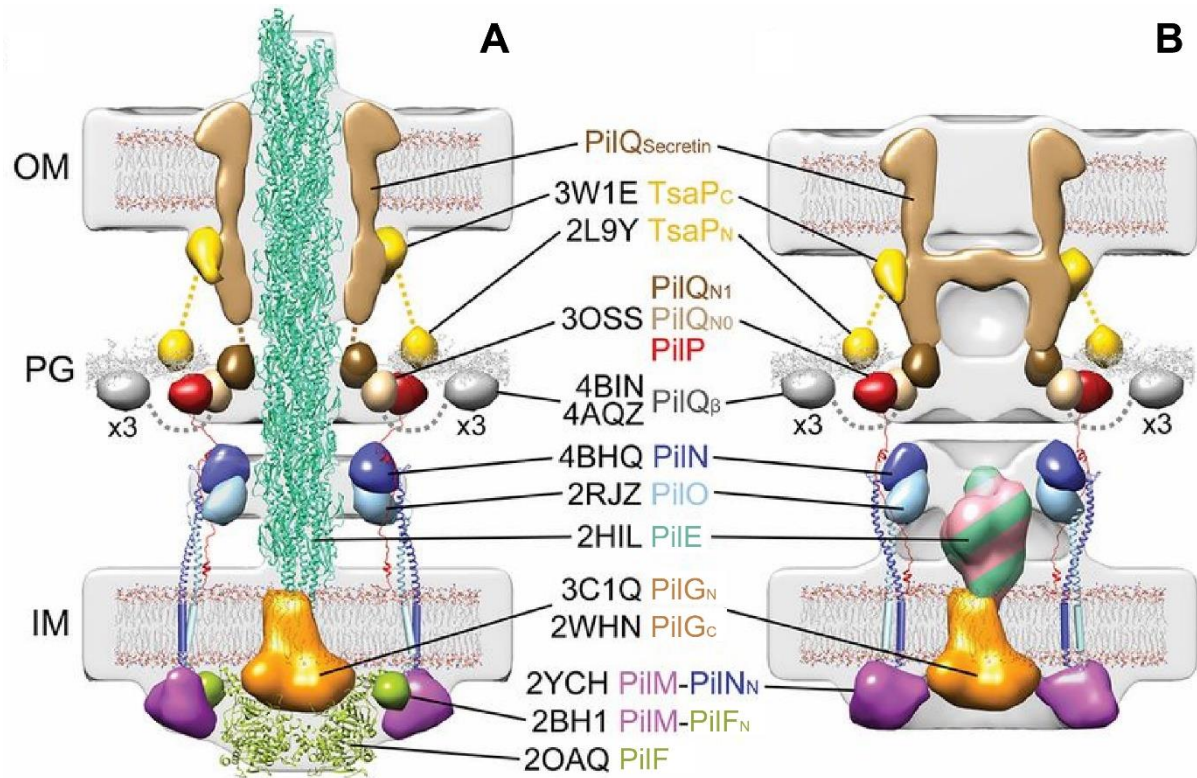


Figure 1.2 Central slices of the architectural models of pilated (A) and empty (B) T4PM basal bodies, respectively, in which atomic models of Tfp machine components are placed in the *in vivo* envelopes according to previously reported constraints and filtered to 3-nm resolution. The transmembrane segments of PilN and PilO are shown as cylinders; “x3” indicates three AMIN domains per PilQ monomer, only one of which is shown. Note that the empty Tfp machines’ basal body is shown with five PilA major pilin subunits in the short stem; however, the short stem likely also contains minor pilins. Image adapted from Chang et al., *Science*, 2016 [163].

1.4.1.1 The type IV pilus fiber

Tfp are proteinaceous fibers that can extend several micrometers from the surface of the cell. They are polymers formed by pilin, a small protein of about 20 kDa. It consists of a hypervariable C-terminal domain and a hydrophobic N-terminal domain [165]. The N-terminal domain anchors the pilin monomers in the cytoplasmic membrane prior to their integration into the Tfp. During polymerization, the N-terminal domains of the pilins attach to each other to form the backbone of a helical pilus fiber with a diameter of approximately 6 nm and five pilin subunits per turn [165][186, 187]. The N-terminal domain contains a leader peptide that is

cleaved by the prepilin peptidase PilD, before the pilins can be integrated into the Tfp fiber [188]. This processing of pilin might also support its translocation through the cytoplasmic membrane [189]. Besides pilin, which is encoded by the *pilE* gene in *N. gonorrhoeae*, various other so called minor pilins are integrated into the pilus fiber, albeit at a lower level. Some of the minor pilins are essential for Tfp formation and might prime pilus assembly [163, 190-192].

1.4.1.2 The minor pilin ComP is the receptor for the neisserial DNA uptake sequence

Efficient transformation in *N. gonorrhoeae* depends on the DNA uptake sequence (DUS) [20, 112, 113]. The DUS occurs as a 10-bp sequence that reads 5'-GCCGTCTGAA-3', yet the 12-bp DUS 5'-ATGCCGTCTGAA-3' enhances transformation more efficiently [6]. In bacterial species closely related to *N. gonorrhoeae*, DUS have been found to differ from this sequence, except for the 5'-CTG-3' core sequence that is essential for recognition. These sequences are called the DUS dialects [20]. The DUS dialects' degree of similarity in two different strains modulates the efficiency of genetic transfer between them [20].

A recent study revealed that the minor pilin ComP is responsible for DUS-mediated enhancement of natural transformation [114]. As a minor pilin, ComP is non-essential for pilus assembly, but absolutely required for efficient transformation [116]. ComP is supposed to bind DNA via an electropositive strip exposed on the assembled pilus fiber and displays an exquisite binding preference for the DNA uptake sequence [114]. Transformation in the presence of DUS is entirely dependent on ComP, which also controls DNA binding in the absence of DUS [193].

PilV, another minor pilin, is known to be an inhibitor of DUS specific natural transformation. DNA uptake and transformation have been shown to be enhanced in *pilV* mutants [175]. PilV inhibits transformation by antagonism of ComP, likely preventing its integration into the Tfp fiber [175].

1.4.1.3 The outer membrane secretins PilQ and TsaP

Pili grow by polymerization on the cytoplasmic membrane. In Gram negative bacteria, they have to pass the outer membrane (OM) in order to protrude from the cell. For this purpose, Gram negative bacteria possess the secretin pore PilQ [194]. Secretins of this type are

homomultimers consisting of 12-14 subunits that form an aqueous pore harboring a central cavity of 6-8.8 nm [195-197]. In *N. gonorrhoeae*, this cavity has a diameter of 6.5 nm, which is sufficient to accommodate the pilus fiber [186, 196]. In the absence of other pilus proteins, *pilQ* forms a rudimentary basal body with a protein called TsaP [166]. One domain of TsaP forms a ring-like structure surrounding PilQ just beneath the OM. A second domain of TsaP interacts with the peptidoglycane layer. Lack of TsaP leads to accumulation of pilus fibers in the periplasm of *N. gonorrhoeae* and fewer pili in *M. xanthus* [164]. Parts of PilQ locate in the periplasm and seem to take part in the alignment of the Tfp machinery [163].

1.4.1.4 The alignment proteins PilM, PilN, PilO and PilP

The four proteins PilM, PilN, PilO, and PilP possess long linker domains and take part in the formation of two periplasmic ring structures, the mid periplasmic ring and lower periplasmic ring [163] (Figure 1.2). PilP builds the mid periplasmic ring together with a part of PilQ [166, 171][163]. The lower periplasmic ring is formed by PilN and PilO, which have been proposed to form heterodimers [163]. Both proteins are critical for the alignment of the Tfp complex [166]. PilP binds PilN to connect the mid periplasmic ring with the lower periplasmic ring [173]. PilM forms a cytoplasmic ring which is required for the incorporation of the motor complex [163]. PilP and PilN interact with PilM via coiled-coil domains [163]. Thus, the entire Tfp machinery is interconnected by a flexible scaffold spanning the entire periplasm.

1.4.1.5 The motor complex for pilus extension and retraction: PilF, PilT and PilG

PilG is a polytopic transmembrane protein with an N-terminal globular domain situated on the cytoplasmic side [179]. It has been proposed to provide the assembly platform for the pilus fiber [198]. In cryo EM data it is characterized by a cytoplasmic dome-like structure at the base of the pilus [163]. PilG depends on PilM for its incorporation in the Tfp complex [163].

PilF and PilT are cytoplasmic proteins that belong to the family of the hexameric secretion or traffic ATPases [182-185]. While PilF is necessary for the formation of the pilus through polymerization, PilT is dispensable [90]. However, PilT is necessary for pilus retraction by depolymerization of the pilus fiber [155]. Both PilF and PilT bind as hexamers to PilG at

the basal body of the Tfp complex. Due to spatial constraints, PilF and PilT are expected to bind in a mutually exclusive manner [163].

1.4.1.6 The mechanism of Tfp elongation and retraction

Based on the structural data, the following model for pilus assembly and function has been proposed [163].

Like the secretin pore PilQ, all proteins taking part in the rings are likely to be arranged in a 12-fold symmetry. This agrees with predictions for Tfp and T2SS [159-161]. The hierarchy of Tfp assembly has been studied in *M. xanthus* using a combination of gene deletions, fluorescent proteins, and protein stability analysis [163]. Pilus assembly is initiated by [PilQ, TsaP], followed by [PilP, PilN, PilO], followed by [PilM, PilG, PilE or minor pilins], followed by PilF or PilT. All the rings of the Tfp complex are linked by flexible protein domains. They align the pilus and connect the outer membrane proteins TsaP and PilQ to the motor complex consisting of PilM, PilG and the traffic ATPases via the scaffold proteins PilP, PilO, and PilN.

No pilus rotation during polymerization and depolymerization of the pilus fiber has been observed. The only Tfp complex protein able to rotate is PilG, as it is not linked to rest of the complex. As PilG is an integral membrane protein it can recruit pilin monomers by hydrophobic interactions with their N-terminal domains and move them between the pilus and the cytoplasmic membrane. According to the electron densities of the Tfp complex structure, PilG is most likely a dimer. When PilF or PilT bind to PilM, they interact with PilG and cause it to rotate by ATP hydrolysis. In this model, it depends on PilGs direction of rotation, whether the pilus polymerizes or depolymerizes. By rotating PilG, the motor proteins PilF and PilT bias the exchange of pilus monomers between the pilus fiber and the cytoplasmic membrane, acting as ratchets. As PilG can be at best a dimer and each subunit is unlikely to contain more than one binding site for pilin, the pilus fiber probably elongates by the incorporation of one pilin subunit at a time [165] [163]. As tension induces conformational changes in the pilus fiber, pilus retraction is hypothesized to be induced by binding of pilin to substrates [199-201]. An involvement of PilN and PilO in sensing signals in the pilus fiber to induce switching from extension to retraction has been discussed [202].

1.4.2 Non-Tfp competence proteins

Variants of the Tfp or T2SS are essential for natural transformation and DNA uptake, but they are not sufficient. This subsection will outline key players in natural transformation that are not associated with Tfp. *N. gonorrhoeae* nomenclature will be used except for proteins unidentified in *N. gonorrhoeae*.

1.4.2.1 The periplasmic DNA binding protein ComE

ComE is a soluble periplasmic protein that binds DNA via a conserved helix-hairpin-helix (hHh) motif [203]. In the absence of ComE, transformation is highly inefficient. The observation that extracellular recombinant ComE inhibits transformation suggests that ComE is actively involved in DNA uptake [203]. There are four *comE* loci in the genome of *N. gonorrhoeae* and by deleting these loci one by one, the transformation efficiency can be gradually reduced.

In *B. subtilis*, lack of the ortholog ComEA impairs DNA binding to the cell surface [204]. ComEA in Gram positive organisms like *B. subtilis* is different than ComE in that it has a more complex structure: The C-terminal domain of ComEA has a hHh motif for DNA binding and is orthologous to ComE [203]. The N-terminal domain that cannot be found in *N. gonorrhoeae* anchors ComEA inside the cytoplasmic membrane [203]. The two domains are connected by a flexible hinge region that is essential for efficient transformation.

B. subtilis ComEA has been proposed to shuttle DNA from the competence pseudopilus to the site of translocation through the inner membrane. Its ortholog ComE in *N. gonorrhoeae* might have the same function [204].

1.4.2.2 Proteins involved in transport through the cytoplasmic membrane

ComA is a polytopic membrane protein essential for transformation in all organisms known to be naturally transformable [120, 205-209]. In *N. gonorrhoeae*, ComA is not necessary for DNA uptake, but in its absence imported dsDNA is retained in the periplasm [210]. In Gram

positive organisms, it is dispensable for DNA binding but essential for transport into the cytoplasm [205].

ComA forms an aqueous channel across the plasma membrane and orthologs of ComE and ComA are listed as ‘DNA translocase’ in the Transport Protein Database [211]. ComA carries a binding-protein domain, a signature motif for ABC transporters and point mutations in this domain reduce transformation [4]. These ubiquitous transporters represent one of the largest protein families and are found both in prokaryotes and eukaryotes [212].

To enter the cytoplasm through ComA, the DNA molecule requires directed movement via active transport. The power source for cytoplasmic DNA import in *N. gonorrhoeae* remains to be elucidated. In *B. subtilis*, the ortholog of ComA interacts with the DNA binding protein ComFA and its deletion results in a 1000-fold reduction of transformation efficiency, but does not affect DNA binding. Its homolog PriA in *E. coli* acts as a DNA partitioning protein and is an ATP driven DNA translocase related to helicases. PriA contains a Walker A and a Walker B motif for ATP binding and hydrolysis. A mutation of Walker A leads to transformation deficiency [205]. ComFA is therefore considered to power DNA transport by interaction with the *B. subtilis* ComA ortholog. Alternatively, it might have a role in unwinding DNA or gating the ComA channel [4]. In Gram negative species including *N. gonorrhoeae*, the ComFA homolog PriA is required for the restart of arrested replication forks. As PriA is required for homologous recombination and thus essential for a different step in the transformation process, its involvement in DNA import has neither been verified nor disproven [213]. .

ComA is associated with nucleolytic activity in *N. gonorrhoeae* and models propose that DNA can only be imported into the cytoplasm as ssDNA [120, 210]. A recent in-silico study on the structure of the *B. subtilis* ComA ortholog revealed a putative zinc binding motif on the periplasmic side [214]. Zinc binding motives are associated with hydrolytic activity suggesting that ComA itself acts as a nuclease to convert incoming DNA to ssDNA before it is transported into the cytoplasm.

1.4.2.3 ComL and Tpc

Tpc (Tetrapac) is a 37 kDa protein with an N-terminal leader sequence typical for lipoproteins [215]. A *tpc* mutant is associated with a rough colony morphology and growth in clusters of four, suggesting a defect in cell division. These cell clusters can be resolved by co-

cultivation with wild-type *N. gonorrhoeae*, indicating Tpc is a diffusible protein. Further, mutation of *tpc* shows a reduced murein hydrolase activity. Importantly, Tpc is absolutely required for natural transformation [216].

ComL is a 29 kDa peptidoglycan-linked lipoprotein. *ComL* is an essential gene a viable mutant of which displays retarded growth due to small cell size. Additionally, *comL* is required for efficient transformation [217].

1.4.2.4 Cytoplasmic DNA binding proteins

After entering the inner membrane via passage through a pore formed by ComA proteins, ssDNA is protected from degradation by ssDNA binding proteins (SSB). The function of these proteins has been extensively investigated in Gram positive *B. subtilis* and other rod-shaped bacteria, where these proteins localize to the cell wall upon establishment of the competence machinery or DNA uptake [218].

RecA is a single-strand-binding protein (SSB) with a central role in the DNA recombination of all bacteria, archae and eukaryotes found in nature [219, 220]. In competent cells, RecA converts the internalized ssDNA into a helical nucleoprotein filament and subsequently promotes the search for homology, leading to integration into the genome of the recipient cell [221, 222]. In addition, RecA requires a set of accessory factors to trigger its nucleation and the extension of the nucleated filament.

These accessory factors are expected to have two main functions in transformation: On one hand, they are expected to protect DNA and delay the onset of recombination into the recipients' chromosome. These SSBs may be called the "guardian" proteins. On the other hand, "mediator" proteins recruit RecA and the recombination machinery resulting in chromosomal integration by homologous recombination [219, 223]. The accessory factors have primarily been investigated in *B. subtilis* and other rod-shaped bacteria, where they are associated with the cell poles. These studies suggest varying functions for the same homolog of a RecA accessory factor in different strains. Thus, it is difficult to attribute a specific function in natural competence to SSBs in coccoid *N. gonorrhoeae* which are less well studied. However, the ssDNA binding protein DprA is absolutely required for transformation in *N. gonorrhoeae* and essential for efficient transformation in various other bacteria [224]. In *S. pneumoniae*, it has been demonstrated to be a mediator protein which can overcome the described inhibitory effect

of guardian proteins and load RecA onto ssDNA [225]. DprA counteracts antigenic variation mediated by homologous recombination in *N. gonorrhoeae* indicating a functional interaction with RecA [224]. DprA is not restricted to naturally transformable bacteria, but ubiquitous in free-living bacteria [218].

1.4.3 The mechanism of DNA import in Gram negative bacteria – state of the art

Based on the structural and functional data of the natural competence machineries' components, an incomplete model of the DNA import mechanism shall be presented (Figure 1.3a): DNA enters the cell via the secretin PilQ, as it is the only membrane pore involved in transformation [226]. With a diameter of 6.5 nm, PilQ can easily accommodate a DNA double helix, measuring 2.4 nm [196]. Nevertheless, the type IV pilus (Tfp), as well as specific binding of the DUS (DNA uptake sequence) to the DNA receptor ComP is required for full efficiency of DNA uptake [114, 226]. As ComP is an integrative part of the pilus fiber, DNA binding is likely to happen outside of the cell, rendering binding of external DNA the primary means of discrimination between self and non-self DNA. In the following, pilus retraction mediated by the ATPase PilT enables DNA uptake. There are two main hypotheses on the role of pilus retraction in the DNA uptake process: 1. PilT drives DNA uptake by pulling it into the periplasm by cycles of pilus retraction and re-extension. 2. Pilus retraction merely initiates DNA uptake, either by clearing a passage for DNA into the periplasm through the PilQ pore, or by actively contriving DNA into the periplasm via PilQ. While the first DNA model would be most efficient with long pili, the second model only requires a short pilus able to reach the surface of the cell. Tfp are used for twitching motility in *N. gonorrhoeae* and hence protrude from the cell surface up to several micrometers. However, protruding pili do not seem to be a requirement for DNA uptake in bacteria using their pili exclusively for competence or bacteria employing competence pseudopili that are derived from the related type II secretion systems (T2SS). Furthermore, a hypercompetent *pilV* deletion mutant has been shown to form less protruding pili in *N. gonorrhoeae* and a non-piliated phenotype still allows for competence in both genetically modified strains and naturally occurring antigenic variants [227-229] [228]. The possible involvement of minor pilins in priming pilus assembly suggests that ComP might prime an alternative, shorter pilus tailored for DNA uptake in *N. gonorrhoeae* [163, 190-192, 227].

Components of the natural transformation machinery and their function

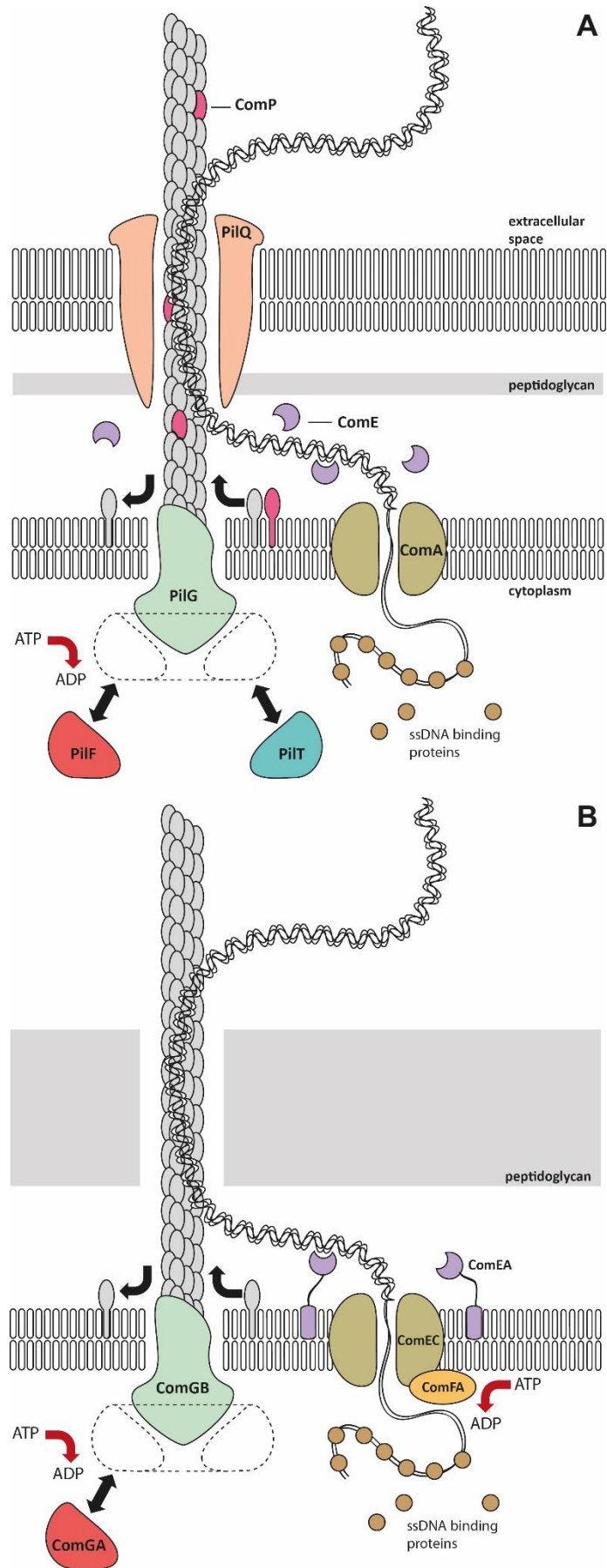


Figure 1.3 A model of the DNA transport machinery in transformation of [A] *N. gonorrhoeae* [B] *B. subtilis*. Only a subset of the proteins required for DNA import are displayed.

In the periplasm, the soluble DNA binding protein ComE represents a possible receptor for incoming DNA. ComE is required for efficient transformation, but its role in DNA uptake from the extracellular space or in DNA import into the cytoplasm remained to be elucidated at the time this thesis started [203]. The roles of Tpc and ComL are unknown. ComA might convert dsDNA to ssDNA by an intrinsic nucleolytic activity and subsequently transports it into the cytoplasm [120, 214]. Cytoplasmic import of ssDNA via ComA is either powered by PriA, another yet unidentified motor protein with a comparable function to *B. subtilis* ComFA or interaction with ssDNA binding proteins in the cytoplasm.

1.4.4 Structural and mechanistic differences to other bacteria

Although the functional components of the DNA import mechanism are usually highly conserved, there are two major cases of variation: Firstly, DNA uptake over the outer membrane is not performed by a type IV pilus in Gram negative *H. pylori*. Secondly, only one membrane needs to be traversed by DNA in Gram positive organisms like *B. subtilis*, resulting in the structural and functional adaption of the Gram positive orthologs (Figure 1.3b).

1.4.4.1 *H. pylori*

In *H. pylori*, uptake of transforming DNA over the outer membrane is mediated by a type IV secretion system (T4SS) [162]. The T4SS is not related to type IV pili which are homologous to type II secretion systems. The T4SS is a transport system composed of 8 individual proteins and has been characterized in *Agrobacterium tumefaciens* where its function is the transfection of plant host cells with effector proteins and DNA, causing tumors [26]. *H. pylori* has a functional ComA ortholog and transport from the periplasm into the cytosol is expected to proceed analogous to other Gram negative bacteria [209] [230]. In contrast to other gram negative systems, the force-velocity relationship of the DNA uptake process has been characterized. In single molecule experiments, *H. pylori* cells take up a DNA molecule at a velocity 1.3 kbp/s. Previously imported DNA can be re-extracted at forces exceeding 23 pN [26].

1.4.4.2 Gram positive bacteria

Gram positive bacteria do not have an outer membrane (OM). Yet, their DNA uptake machinery requires a type IV pilus (Tfp) or a pseudopilus synthesized by a type II secretion system [206, 231]. The most important consequence of a missing outer membrane is the absence of the PilQ secretin pore, as it is not needed to get the pilus fiber to the surface of the cell (Figure 1.3b). The ComE ortholog in Gram positive organisms is named ComEA. It is not soluble, as it would be lost from the cell without an OM. Additionally to the C-terminal DNA binding domain orthologous to *N. gonorrhoeae* ComE, the *B. subtilis* ComEA possesses an N-terminal membrane binding domain [204]. It is connected to the C-terminal domain via a flexible hinge region, thereby anchoring ComEA in the cytoplasmic membrane [204]. If the peptidoglycane layer is removed, the competence pilus is not required and ComEA can bind external DNA on its own [232]. From ComEA, the DNA is expected to be passed on to the ComA ortholog ComEC, which transports ssDNA into the periplasm, analogous to Gram negative organisms [233]. In *B. subtilis*, transport of ssDNA through ComEC is known to be powered by the ATPase ComFA [234]. Moreover, there is no ortholog of the pilus retraction ATPase PilT in the natural transformation machinery of Gram positive bacteria [235]. Hence, it has been hypothesized that the competence pilus is merely needed to provide space within the peptidoglycane layer for DNA to fit through.

1.5 Aims of this study

Horizontal gene transfer by natural genetic transformation contributes to diversity and adaptability of microbial life. Understanding the mechanism for this kind of genetic transfer has the potential to open new perspectives in medicine and biotechnology. In this study, we are seeking to elucidate the mechanistic function of previously identified components of the natural transformation machinery in Gram negative bacteria. Our model organism is *Neisseria gonorrhoeae*, a human pathogen that is stably transformable under laboratory conditions.

In the first part of this study, we set out to ask what the mechanistic purpose of the periplasmic DNA binding protein ComE is. We hypothesize that ComE binds DNA after entry into the periplasm and escorts it to the inner membrane DNA transporter ComA, before it enters the cytoplasm. To test this hypothesis, we aim to assess the capacity, kinetics, stability, localization and possible rearrangements of DNA within the cytoplasm in response to altering ComE levels. To accomplish this aim, we plan to observe cells during and after uptake of fluorescently labeled DNA at varying concentrations of ComE. Further, we aim to track ComE after DNA binding. If ComE can be shown to colocalize with DNA after uptake, stability, localization and rearrangements of the ComE-DNA complex can be assessed. The results of these experiments will help us to substantiate our hypothesis on ComE function.

In the second part of this study, we ask what powers DNA uptake into the periplasm. Based on previous results, we hypothesize that the binding of ComE molecules inside the periplasm drives the uptake of DNA through a translocation ratchet mechanism. To test this hypothesis, we investigate the force-velocity relationship during the uptake of a single DNA molecule. For this purpose, we perform single molecule experiments using optical tweezers in force-feedback mode. To provide evidence for a direct involvement of ComE in the uptake process, we test whether the force-velocity relationship changes upon varying the ComE concentration. Further, we plan to compare our experimental data to a theoretical model describing a translocation ratchet. Finally, we compare our data with pilus retraction to exclude the alternative hypothesis that DNA uptake is powered by retracting pili.

In the third part of this study, we address the question whether single stranded DNA is an efficient substrate for DNA uptake. Earlier results show that *N. gonorrhoeae* can be naturally transformed by ssDNA. Moreover, *N. gonorrhoeae* secretes ssDNA, resulting in elevated transformation levels. We hypothesize that efficient transformation of ssDNA requires efficient

ssDNA uptake and that uptake of ssDNA and dsDNA should therefore be comparable. To test this hypothesis, we set out to compare the uptake efficiencies of fluorescently labeled ssDNA and dsDNA. We assume specific recognition of the DNA uptake sequence (DUS) and transport of DNA are mediated by different DNA receptors. Hence, we design several hybrid fragments containing stretches of both ssDNA and dsDNA to separately test for recognition and uptake. Further, in comparing the uptake kinetics of the different DNA species, we hope to draw further conclusions about the mechanism of DNA uptake.

2 Materials and Methods

2.1 Media and solutions

Gonococcal base medium (GC)

NaCl	5 g/l
K ₂ HPO ₄	4 g/l
KH ₂ PO ₄	1 g/l
Bacto™ Proteose Peptone No. 3	15 g/l
D-glucose	1 g/l
L-glutamine	0.1 g/l
L-cysteine	0.289 g/l
thiamine pyrophosphate	1 mg/l
Fe(NO ₃) ₃	0.2 mg/l
thiamine HCl	0.03 mg/l
4-aminobenzoic acid	0.13 mg/l
β-nicotinamide adenine dinucleotide	2.5 mg/l
vitamin B ₁₂	0.1 mg/l

Gonococcal base agar (GC agar)

soluble starch	0,5 g
Bacto™ agar	10 g
GC	to 1 L

DNA uptake medium

GC	
MgCl ₂	7 mM

Annealing buffer 1x

Tris-HCl pH 8.0	10 mM
NaCl	50 mM
EDTA	1 mM

PBS

K-PO ₄ pH 7.45	10 mM
KCl	50 mM
NaCl	1 mM

DNA uptake retraction assay medium (DRAM)

DMEM	
L-glutamine	2 mM
sodium pyruvate	8 mM
HEPES	30 mM
MgCl ₂	7 mM
BSA	0.4 g/l

TAE buffer 1x

Tris	40 mM
acetic acid	20 mM
EDTA	1.4 mM

EtNA extraction solution

NaOH	240 mM
EDTA	2.7 mM
ethanol	74% (v/v)

EtNA suspension solution

Tris-HCl pH 8.0	50 mM
EDTA	0.1 mM
Triton-X-100	1% (v/v)
Tween-20	0.5% (v/v)

NaCl, KCl, HCl, acetic acid, ethanol, Triton X-100TM, Tween-20TM, Tris, HEPES, K₂HPO₄, KH₂PO₄, D-glucose, L-glutamine, L-cysteine-HCl, thiamine-HCl, β-nicotinamide adenine dinucleotide, BSA were purchased from Roth, Darmstadt, Germany. BactoTM Proteose Peptone No. 3 and BactoTM agar were purchased from BD Biosciences, MA, USA. Soluble starch, thiamine pyrophosphate, Fe(NO₃)₃, 4-aminobenzoic acid and vitamin B₁₂ were purchased from Sigma-Aldrich, St. Louis, MO, USA. PBS was purchased as tablets from Thermo Scientific, Waltham, MA, USA.

2.2 Molecular biological methods

2.2.1 Plasmid isolation from *E.coli*

The strain containing the plasmid was inoculated in 5 ml LB broth (Roth, Darmstadt, Germany) containing an appropriate antibiotic and incubated overnight at 37°C, 250 rpm. DNA was isolated using QiaprepTM Spin Miniprep Kit (Qiagen, Hilden, USA) according to the manufacturer's protocol. The DNA concentration of the isolate was determined by measuring the

absorbance at wavelengths of 260 nm and 280 nm using a Genesys™ 10S UV-Vis photometer (Thermo Scientific, Waltham, MA, USA).

2.2.2 Genomic DNA isolation from *N. gonorrhoeae*

Cells were grown overnight on GC agar (2.1). The cells were resuspended in 1 ml GC (2.1) to $OD_{600} \approx 1$ and pelleted for at 5000 rpm. Genomic DNA was purified from the pellet using DNeasy Blood & Tissue Kits (Qiagen, Hilden, USA) according to the manufacturer's protocol.

2.2.3 Polymerase chain reaction

Polymerase chain reactions (PCR) were performed using previously described methods (Sambrook et al., 2001). For preparative PCR reactions, the following polymerases were used: High Fidelity PCR Enzyme Mix (Thermo Scientific, Waltham, MA, USA), Phusion™ polymerase (Thermo Scientific) and Q5™ polymerase (New England Biolabs, Ipswich, MA, USA). Additionally, Taq polymerase (Thermo Scientific) and DreamTaq™ Green MasterMix (Thermo Scientific) were used for analytical PCR reactions. PCR reaction mixtures and cycling conditions were adopted from the manufacturers' protocols. Oligonucleotide primers were designed for an annealing temperature of 55°C, utilizing a freely available online tool provided by the Northwestern University, IL, USA [236]. For this, the basic melting temperature for the part of the sequence that anneals to the template was adjusted to $58 \pm 1^\circ\text{C}$.

In this work, up to four DNA fragments were joined by PCR fusions. First, the fragments to be joined were individually amplified by PCR. The primers to obtain each fragment carried extensions at their 5' end to introduce flanking sequences overlapping with the adjacent fragments. In the next step, a PCR reaction was run containing all the fragments to be joined as well as the two terminal primers of the desired fusion product.

2.2.4 Agarose gel electrophoresis

To analyze fragment size and separate DNA fragments for preparation, agarose was dissolved in 1x TAE buffer (2.1) to a concentration of 0.7 – 1%. The DNA sample was mixed with 6x DNA loading buffer (Thermo Scientific, Waltham, MA, USA). Electrophoresis was run for 50 min at 120 V in 1x TAE buffer. “GeneRuler™ 1 kb Plus DNA Ladder” (Thermo Scientific) served as molecular size marker. The fragments were stained with GelRed™ dye (Biotium, Hayward, CA, USA) or PeqGreen™ dye (Peqlab, Erlangen, Germany). A Geni™ gel documentation system (Syngene, Frederick, MD, USA) was used to visualize DNA fragments by UV trans-illumination.

2.2.5 DNA isolation by gel extraction

To recover DNA fragments from agarose gels, the band containing the required fragment was excised with a blade on a UV-table. The gel piece was purified using the manufacturer’s supplied protocol for QiaQuick™ Gel Extraction Kit (Qiagen, Hilden, USA), collected in the 10 mM Tris-HCl (pH 8) elution buffer and stored at -20 °C for future use.

2.2.6 DNA restriction

For insertion into plasmid vectors, DNA fragments were digested with restriction enzymes (New England Biolabs, Ipswich, MA, USA and Thermo Scientific, Waltham, MA, USA). Up to 1 µg of DNA was digested with 5-10 units of a restriction enzyme according to the manufacturers’ protocols. After incubation, the restriction enzymes were deactivated for 20 min at 65°C. The digestion was controlled by agarose gel electrophoresis (2.2.4). Digested products were purified using „QIAquick™ PCR Purification Kit (Qiagen, Hilden, USA).

2.2.7 Dephosphorylation

To prevent religation of linearized plasmid after digestion, Shrimp Alkaline Phosphatase (Thermo Scientific, Waltham, MA, USA) was used. This enzyme catalyzes the dephosphorylation of 5' and 3' ends of DNA. The vector was treated using the manufacturer's supplied protocol.

2.2.8 Ligation

To ligate DNA fragments with complementary overhangs obtained by restriction, T4 DNA ligase (Thermo Scientific, Waltham, MA, USA) which catalyzes the formation of phosphodiester bonds between neighboring 3'-OH and 5'-phosphate ends was used. For cloning of PCR fragments into plasmid vectors, 50 ng of digested vector was added to 1x T4-DNA Ligation Buffer (Thermo Scientific) and supplemented with 0.5 μ l of 10 mM ATP (Thermo Scientific). The required amount of DNA insert was calculated with respect to the insert to vector ratio of 3:1. After addition of 1 μ l of T4 DNA ligase to the reaction mix, it was incubated for ≥ 1 h at 22°C.

2.2.9 Transformation of chemically competent *E.coli*

An aliquot of 50 μ l of competent *E.coli* DH5 α cells was thawed on ice, 50 – 500 ng of plasmid DNA were added to the cells and incubated on ice for 30 min. After incubation, the cells were placed at 42°C for 90 sec and then incubated on ice for additional 5 min. Subsequently, 950 μ l of LB medium (Roth, Darmstadt, Germany) were added to the tube and cells were incubated at 37°C for 1 h under at 250 rpm. 50 μ l of transformed sample was plated on LB agar containing the appropriate antibiotic. In addition, the remaining 950 μ l were concentrated to 50 μ l via centrifugation and plated separately. After an overnight incubation at 37°C, single colonies were picked and screened for the presence of the insert (2.2.11).

2.2.10 Transformation of *N. gonorrhoeae*

For transformation in *N. gonorrhoeae*, 5 µl of a PCR reaction, 500 ng plasmid DNA or 5 µg genomic DNA were applied to GC agar. When a strain carrying an IPTG-inducible *recA* allele was to be transformed, the GC agar was supplemented with 1 mM IPTG. After the added DNA sample had dried on the agar, cells were spread on the spot where DNA had been added previously. After overnight incubation at 37 °C and 5 % CO₂, cells were harvested and resuspended in 50 µl of GC. The suspension, as well as its 1:10⁻² and 1:10⁻⁴ dilutions were plated on GC agar containing the appropriate antibiotics. After 24 - 48 h at 37°C and 5% CO₂, single colonies were picked and spread on another GC plate containing the antibiotic. The plate was incubated overnight at 37°C and 5% CO₂. After outgrowth, the clones were screened for the presence of the insert by colony PCR (2.2.11). Genomic DNA for the positive clones was amplified by PCR and sequenced (2.2.12). Clones carrying the correct sequence were converted to stocks in a 10% non-fat milk powder (Roth, Darmstadt, Germany) solution.

2.2.11 Colony PCR

A portion of a bacterial colony was picked with a sterile 1 µl inoculation syringe and transferred to a tube, containing 20 µl of water. The sample was incubated at 95°C for 10 min. An aliquot of 1 µl of the cell lysates was used as a DNA template for PCR. To determine the correct position and orientation of the insert, a combination of gene-, vector- and insert-specific primers were used.

For analysis of some genomic loci of *N. gonorrhoeae*, it was necessary to apply a different procedure to obtain amplifiable DNA [237]. The cells were resuspended in 100 µl PBS and mixed with 455 µl EtNA extraction solution (2.1). The mixture was incubated at 80°C for 10 min. After centrifugation at 16000 x g for 10 min, the supernatant was removed and 100 µl EtNA resuspension solution (2.1) was added. An aliquot of 1 µl of the product was used in PCR as described above.

2.2.12 Sequencing

Sanger sequencing of plasmids and PCR products from genomic DNA was carried out by GATC Biotech AG, Konstanz, Germany to verify the exact sequence of the insert. For this purpose, purified plasmid DNA (2.2.1) or purified PCR products were dissolved in 10 mM Tris-HCl (pH 8) according to the sequencing service's instructions. The sequencing primer was added and the sequencing reaction by GATC was started within 48 h.

2.3 Bacterial strains, growth conditions and selection conditions

N. gonorrhoeae was grown at 37°C and 5% CO₂ on agar plates containing GC agar (2.1). In transformation assays, Antibiotics and IPTG were used at the following concentrations: 50 µg/ml kanamycin (Roth), 50 µg/ml apramycin (Sigma-Aldrich), 2.5 µg/ml erythromycin (Sigma-Aldrich), 10 µg/ml chloramphenicol (Roth), 40 µg/ml spectinomycin (Sigma-Aldrich), 2 µg/ml tetracyclin (Roth), 1 mM IPTG (Roth).

Table 2.1: *N. gonorrhoeae* strains used in this work

Strain	Relevant genotype	Source/Reference	strains collection entry
N400	<i>recA6ind(tetM)</i>	[238] [239]	Ng003
GP117	<i>recA6ind(tetM)</i> <i>iga::P_{pilE}comP erm^R</i>	[226]	Ng033
GV1	<i>recA6ind(tetM) pilVfs (G-1)</i>	[240]	Ng005
<i>ΔpilQΔpilV</i>	<i>pilQ::m-Tn3cm</i> <i>recA6ind(tetM) pilVfs</i>	This work, [241]	Ng055
<i>ΔpilTΔpilV</i>	<i>pilT::m-Tn3cm</i> <i>recA6ind(tetM) pilVfs</i>	This work, [242]	Ng056

<i>ΔcomAΔpilV</i>	<i>comA::TnMax1 recA6ind(tetM) pilVfs</i>	This work, [120]	Ng098
<i>ΔcomE1ΔpilV</i>	<i>comE1::Apra recA6ind(tetM) pilVfs</i>	This work	Ng047
<i>ΔcomE2ΔpilV</i>	<i>comE2::Erm recA6ind(tetM) pilVfs</i>	This work*, [203]	Ng048
<i>ΔcomE3ΔpilV</i>	<i>comE3::Clm recA6ind(tetM) pilVfs</i>	This work*, [203]	Ng049
<i>ΔcomE4ΔpilV</i>	<i>comE4::Kan recA6ind(tetM) pilVfs</i>	This work*, [203]	Ng050
<i>ΔcomE34ΔpilV</i>	<i>comE4::Kan comE3::Clm recA6ind(tetM) pilVfs</i>	This work	Ng051
<i>ΔcomE234ΔpilV</i>	<i>comE4::Kan comE3::Clm comE2::Erm, recA6ind(tetM) pilVfs</i>	This work	Ng052
<i>ΔcomE1234ΔpilV</i>	<i>comE4::Kan, comE3::Clm, comE2::Erm, comE1::Apra recA6ind(tetM) pilVfs</i>	This work	Ng053
<i>comE-mcherry ΔpilV</i>	<i>pilE4-mcherry Kan recA6ind(tetM) pilVfs</i>	This work	Ng068
<i>Δnuc ΔpilV</i>	<i>nuc::Kan recA6ind(tetM) pilVfs</i>	This work	Ng058
<i>Δnuc</i>	<i>nuc::Kan</i>	This work	Ng164
<i>Δnuc ΔpilT ΔpilV</i>	<i>nuc::Kan pilT::m-Tn3cm recA6ind(tetM) pilVfs</i>	This work	Ng162
<i>Δnuc ΔpilQ ΔpilV</i>	<i>nuc::Kan pilQ::m-Tn3cm recA6ind(tetM) pilVfs</i>	This work	Ng1
<i>comA-mcherry</i>	<i>comA-mcherry Kan</i>	This work	Ng111
<i>ΔpilV comA-mcherry</i>	<i>comA-mcherry Kan recA6ind(tetM) pilVfs</i>	This work	Ng112
<i>dprA-eyfp</i>	<i>dprA-eyfp Erm</i>	This work	Ng113
<i>ΔpilV dprA-eyfp</i>	<i>dprA-eyfp Erm recA6ind(tetM) pilVfs</i>	This work	Ng114
<i>ΔdprA</i>	<i>dprA::Erm</i>	This work	-

2.4 Construction of mutant strains

2.4.1 Construction of $\Delta pilQ \Delta pilV$, $\Delta pilT \Delta pilV$, $\Delta comA \Delta pilV$

These strains were created by Stephanie Müller. $\Delta pilQ \Delta pilV$, $\Delta pilT \Delta pilV$ and $\Delta comA \Delta pilV$ were constructed by transforming genomic DNA from existing deletion mutants in the N400 background into GV1 ($\Delta pilV$) [243]. The genomic DNA was isolated from GQ21 [241], GT17 [229] and $\Delta comA$ (derived by transformation of N400 with the $\Delta comA$ allele originally detailed in Facius and Meyer 1993 [120]).

2.4.2 Construction of *comE* deletion strains

Single comE deletions. Genomic DNA of a complete knockout of all four *comE* copies in MS11 has been kindly provided by Ines Chen [203]. The genomic DNA was transformed into N400 and the cells were plated separately on the four different antibiotic markers: Erythromycin for $\Delta comE2$ (*ermC*, M13761.1), chloramphenicol for $\Delta comE3$ (*clmR*) and kanamycin for $\Delta comE4$ (*kanR*). The markers were assigned slightly differently compared to the publication cited above. Genomic DNA was isolated from $\Delta comE2$, $\Delta comE3$ and $\Delta comE4$ in the N400 background strains for further constructions of knockouts in GV1. The insertion of the Omega-fragment, which carries the spectinomycin resistance cassette, in $\Delta comE1$ resulted in a negative polar effect on the downstream *comP* [203], although *comP* is apparently not organized in an operon with *comE1*. The reason for the knockdown effect remains elusive, but possibly the large inserted Omega fragment and the distance between the stop-codon of the spectinomycin resistance gene to the following gene region downstream of *comE1* caused this strong polar effect. Hence, a non-polar knockout of *comE1* has been constructed in this work. For this, the apramycin resistance gene from pUC1813Apra was amplified using primers NG51 and NG52 and has been inserted directly into the start and stop codons of *comE1* using overlap extension PCRs with the amplified up and downstream regions of *comE1*. The GTG start codon of the apramycin resistance cassette has been replaced by the original *comE1* start codon ATG in this step. All regulatory units like the promoter regions or possible Shine-Dalgarno sequences

up or downstream of *comE1* should be preserved by this procedure. As the transformation of PCR-fragments, although containing the DUS, did not work with the *comE1*-knockout construct, the upstream region of *comE1* was amplified for the overlap extension PCR with primers NG53-2 and NG54 (Table 2.2), inserting a *EcoRI* restriction site into the fragment (Table 2.2, marked bold in NG53-2). In the downstream region, a *BamHI* restriction site (marked bold in NG56-2) was inserted by the amplification with primers NG55 and NG56-2. The restriction sites were necessary for the incorporation of the *comE1::Apra* fragment into the transformation vector pUP6. After fusing the *comE1* upstream and downstream PCR fragments with the apramycin resistance cassette using the outer primers NG53-2 and NG56-2, both the PCR-fragment and the backbone vector pUP6 were double digested with *EcoRI* and *BamHI*. Subsequently, the PCR fragment was ligated into the linearized plasmid after dephosphorylation of the 5'- sticky endings of pUP6. The construct was transformed into GV1 and cells were selected on apramycin.

Gradual comE deletions. For the construction of multiple *comE* knockouts, the genomic DNA of these single knockouts in GV1 was isolated. Then, a successive transformation of genomic DNA produced the following gradual knockouts: $\Delta comE4/3$ by transforming genomic DNA from $\Delta comE3$ into $\Delta comE4$; $\Delta comE4/E3/E2$ by transforming $\Delta comE2$ into $\Delta comE4/E3$; and finally, $\Delta comE4/E3/E2/E1$ by transforming $\Delta comE1$ into $\Delta comE4/E3/E2$.

All single and gradual *comE* knockout strains were controlled via PCR for the correct genotype in all four *comE* loci after transformation and selection on the respective antibiotic markers. The upstream regions of the *comE* loci are homologous to each other up to approximately 6000bp (according to the sequence from strain FA1090), so the same primer, NG2, was always used as upstream primer for all *comE* loci. For this reason, special care was taken that the downstream primers bind very specifically to the respective downstream *comE* loci. In particular, *comE1* is the only locus with no homologue region to the other three *comE*-loci directly after the stop codon, whereas *comE2*, *comE3* and *comE4* share the same downstream sequence up to approximately 150bp, *comE2* and *comE4* even up to 350bp. Thus, all downstream primers were designed at least 600bp downstream of the respective *comE* stop codon. These primers were NG23 for *comE1*, NG24-2 for *comE2*, NG25 for *comE3* and NG26 for *comE4*.

2.4.3 Construction of a *comE-mcherry* fusion strain

ComE4 was selected to be replaced with a C-terminal fusion construct of *comE* and *mcherry*, connected by a (PS)₄ spacer. For this purpose, a PCR construct was designed, comprising the *comE-mcherry* fusion, an antibiotic resistance cassette and the 5' and 3' flanking regions of the *comE4* locus required for homologous recombination. The *comE*-ORF and its 5' flanking region was amplified by PCR using primers KHpam1 and KHpam2imp. The coding sequence for mCherry was amplified from *pGCC4-mcherry* (provided by Nadzeya Kouzel) by primers KHpam3 and KHpam4 (Table 2.2), introducing the spacer at the 5' end. The kanamycin resistance cassette was amplified from *pUP6* by KHpam5 and KHpam6, introducing a Shine-Dalgarno sequence at its 5' end. The 3' region of ComE4 was amplified by primers KHpam7 and KHpam8. All fragments were joined together by fusion PCR to the construct, which was directly transformed into *N. gonorrhoeae* GV1. To verify the correct insertion of the construct, colony PCR of single clones was performed using primers NG2 and NG26. The PCR product was used as a template for sequencing of the recombinant *comE-mcherry* construct.

2.4.4 Construction of a *nuc* deletion strain

This strain was created by Heike Gangel. The *nuc* deletion strain was generated by an in-frame replacement of the *nuc* ORF by the short *kanR* ORF. A 504 bp fragment upstream of the *nuc* ORF was generated using primers HG3 and HG4 (Table 2.2). The *kanR* ORF from pUP6 was amplified using primers HG1 and HG2. A 564 bp fragment downstream of the *nuc* ORF was generated using primers HG5a and HG6. The three fragments were joined by fusion PCR using primers HG3 and HG6. The PCR product was purified and subsequently amplified using primers HG11 and HG12. After purification, GV1 was transformed with the PCR product, resulting in a replacement of the *nuc* ORF by the *kanR* ORF ($\Delta nuc \Delta pilV$). The transformants were selected on GC agar containing kanamycin. Insertion was verified by PCR using primers HG3 and HG6 and sequencing of the purified PCR product.

2.4.5 Construction of a *comA-mcherry* fusion strain

Similarly to ComE, a strain expressing ComA with C-terminally fused with mCherry was constructed. For this purpose, the C-terminal 515bp of the *comA* ORF were amplified using primers NGCH125 and NGCH126_2 (Table 2.2). The *mcherry* ORF was amplified from GV1 *comE-mcherry* genomic DNA by primers NGCH127 and NGCH169. The kanamycin resistance cassette was amplified using primers NGCH170 and NGCH132. Finally, the 3'-UTR of *comA* was amplified using primers NGCH133 and NGCH134. The primers were designed to insert a (PS)₄ spacer between *comA* and *mcherry* and a DUS at the 5' end. Additionally, an artificial promoter was introduced upstream of the *kanR* cassette to ensure effective selection. The artificial promoter sequence was obtained from the promoter of *comE* as identified using an online tool provided by the Berkeley Drosophila Genome Project [244]. The putative Shine-Dalgarno sequence could not be identified and was replaced by the one for *pilE*. The four fragments were joined by fusion PCR, the fusion product was transformed into MS11 and transformants were selected on kanamycin. To obtain a *ΔpilV comA-mcherry* strain, genomic DNA of MS11 *comA-mcherry* was isolated and transformed into GV1, transformants were selected on kanamycin. Insertion into the genome was verified by PCR using primers NGCH165 and NGCH134. The construct was verified by sequencing using primer NGCH195.

2.4.6 Construction of a *dprA-yfp* fusion strain

The 387bp C-terminal end of the *dprA* ORF was amplified using primers NGCH173 and NGCH174 (Table 2.2). A 1580bp region from *pIGA-eyfp-ermC* (provided by Nadzeya Kouzel) containing *eyfp* and *ermR* under a separate promoter was amplified by NGCH175 and NGCH178. Finally, the 3' UTR of *dprA* was amplified using primers NGCH179 and NGCH180. The three fragments were joined by fusion PCR using primers NGCH173 and NGCH180. The primers were designed to separate *dprA* and *eyfp* by a (PS)₄ spacer and for the fragment to include the DUS at its 5' end. The PCR product was used for transformation of MS11 and transformants were selected on erythromycin. Insertion into the genome was verified by PCR using primers NGCH173 and NGCH180 and the construct was verified by sequencing with primers NGCH173 and NGCH175.

2.4.7 Construction of a *dprA* deletion strain

The *dprA* 5' UTR was amplified using primers NGCH196 and NGCH197 (Table 2.2). The *ermR* cassette was amplified from *pIGA-gfp-ermR* (created by Nadzeya Kouzel) using primers NGCH198 and NGCH199. Finally, the 3' UTR of *dprA* was amplified by primers NGCH200 and NGCH201. The three fragments were joined by fusion PCR using primers NGCH196 and NGCH201. The primers were designed to generate a DUS at the 5' end. The PCR product was transformed into MS11 and transformants were selected on erythromycin. Insertion into the genome was verified by PCR using primers NGCH196 and NGCH201.

Table 2.2: Primers and oligonucleotides used in this work

Primers	Sequence
NG51	5'-CAATACGAATGGCGAAAAGCCGAG-3'
NG52	5'-TCATGAGCTCAGCCAATCGACTG-3'
NG53-2	5' GCGAATTC ATGCCGTCTGAAGCCCGTGAGGCTTGACTCTAT-3'
NG54	5'CTCGGCTTTTCGCCATTTCGTATTGCATGGTTTTTCTTTAAGGGTTGCAAAC-3'
NG55	5'-CAGTCGATTGGCTGAGCTCATGAAGTGGGAAATATGCATACTGCTGAATG-3'
NG56-2	5'- GCGGATCC ATGCCGTCTGAACCATCAAGGCGGAAAACCGCAC-3'
NG2	5'-ATGGCGGGACGGCATCTGTAC-3'
NG23	5'-CAGCAGGACAAGGTTTCGCGATG-3'
NG24-2	5'-GCAAAAGGAGCTTGCCTTGAACAGC-3'
NG25	5'-CCGATCGAACAATACCTGAACCGTC-3'
NGCH001	5'-ATGCCGTCTGAACGGTTTAAGGCGTTTCCGTTCTTC-3'
NGCH002	5'-CGGTTTAAGGCGTTTCCGTTCTTC-3'
NGCH003	5'-GGCATAACCATTTTATGACGGCGG-3'
NGCH005	5'-CATCACCATCCGTCGGCAACC-3'
NGCH008	5'-CCGTTTTTTCGTCTCGTCGCTGG-3'
NGCH009	5'-CGACGAATTTTCGCCGCCCC-3'
NGCH120	5'-CGACGAATTTTCGCCGCCCC-3'
NGCH125	5'-ATGCCGTCTGAAGGATTTATGCCGGACAGCCGG-3'
NGCH126_2	5'-GACGGAGATGGTCACTCAAACGGTTTTTTTCTGCCAATAG-3'

Construction of mutant strains

NGCH127	5'-CCGTTTGAGTGACCATCTCCGTCACCATCGCC-3'
NGCH132	5'-GCCTTCCCCTTCAGAAGAAGCTCGTCAAGAAGGCG-3'
NGCH133	5'-CGAGTTCTTCTGAACGGGAAGGCTGGTGCCG-3'
NGCH134	5'-ATGCCGTCTGAAGAACGCTTCCGCCGCCTC-3'
NGCH162	5'-TGTGAAGGCGATGTATG-3'
NGCH165	5'-TTTGGATCCATGCCGTCTGAAGATTTTCGAGTTTTTGAGGCCGTCTG-3'
NGCH169	5'GGGTCAATTCTAAAATGAATATCCCAAAGTTTCAAGCCGTTTCACTTGTACAGCT CGTCCATGCC-3'
NGCH170	5'-GAAACTTTGGGATATTCATTTTAGAATGACCCGTTTTATAGCAGGAGTAATTT TATGATTGAACAAGATGGATTGCACGCAG-3'
NGCH171	Cy5 -5'-CTCCTGACTGTTTCGCGCCCAGAATAAAAATCCATCGCTGACTGCGTATCCA GCTCACTCTCAATGGTGGCGGCATACATCGCCTTACATTCAGACGGCAT-3'
NGCH172	5'-CTCCTGACTGTTTCGCGCCCAGAATAAAAATCCATCGC[T-Atto647N]GACTGCGT ATCCAGCTCACTCTCAATGGTGGCGGCATACATCGCCTTACATTCAGACGGCAT -3'
NGCH173	5'-ATGCCGTCTGAACACAGCAAAGGCTGCCACAAACTG-3'
NGCH174	5'-GGCGATGGTGACGGAGATGGAGTTCGGATACGCTGGTATCTGCC-3'
NGCH175	5'-CCATCTCCGTCACCATCGCCTTCAATGGTGAGCAAGGGCGAGGAG-3'
NGCH178	5'-CTTAATATAAAGTGCCTGGATGCAGTTTATGCATCCCTTAACTTAC-3'
NGCH180	5'-ATGCCGTCTGAACGGGCAGCTCGCTCTTGTGTTG-3'
NGCH195	5'-CGAAACGGCATTGAGGAACACGC-3'
NGCH196	5'-ATGCCGTCTGAAGTCGTGACAACGCTGCTGCTG-3'
NGCH197	5'-CTTATAAAATTAGTATAATTATAGCACTTGAGCTCCCATCCCCTTACGATTC CAGACG-3'
NGCH198	5'-GGGAGCTCAAGTGCTATAATTATACTAATTTTATAAGGAG-3'
NGCH199	5'-CATTCGTGTTCCGGATGCAGTTTATGCATCCCTTAACTTAC-3'
NGCH200	5'-CATAAACTGCATCCGGAACACGAATGACCGAAGTCATCG-3'
NGCH201	5'-ATGCCGTCTGAAGATGTGCATGAGCGCGTGGATG-3'
NGCH_L01	5'-CGCGGTAATCAGGGTGGCGACCTCTTGGCTGGCGAGCATTTTTTCAAACGTC CTTTTTTCGACGTTCAAATTTTACCTTTGAGCGGCAAATCGCTTGAATTTGCG GTCGCGGCCCTGCATGGCGGAACCGCCTGCGGAGTTGCCCTCGACGAGGTAGAG TTCAGACAGGGCAGGGTCTTTTTCTTGGCAGTCGGCGAGTTGCCGGGCAGTCCC AAGCCGTCCATCACGCCTTTGCGGGGGGTGATTTTCGCGGGCTTTGCGGGCGGCTT CGCGTGCGCGGGCGGCTTCAGACGGCAT -3'
KHpam1	5'-GGATCCATGCCGTCTGAACGTCGCAAGATGCGG-3'

KHpam2imp	5'TGAAGGCGATGGTGACGGAGATGGTTTTTTAACCGCAGGCAGCACCGGTTTGG CGGG-3'
KHpam3	5'-CCATCTCCGTCACCATCGCCTTCAATGGTGAGCAAGGGCGAGG-3'
KHpam4	5'-TTATTCTCCTAGTTAGTCACTTGTACAGCTCGTCCATGCCG-3'
KHpam5	5'CTGTACAAGTGACTAACTAGGAGGAATAAATGATTGAACAAGATGGATTGCTC GCAG-3'
KHpam6	5'-CCCCTTCCTTTACAGGTTCCCTATCAGAAGAAGTTCGTCAAGAAGGCGATAG- 3'
KHpam7	5'-TAGGGGAACCTGTAAAGGAAGGGGCATCGGCTGCCGCCGGC-3'
KHpam8	5'-GAATTCTTGCTTCCACCCTTCG-3'
KH33	5'- ATGCCGTCTGAAGCCGCCCGCACGC-3'
KH34	5'- CGCGGTAATCAGGGTGGCGAC-3'
HG1	5'-ATGGCTAAAATGAGAATATCACCGGAATTGAAAAAACTG-3'
HG2	5'-CTAAAACAATTCATCCAGTAAAATATAATATTTTATTTTCTCCCAATCAG -3'
HG3	5'-ATGCCGTCTGAAGTCCCTGAACGAAGTGTCCGGTTTG -3'
HG4	5'-CAGTTTTTTCAATTCCGGTGATATTCTCATTTTAGCCATCTCTGAACCGGAT TTCAGACGGCATC-3'
HG5a	5'-CTGATTGGGAGAAAATAAAATATTATATTTTACTGGATGAATTGTTTTAGAGA CACCGCACGGCCTTGAACG-3'
HG6	5'-ATGCCGTCTGAACCCGAGTTGGCGATCAGTGCC-3'
HG11	5'-ACTGCCCGTGGAAGCCGTTCG-3'
HG12	5'-GGACGAAAAACGGAAACCACACATACG-3'

2.5 Preparation of fluorescently labeled DNA

2.5.1 Preparation of continuously labeled DNA fragments

Fragments for DNA uptake were amplified from λ -DNA (Roche, Rotkreuz, Switzerland) by PCR. The forward primer was either containing or lagging a DUS (NGCH001 and NGCH002). The fragment length was defined by the reverse primers, yielding fragments

of 300 bp, 1 kbp, 6 kbp, 10 kbp by use of primers NGCH003, NGCH005, NGCH008, NGCH009 respectively (Table 2.2). The covalent attachment of Cy3 and Cy5 dyes to DNA was achieved with the help of the *Label IT Nucleic Acid Labeling Kits* (Mirus Bio, Madison, WI, USA). According to the manufacturer, the Label IT reagent is bound by a reactive alkylating group to any reactive heteroatom of the DNA without altering the structure of the nucleic acid. The labeling reagent, labeling buffer and 5 μ g of DNA were mixed in Milli-Q-H₂O to a total volume of 50 μ l according to the manufacturer's protocol with a 1:1 (v/w) ratio of Label IT reagent to DNA. The incubation time at 37°C was elongated to 2 h to improve the labeling density. The samples were purified subsequently by using the provided microspin columns. For comparative quantifications, only labeled DNA from the same labelling reaction was used.

2.5.2 DNA fragments with a single fluorophore

For a more accurate quantification of DNA uptake, oligonucleotides carrying a single fluorophore were purchased from Sigma-Aldrich (St. Louis, MO, USA). The sequence was derived from 100bp stretch of λ DNA. The oligonucleotide NGCH171 carried a Cyanine-5 modification at its 5' end, while NGCH172 carried a covalent modification of the internal thymidine at position 37 by Atto647N. Double-stranded DNA fragments were obtained by hybridization with complementary sequences. For this, a labeled oligonucleotide and its unlabeled complementary oligonucleotide were mixed in annealing buffer (2.1). Subsequently, the following program was run in a thermocycler:

Temperature [°C]	Time[min]
95	2:00
85	2:00
75	2:00
65	2:00
55	2:00
45	2:00
35	2:00

Hybridization of the complementary strand to an ssDNA fragment with a single dye molecule attached did not significantly affect the fluorescence intensity. Spectroscopic analysis of the fluorescence intensity showed a difference of less than 8 % between ssDNA and dsDNA both carrying a single dye.

2.6 DNA uptake assays

Several bacterial colonies of 16 h – 20 h old cultures grown on GC-agar were resuspended with a 10 μ l inoculation syringe in 100 μ l DNA-uptake-medium (2.1) to an OD₆₀₀ of 0.1. Fluorescently labeled dsDNA was added to the cell suspension to a final concentration of 1 ng/ μ l. For entirely or partially single stranded DNA, the molar equivalent to 1 ng/ μ l dsDNA was added. The cells were incubated with DNA at 37°C with 5% CO₂ and subsequently treated with 10 U DNase I (recombinant, Thermo Scientific, Waltham, MA, USA) for further 15min at 37°C. 50 μ l of this dilution were applied to cover slips for microscopic analysis. For each comparative experiment, the different strains or conditions were characterized on the same day using the same stock of labeled DNA. Each condition was characterized independently on at least three different days.

2.7 Microscopy and quantitative analysis of single-cell fluorescence

2.7.1 Image acquisition

Fluorescence microscopy was conducted with two experimental settings. Firstly, fluorescence quantification and real-time experiments were conducted at an inverted microscope (Eclipse TE2000 *Nikon*) in epi-fluorescence mode at 37°. A 120 W metal halogenide fluorescence lamp (X-Cite, *EXFO*) served as illumination source. Images were

taken with an EMCCD camera (Cascade II:512, *Photometrics*). The 100x oil immersion CFI Plan Fluor objective (NA 1.3, *Nikon*) was used in all applications. Secondly, fluorescence quantification, ComE-mCherry / Cy5-DNA co-localization and single molecule fluorescence experiments were conducted at an inverted microscope (TI-E *Nikon*) at room temperature. A 120 W metal halogenide fluorescence lamp (Intensilight *Nikon*) served as illumination source. Images were taken with an EMCCD camera (IXON X3897 *Andor*). A 100x oil immersion CFI apochromat TIRF objective (NA 1.49, *Nikon*) was used. Day to day variations in the brightness of the fluorescence lamp were detected by using the test beads on the *Focal Check Fluorescence Microscope Test Slide #3 (Invitrogen)*. The intensities from day to day stayed relatively stable with no more deviations than $\pm 10\%$. A correction factor to this reference intensity was calculated for every day and was applied to the respective data sets.

2.7.2 Quantification of fluorescent DNA import at the single cell level

Cells were analyzed using routines written in MATLAB by Enno Oldewurtel. Bacteria were automatically detected in the bright-field channel and accepted or rejected depending on shape and distance to the nearest neighbors. Thus, positions of individual single mono- or diplococci were found. Optionally, the automatic selection was further refined manually (Figure 2.1a, b). Each cell was assigned a 30x30 pixels large region of interest (ROI). The pixel intensities I inside a ROI were fitted with a Gaussian function, $g(I) = a \cdot \exp(-(I - I_{back})^2/b^2)$, to determine the local background. After background subtraction by shifting the distribution by $-I_{back}$ the sum over the pixel intensities gives a measure for the total single cell fluorescence (Figure 2.1c). This routine allowed to quickly analyze a large number of cells and gain information over the total fluorescence of each cell, irrespective of a strongly localized or weakly diffusive distribution.

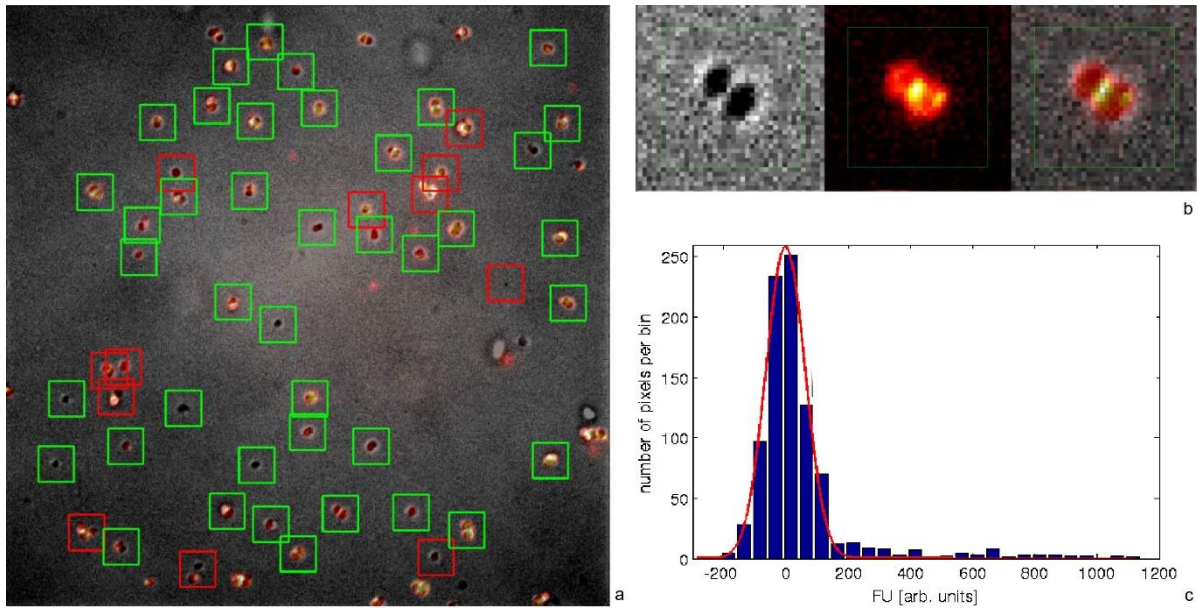


Figure 2.1 Quantification of single cell fluorescence. a) Cells are automatically detected in the bright-field channel and accepted (green squares) or rejected (red squares) depending on shape or distance to neighbors. b) Regions of interest (ROIs) of size 30x30 pixel are taken about the center of each bacterium for single cell analysis. Left: brightfield, center: fluorescence, right: merge. c) Blue bars: Histogram of intensity of individual pixels in ROI (30x30). The local background is determined by a gauss fit over the intensity distribution inside each ROI (red line). After background subtraction the sum over all pixel values inside a ROI gives the value for single cell fluorescence. Image adapted from [245].

2.8 Real-time quantification of DNA import and degradation

Cells selected for piliation were grown on a GC agar plate for < 20 h, harvested, resuspended in DNA-uptake-medium (2.1). If DNA uptake was to be recorded for less than 20 min, the OD_{600} was adjusted to 0.1 and pre-warmed to 37°C. DNA was added at a concentration of 1 ng/ μ l. 50 μ l of this dilution were applied to cover slides for microscopic analysis. If the observation times were greater than 20 min, oxygen depletion in the medium was a point of concern. Therefore, the cells were adjusted to $OD_{600} = 0.01-0.02$. 150 μ l of the suspension were applied to a polystyrene-coated coverslip inside an open microscopy chamber to ensure oxygen supply. The cells were incubated for 10 min on the microscope stage to settle. Under these conditions, the cells are more motile than in a sealed specimen. This enables the cells to aggregate to microcolonies, which was suppressed by the prior reduction of the OD_{600} . Subsequently, 1.4 μ g of 300 bp labeled DNA diluted in 100 μ l DNA-uptake-medium was added and DNA uptake was recorded. To remove DNA bound to the exterior of the cells, 10 U/ml of

DNaseI (*Fermentas*) was added and fluorescence intensity was recorded for another 15 min. To monitor degradation of imported DNA, cells were adjusted to $OD_{600} = 0.1$ and incubated with 1 ng/ μ l dsDNA for 1h at 37°C and 250 rpm. Subsequently, DNA was removed by washing with DNA uptake medium twice and incubation with 10 U/ml of DNaseI for another 15 min at 37°C and 250 rpm. After DNA removal, 50 μ l of the sample were applied to a glass cover slip and monitored for 60 min at 37°C.

2.9 Duplex PCR for investigating degradation of DNA in the periplasm.

Cells grown on GC-agar for 16-10 h were resuspended in 500 μ l of DNA uptake medium (2.1) to an OD_{600} of 0.1, incubated with 1 ng/ μ l 10 kbp PCR fragment containing a single DUS at 37°C for 60 min and treated with DNaseI (10 U/ml, Fermentas) for 15 min. To test for degradation over a larger timescale, DNaseI incubation time was extended. To remove DNase along with residual DNA, the samples were vortexed for 3 min and washed in DNA-uptake-medium several times. The pellets were resuspended in MilliQ-H₂O and incubated at 98°C for 5 min, vortexed shortly and pelleted at 13000 rpm for 5 min. The supernatant was stored at -20°C or immediately used for the PCR reaction. PCR was carried out using DreamTaq MasterMix (Thermo Scientific, Waltham, MA). Genomic DNA was amplified using primers NG2 and NG23, while PCR fragment was amplified using primers NGCH002 and B260, yielding a 3 kbp PCR product (Table 2.2). The ratio between genomic and fragment primers in the PCR sample was 1:15. In the GV1 background, the annealing temperature was increased to 65°C to suppress the formation of unspecific PCR artifacts.

2.10 Transformation assays

Cell cultures of MS11 wt grown for 16 h on GC agar were harvested in GC uptake medium (2.1) and diluted to OD₆₀₀ 0.2. Application of transformation medium (2.1) was not necessary, as *recA* was constantly being expressed in those cells. MgCl₂ is a cofactor in DNA uptake and strongly increases the transformation efficiency. 500 µl of the cell suspension were mixed with 2.5 µg of the transformation plasmid pSY6, isolated from *Escherichia coli* DH5α-pSY6 by a plasmid maxi-preparation or 45 pmol of a synthetic DNA fragment, and was incubated for 30 min at 37° C at 250 rpm. Afterwards, the cell and DNA mixture was diluted by adding it to 2ml transformation medium in cell culture flasks with ventilation caps. The cell culture flasks were incubated for 3 h at 37° C and 250 rpm at 5% CO₂. The above mentioned pSY6 is a transformation plasmid containing the DNA uptake sequence and a modified gyrase-B-subunit, leading to nalidixic acid resistance only when the subunit is incorporated into the genome. The synthetic fragments are either double or single stranded and consist of the 300 bp stretch flanking the mutation in pSY6, which confers the nalidixic acid resistance, as well as a terminal DUS to support DNA uptake. After incubation, the cells were resuspended in 200 µl of transformation medium, which corresponds to a dilution factor of 10⁰. Finally, 50 µl of several serial dilutions were evenly spread on GC agar plates (dilutions 10⁻⁵, 10⁻⁶, 10⁻⁷ & 10⁻⁸) and on GC agar plates with 2 µg/ml nalidixic acid (dilutions 10⁻⁴, 10⁻⁵, 10⁻⁶ & 10⁻⁷ for pSY6; 10⁰, 10⁻¹, 10⁻² & 10⁻³ for synthetic DNA fragments) respectively. The cells were grown for further 45 h at 37° C at 5 % CO₂ before the number of colonies on each plate was counted separately.

2.11 Preparation of biotinylated DNA fragments for optical tweezers assays

A 10 kbp fragment from λ DNA (Invitrogen) was amplified by LongAmp polymerase (NEB) using primer 5'- ATGCCGTCTGAACAGGTGGTAAGCACTTCCTGCTC (Sigma-Aldrich) containing the DUS and primer 5'-[Btn]AAAA[BtndT]TT[BtndT]CCGGTTT-

AAGGCGTTTCCGTTCTTCTTCGTCATAAC (Sigma-Aldrich) containing three biotin modifications (Figure 2.2). The PCR sample was precipitated at RT using 0.1 volumes of 3M sodium acetate pH5 and 0.7 volumes of isopropanol. After precipitation, the DNA was washed with 70% ethanol at RT and resuspended in buffer EB (Qiagen) to yield a concentration of 0.5 to 1 $\mu\text{g}/\mu\text{l}$. The DNA was stored in solution at 4°C.



Figure 2.2 The DNA fragment attached to the beads is a 10 kbp PCR derivative of λ DNA. On one end 3 biotin residues are introduced as part of the PCR primer, one covalently attached to the 5'-end and two more covalently attached to thymines within the primer sequence. On the opposite end, a DUS is introduced in order to face away from the bead and to be recognized for DNA uptake.

2.12 Preparation of DNA coated beads for optical tweezers assays

40 μl 2.0 μm streptavidine-coated polystyrene beads (Kisker) were washed with 400 μl DNA coupling buffer (2.1) three times. Subsequently, the washed beads were resuspended in 40 μl DNA coupling buffer and incubated with 2 μg of biotinylated DNA overnight at 4°C head-over-tail. To remove unbound DNA, the DNA-coated beads were washed 4 times with PBS pH 7.45 (2.1) and stored head-over-tail at 4 °C.

2.13 Laser tweezers setup and data analysis

The sample was mounted on a temperature-controlled microscope (37°C) (Zeiss Axiovert 200). The optical tweezers setup was described before [199]. In brief, positional data

of the bead trapped in the laser beam were acquired at 20-kHz time resolution with a four-quadrant photodiode (QPD). Positional data was verified by recording videos at 10 Hz and subsequent tracking of both bead and bacterium using a MatLab routine employing a Hough grid [246, 247]. Force feedback was activated after the force reached a preprogrammed level, and the position of the piezo table was adjusted so that the force remained constant but controllable by the user. The trap stiffness was calibrated by the power spectrum analysis of the bead's Brownian motion and verified by the viscous drag method. Data from the stage movement were down-sampled to 20 data points per second by MatLab routines, leading to velocity values for 50 ms intervals after differentiation. Each data point in Figure 3.17 depicts the average velocity between two consecutive changes of the external force as illustrated in Figure 3.16. As data on bead displacement obtained from video tracking was more reliable compared to QPD data, it was used to calculate the actual forces for the evaluation.

2.14 Data acquisition of DNA uptake in the optical tweezers assay

After 24h growth, 10 piliated colonies were picked and transferred to a new plate. After 16-20h of growth, about 5 clones were picked and resuspended in 100 μ l DNA uptake retraction assay medium (2.1). The DNA coated beads were diluted 1:5 in PBS (2.1) and 1 μ l of beads was mixed with 20 μ l of bacterial suspension and mounted on the optical tweezers setup. A bead was trapped in the optical tweezers and placed next to a diplococcus. After 10-30 s it was slowly removed from the cell in 100 nm steps. If a persistent deflection of the bead due to a binding event could be detected, the acquisition was started. Force clamp mode at a starting force of 10 pN was triggered automatically, either instantly due to the initial deflection of the bead or eventually due to the increased deflection by further moving the bead away from the cell. If DNA uptake could not be readily detected, the force was decreased stepwise down to 2 pN. If DNA uptake did not start upon decreasing the force, it was increased to extract DNA potentially already taken up into the periplasm. Once DNA could be successfully extracted, the force was decreased again to observe uptake. An attempt was ceased, if extraction of DNA failed or the extracted DNA could not be re-imported. During DNA uptake, the force was varied

to observe DNA uptake or extraction velocity at different forces. DNA uptake at a constant force was monitored for up to 30 s, depending on a reasonable time frame for the observed velocity. Ideally, varying forces were applied such that they permitted multiple rounds of extraction and elongation of a single DNA fragment.

3 Results

The results part of my thesis is divided in three sections. In section 3.1, we seek to gather more information about the mechanism of DNA uptake over the outer membrane. To this end, we characterize the spatio-temporal dynamics of imported DNA and the periplasmic DNA binding protein ComE. We find that ComE binds to DNA at the site of DNA uptake and determines the DNA capacity of the periplasm in a gene-dosage dependent manner. In section 3.2, we test whether ComE is directly involved in the DNA uptake process by measuring the force-velocity relationship of DNA uptake at different ComE concentrations. We compare our results to the theoretical predictions for a translocation ratchet mechanism and conclude that it fits our observations. In section 3.3, we seek to clarify whether both DUS-specific binding and unspecific transport are efficient during uptake of single-stranded DNA.

3.1 Concerted spatio-temporal dynamics of imported DNA and ComE DNA uptake protein during gonococcal transformation

In the case of Gram negative systems, a key step of transformation is the import of DNA across the outer membrane. Although various factors are known to affect DNA transport, little is known about the dynamics of the DNA import process. In this section, we try to answer the following central questions about the DNA uptake process: 1. How efficient is DNA uptake over the outer membrane? 2. Are there specific sites associated with DNA import as seen in

Gram positive species? 3. How stable is DNA after import into the periplasm? 4. Are DNA uptake events over the outer and inner membrane spatially coupled? To answer these questions, we monitor the uptake of both fluorescently labeled and native DNA and characterize the interaction of DNA with the periplasmic DNA binding protein ComE. The results presented in this section are my contribution to the following publication, unless stated differently in the text:

Gangel*, H., Hepp*, C., Müller*, S. et al. *Concerted spatio-temporal dynamics of imported DNA and ComE DNA uptake protein during gonococcal transformation. PLoS Pathogens*, 2014. 10(4): p. e1004043. [245].

3.1.1 *N. gonorrhoeae* imports Cy3-DNA in a DNase-resistant state

First, we investigated whether Cy3-DNA could be used to study DNA uptake in gonococci. The experiments described in this subsection 3.1.1 were performed by Stephanie Müller. DNA was labeled randomly along its entire contour (2.5.1). Throughout this work, we used a *recA_{ind}* background without induction to prevent the cells from antigenic variation of *pilE* (Table 2.1, Ng003). The *recA_{ind}* strain will be labeled wt in the following, since it shows wt behavior in terms of DNA import through the cell envelope. Wt cells were associated with fluorescent foci that were clearly distinguishable from the fluorescence background (Figure 3.1), indicating that Cy3-DNA was imported into a DNase-resistant state.

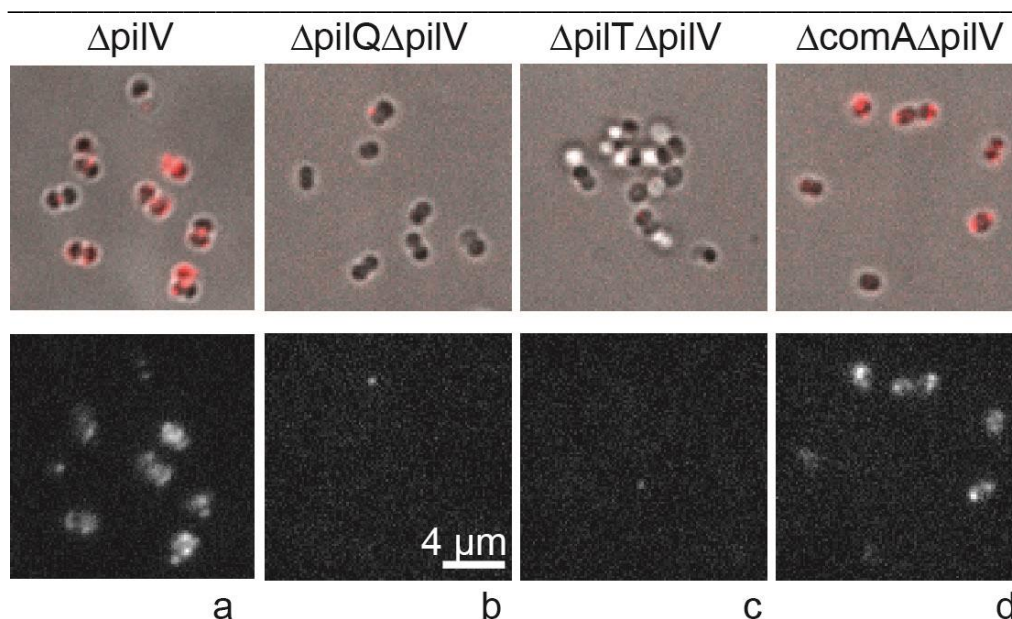


Figure 3.1 The minor pilins PilV and ComP differentially influence the amount of imported Cy3-DNA. **Upper line: merged images of brightfield and fluorescence, lower line: fluorescence images.** Gonococci were incubated with Cy3-DNA for 30 min and subsequently treated with DNase. a) wt with enhanced contrast, b) wt with contrast adjusted to c, d. c) $P_{pilE}COMP$, d) $\Delta pilV$. Image adapted from [245].

The minor pilins ComP and PilV have been shown to strongly affect DNA uptake at the level of DNA binding [175, 226]. Following the uptake of Cy3-DNA, both strains showed a strongly increased fluorescence signal (Figure 3.1b-d), indicating that more Cy3-DNA was imported within 30 min. Since the high signal of the $\Delta pilV$ strain was very convenient for data analysis, we performed all following experiments in this background.

To determine the background level of fluorescence, we repeated the experiment using a strain with a deletion in the retraction ATPase PilT (Table 2.1, Ng056) which is unable to import DNA [226]. Furthermore, we investigated a $pilQ$ deletion strain (Table 2.1, Ng055) that does not form the outer membrane pore, is thus deficient in DNA uptake. Upon incubation with Cy3-DNA, both strains showed a drastic reduction in fluorescence signal.

Moreover, we investigated whether import of Cy3-DNA into a DNase-resistant state was dependent on the putative inner membrane channel formed by ComA. When repeating the DNA uptake experiment using a $comA$ deletion strain ($\Delta comA \Delta pilV$, Table 2.1, Ng098) we found that the fluorescence distribution was not significantly different from the $\Delta pilV$ strain, indicating that the imported DNA accumulated in the periplasm. This result was analogous to what was observed previously for *H. pylori* [230].

Transformation of *N. gonorrhoeae* depends on the DNA uptake sequence (DUS). ComP has been shown to be a positive effector of sequence-specific DNA binding and that it is directly involved in binding of DUS-containing DNA [226][114]. The DNA uptake assay with fragments lacking the DUS showed strongly reduced fluorescence. Thus, the uptake of Cy3-DNA was strongly enhanced by the DUS.

We conclude that Cy3-DNA is imported into the periplasm of gonococci and that DUS-related import is dependent on the outer membrane channel formed by PilQ as well as the T4P retraction ATPase PilT, but not on the inner membrane channel ComA. Since these results are consistent with previous DNA uptake studies using radioactively labeled DNA, they validate our method for studying DNA uptake in *N. gonorrhoeae* using Cy3-DNA. In contrast to the classic method using radioactively labeled DNA, our approach enables us to study DNA uptake at the single cell level and thus reveals strong cell-to-cell variability in terms of the total amount of DNA imported after 30min.

3.1.2 The periplasm of *N. gonorrhoeae* can retain ample amounts of DNA

Up until now, DNA uptake by *N. gonorrhoeae* has been investigated at the population level. Therefore, it is unclear whether there is heterogeneity in this process at the level of single cells. To investigate any potential for heterogeneity, we measured the distribution of DNA uptake efficiencies of individual cells. We incubated gonococci with the 300 bp, 1 kbp and 10 kbp Cy3 fragments for 60 min, treated the cells with DNase and subsequently quantified the fluorescence intensity of individual cells (Figure 3.2). We found that the distribution of fluorescence intensities was very broad (Figure 3.2). A fraction of cells showed no import of DNA and this fraction was variable between different experiments.

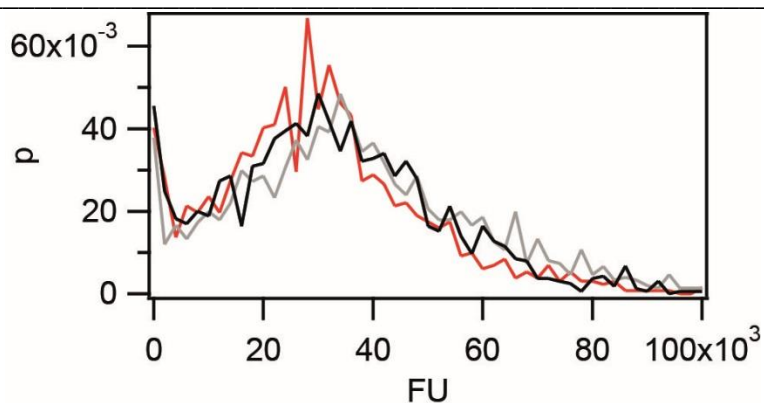


Figure 3.2 The amount of imported Cy3-DNA after 1 h is independent of fragment length. Probability distribution of the total fluorescence intensity of individual cells with a length of 300 bp (red), 1 kbp (grey), 10 kbp (black). ($N > 1300$ for each condition). Image adapted from [245].

We investigated whether the periplasm acts as a reservoir for imported DNA. *ApilV* cells were incubated with Cy3-DNA for 1 h, treated with DNase and subsequently single cell fluorescence was measured. The total fluorescence intensity per cell did not vary when incubated with Cy3-DNA with fragment lengths of 0.3 kbp, 1 kbp, and 10 kbp at equimolar concentrations (Figure 3.2), indicating that the total amount of imported DNA was independent of fragment length. To convert fluorescence intensity into amount of DNA, we quantified the fluorescence intensity of individual 6 kbp fragments (Fig. 3.3) [248] and compared them to the total fluorescence of individual cells that were incubated with Cy3-DNA from the same labeling reaction for 1 h. We found that the periplasm contained ~ 40 kbp of Cy3-DNA. We note that this value might be biased slightly by binding of proteins to the DNA in the periplasm [249]. Furthermore, the Cy3-labeling efficiency is somewhat variable and therefore the fluorescence intensity cannot be directly compared to other experiments using different Cy3-DNA stocks.

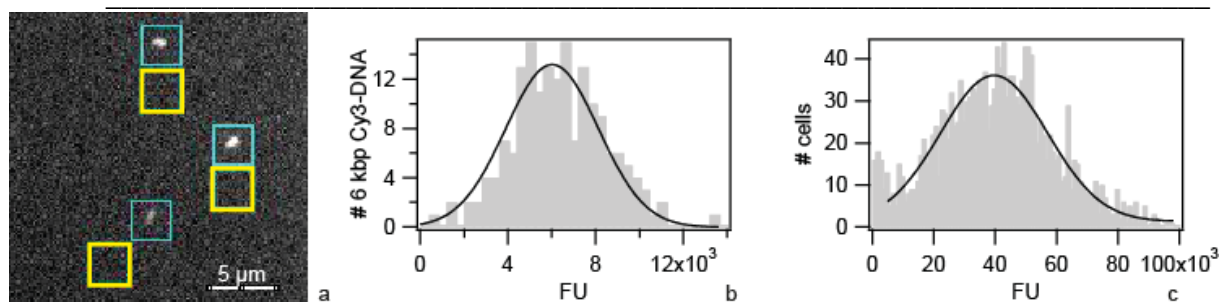


Fig. 3.3 Quantification of imported Cy3-DNA. a) Typical image of single 6 kbp Cy3-DNA fragments immobilized on a cationic lipid membrane [33]. Blue squares: ROI for fluorescence signal of single DNA fragment, yellow squares: ROI for background subtraction for adjacent DNA fragment. b) Grey: Distribution of fluorescence intensities of single 6 kbp Cy3-DNA. Full line: Gaussian fit with a center of mass of (6010 ± 120) FU. c) Grey: Distribution of single cell fluorescence after incubation of the *ΔpilV* strain with 6 kbp Cy3-DNA from the same batch for 1 h. Full line: Gaussian fit with a center of mass of (39621 ± 586) FU. Image adapted from [245].

Next, we examined the stability and integrity of the imported DNA. Cells were incubated with unlabeled 10 kbp fragments for 1 h, subsequently treated with DNase, and further incubated for various periods of time. Exploiting a protocol recently developed for *Vibrio cholerae* [250], we used duplex PCR with primer pairs against the newly imported 10 kbp fragment and against gDNA of gonococci. We found that the 3 kbp DNA fragments amplified from the imported DNA were clearly detectable even after 60 min after DNase treatment in *ΔpilV* and *ΔpilV ΔcomA* backgrounds (Figure 3.4). Using wt, the 3 kbp DNA fragments were still detectable after 30 min. Since the signal was lower for wt cells, we did not attempt to amplify DNA at later time points. This data shows that DNA import through the outer membrane occurs independently of inner membrane transport and that large amounts of DNA can be amassed in the periplasm over a time scale of hours.

Concerted spatio-temporal dynamics of imported DNA and ComE DNA uptake protein during gonococcal transformation

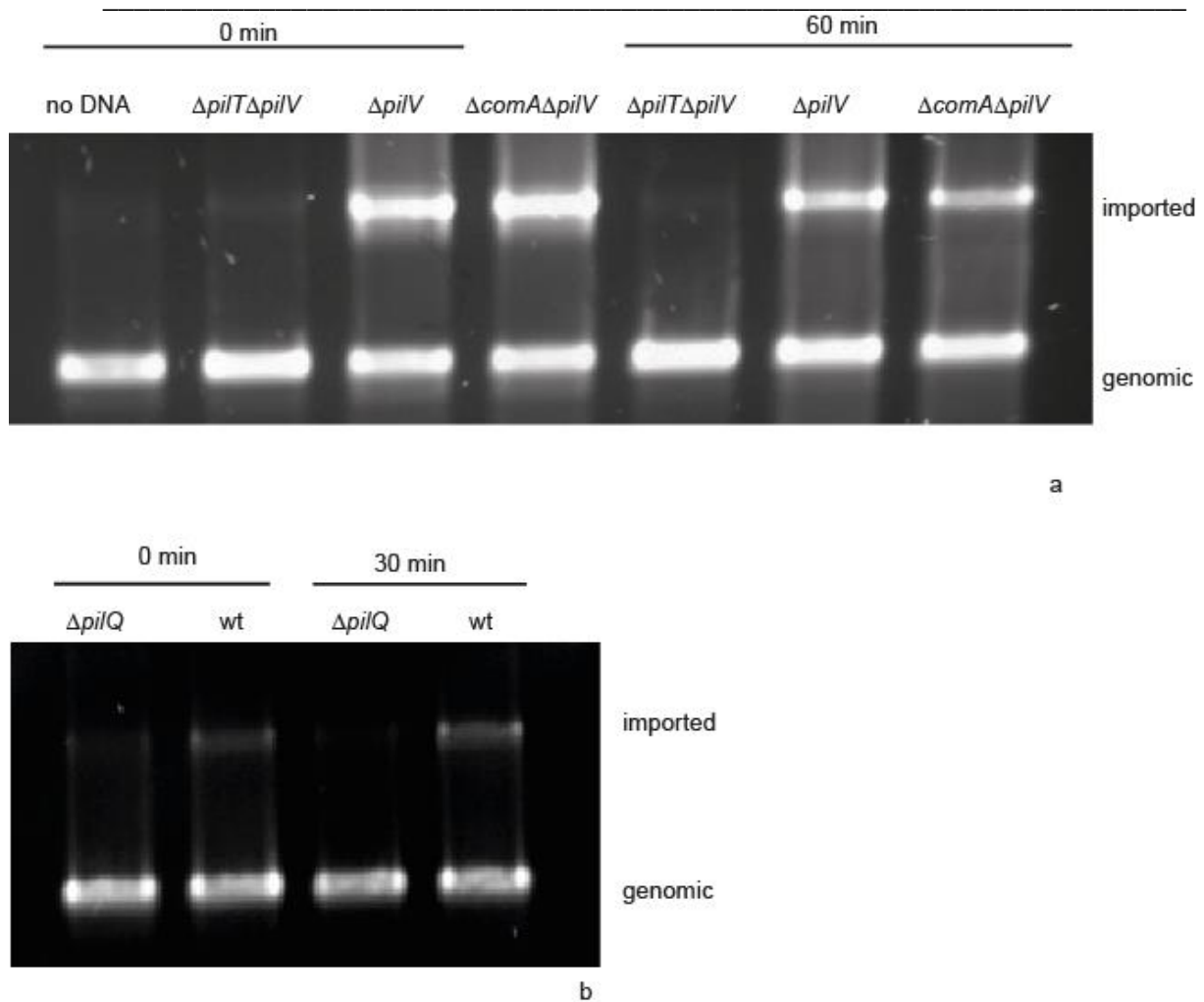


Figure 3.4 Duplex PCR of imported DNA. Imported DNA fragments were amplified at varying time periods after DNase treatment for a) $\Delta pilV$ b) wt. Image adapted from [245].

3.1.3 Kinetics of Cy3-DNA import into the periplasm

We next investigated the temporal dynamics of Cy3-DNA during DNA uptake by monitoring single $\Delta pilV$ cells during incubation with 300 bp Cy3-DNA in real-time. The fluorescence intensity per cell showed a saturating kinetics with $FU(t) = FU_{max}(1 - \exp(-t/\tau))$ with $\tau = (4.5 \pm 0.6)$ min (Figure 3.5a, b). FU_{max} is a measure for the total amount of Cy3-DNA that can be imported into the periplasm. Cy3-DNA tended to accumulate at the septa of diplococci. To test whether the kinetics characterized binding or import of Cy3-DNA, we repeated the experiment in $\Delta pilT\Delta pilV$ and $\Delta pilQ\Delta pilV$ backgrounds. During 30 min, we did not detect an increase in fluorescence intensity (Figure 3.5c), demonstrating that Cy3-DNA was imported with a characteristic time of 4.5 min in the $\Delta pilV$ strain.

In conclusion, the periplasm saturates with short Cy3-DNA fragments within minutes.

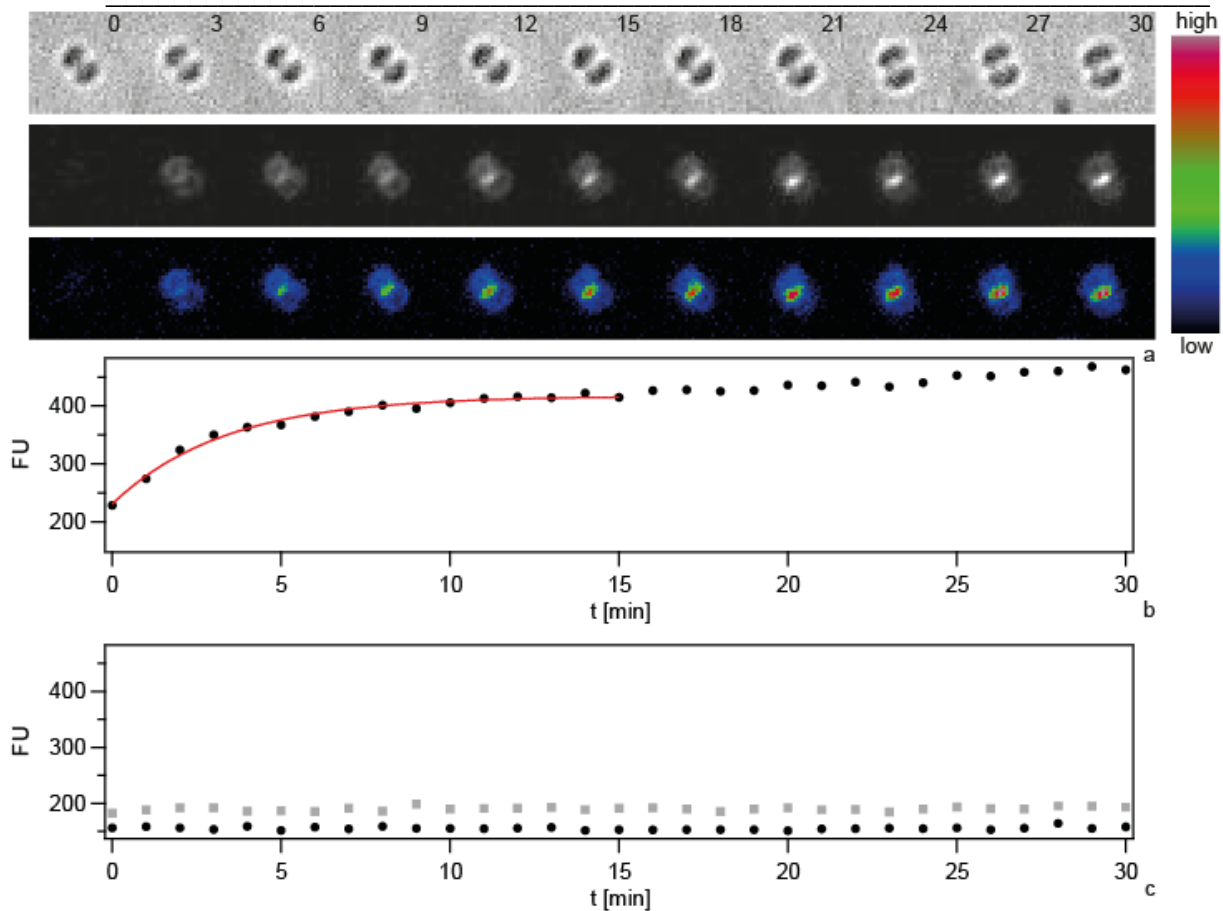


Figure 3.5 Dynamics of focus formation ($\Delta pilV$) with 300 bp fragments of Cy3-DNA. a) Time lapse of binding and import of Cy3-DNA. Upper line: brightfield image, middle line: fluorescence image, lower line: pseudocolored intensity image. b) Black circles: Fluorescence intensities of cells shown in a. Red line: Exponential fit. c) Fluorescence intensities of individual $\Delta pilQ\Delta pilV$ (black circles) and $\Delta pilT\Delta pilV$ (grey boxes). Image adapted from [245].

3.1.4 The periplasmatic DNA binding protein ComE quantitatively increases the amount of Cy3-DNA imported into the periplasm

It has been shown previously that ComE is necessary for DNA uptake into a DNase-resistant state and transformation [203]. The experimental work in this section was done in collaboration with Stephanie Müller. We investigated whether ComE acted by increasing the carrying capacity of the periplasm or by speeding up DNA import. To this end, we generated isogenic backgrounds varying in *comE* copy number. Since the amount of imported Cy3-DNA was similar for the backgrounds with four and three copies and for one or no *comE* copies (Figure 3.6), we concentrated on strains with two ($\Delta comE_{34}$) versus no ($\Delta comE_{1234}$) alleles in the following (Table 2.1, Ng051, Ng053). In a first set of experiments, we incubated $\Delta pilV$ cells

with 3 kbp DNA for variable amounts of time before treating them with DNase (Figure 3.7a, b). Comparing the patterns formed in $\Delta pilV$ and $\Delta comE_{34}\Delta pilV$ at various time points did not reveal a striking difference. For example, at 1 h both mutants showed multiple foci (Figure 3.7c, d). The kinetics could be well described by a single exponential function $FU(t) = FU_{max}(1 - \exp(-t/\tau))$ (Figure 3.7e). In the $\Delta comE_{34}\Delta pilV$ strain, that carries two copies of the *comE* gene, the capacity was decreased by a factor of ~ 3 as compared to the $\Delta pilV$ strain (Figure 3.7g). The complete *comE* deletion strain $\Delta comE_{1234}\Delta pilV$ showed a decrease of fluorescence intensity by a factor of ~ 24 . This reduction is similar to the reduction in a *pilQ* deletion strain in agreement with ComE being necessary for DNA uptake. We note, however, that residual fluorescence was observed in some cells. The characteristic time to saturation was $\tau = (100 \pm 17)$ min in $\Delta pilV$. If ComE would enhance the speed of DNA import, then we would expect that reduction of the ComE concentration leads to an increase in the characteristic time. Instead, we observed a decrease to $\tau = (62 \pm 12)$ min in $\Delta comE_{34}\Delta pilV$ (Figure 3.7f).

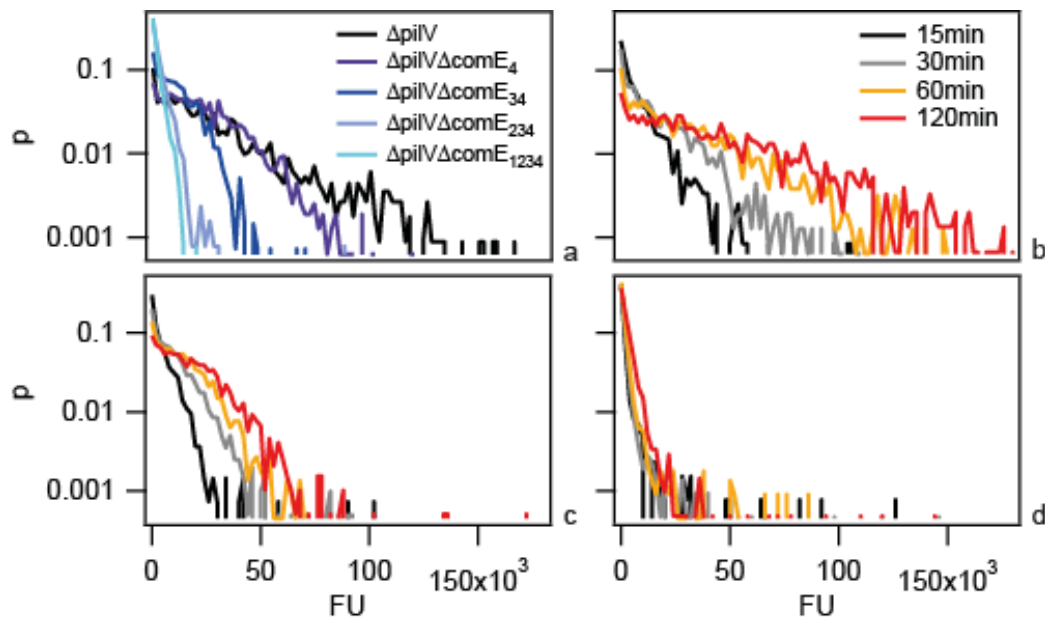


Figure 3.6 Fluorescence distribution of individual cells with varying *comE* expression. a) After 1 h incubation with 3 kbp Cy3-DNA. b) $\Delta pilV$ c) $\Delta pilV \Delta comE_{34}$ d) $\Delta pilV \Delta comE_{1234}$ after varying periods of incubation with 3 kbp Cy3-DNA. Image adapted from [245].

Concerted spatio-temporal dynamics of imported DNA and ComE DNA uptake protein during gonococcal transformation

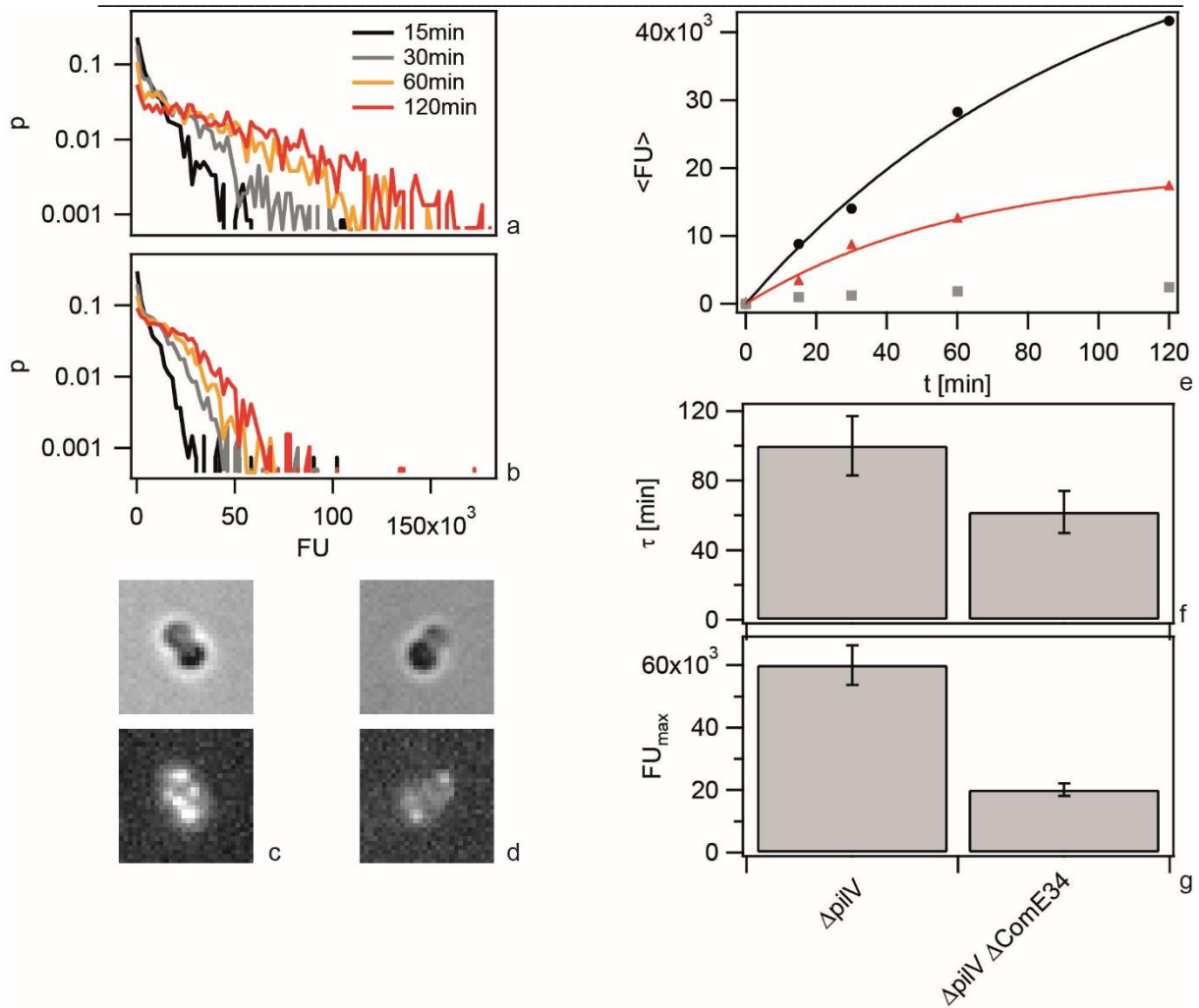


Figure 3.7 Dynamics of 3 kbp Cy3-DNA import depends on ComE. a, b) Probability distribution of the total fluorescence intensity of individual a) $\Delta pilV$ and b) $\Delta comE_{34}\Delta pilV$ as a function of time. c, d) Typical fluorescence images after 1 h for c) $\Delta pilV$ and d) $\Delta comE_{34}\Delta pilV$. e) Average fluorescence intensity per cell as a function of time with 3 kbp Cy3-DNA for $\Delta pilV$ (black circles), $\Delta comE_{34}\Delta pilV$ (red triangles), $\Delta comE_{1234}\Delta pilV$ (grey squares). Full lines: fits to exponential function. f) Saturation value for average fluorescence intensity per cell obtained from fits in e). g) Characteristic times obtained from fits in e). ($N > 1500$ for each condition). Image adapted from [245].

Since we found that ComE increased the carrying capacity of the periplasm, we tested whether ComE was necessary for importing very short DNA fragments of 100 nm. As Cy3-DNA import showed saturation within minutes, we quantified single cell fluorescence in real-time during incubation with 300 bp Cy3-DNA (Figure 3.8). We found that Cy3-DNA import of short fragments was dependent on ComE. A full *comE* null mutant did not show any increase in fluorescence, indicating that ComE was essential for Cy3-DNA import. The saturating fluorescence intensity F_{max} was strongly decreased in the $\Delta comE_{34}$ strain, confirming that ComE quantitatively controls the carrying capacity of the periplasm.

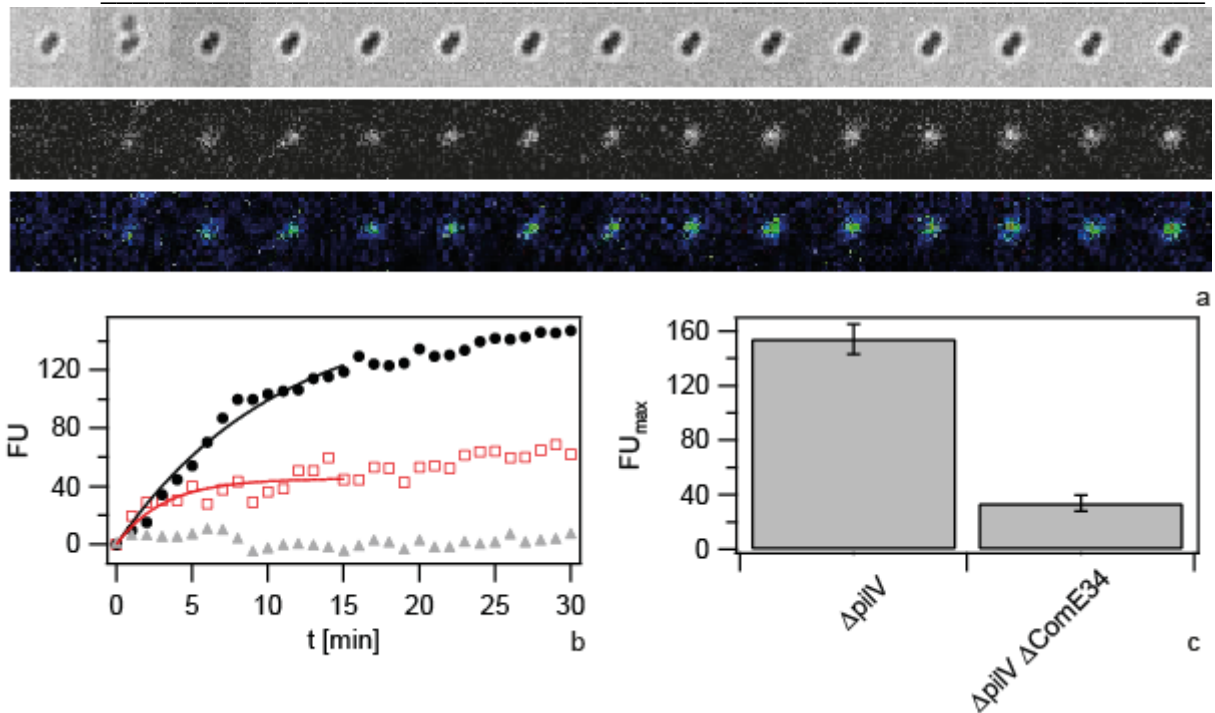


Figure 3.8 Dynamics of focus formation ($\Delta pilV$) with 10 kbp fragments of Cy3-DNA. a, c) Examples for time lapse of binding and import. Upper line: brightfield image, middle line: fluorescence image, lower line: pseudocolored intensity image. $\Delta t = 3$ min b, d) Fluorescence intensities of cells shown in a, c). e) Distribution of initial location of Cy3-DNA foci normalized to length of diplococcus. Black circles: Cy3-DNA, red squares: YOYO-DNA. Image adapted from [245].

3.1.5 ComE-mCherry relocates to DNA foci

As Cy3-DNA was not homogeneously distributed within the periplasm (Figure 3.1), it was investigated whether the periplasmic DNA-binding protein ComE co-localized with DNA. To this end, a strain was generated in which one of the *comE* genes was fused to an *mcherry* ORF (Table 2.1, Ng068). In the absence of transforming DNA, ComE-mCherry showed a mostly ring-like distribution, indicating that it was homogeneously distributed within the periplasm (Figure 3.9a). Some cells showed pronounced foci which were most often located at the septa between the cocci of diplococci. To test whether these foci arise from DNA that was present due to lysed cells, cells were incubated with DNase for 30 min and subsequently grown for three generations in liquid culture. Upon this treatment, the foci disappeared almost completely revealing homogeneous distribution of ComE-mCherry in the periplasm (Figure 3.9b, Figure 3.10a).

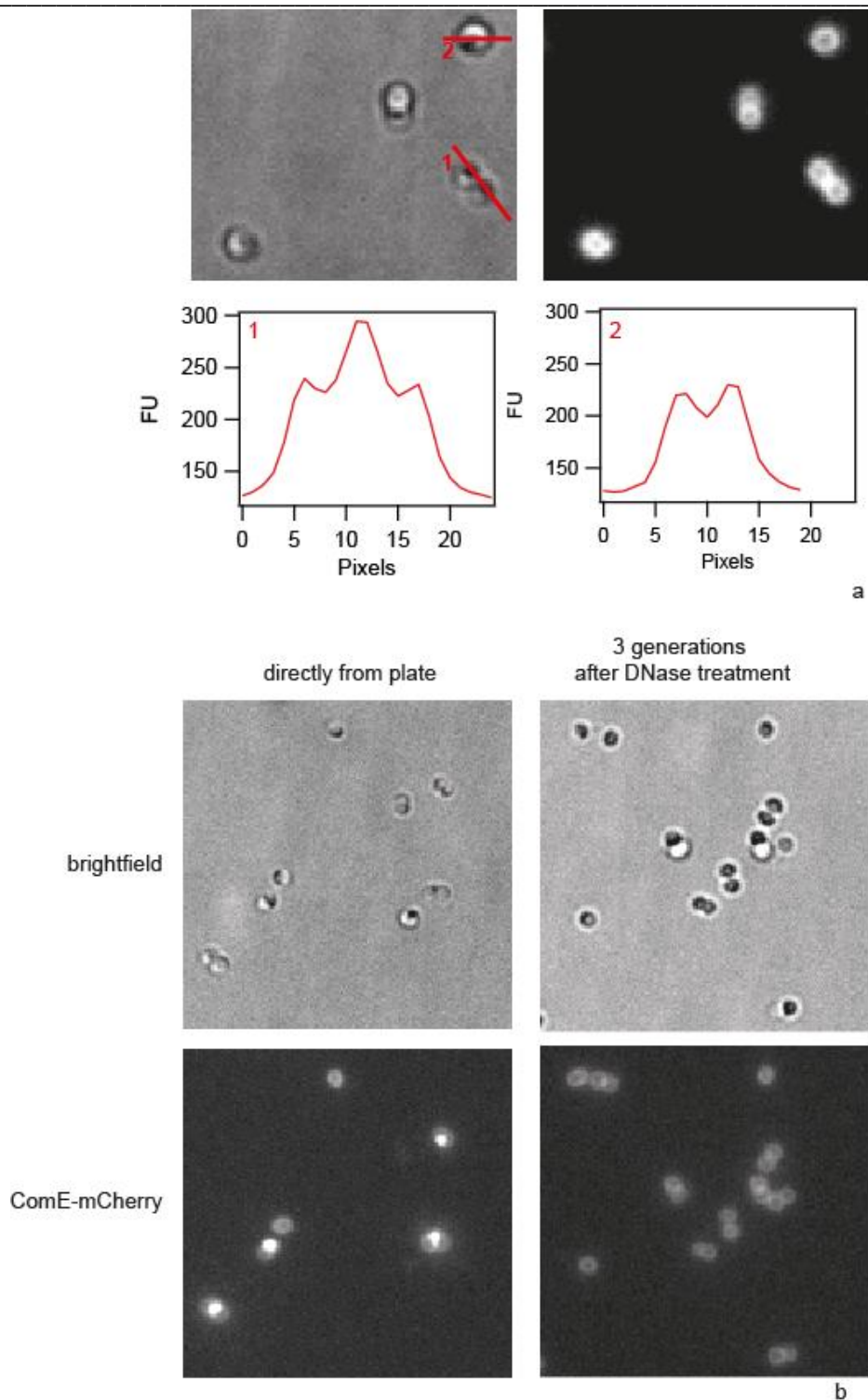


Figure 3.9 Distribution of ComE-mCherry in the absence of transforming DNA. a) Example of mCherry fluorescence and intensity plots through the fluorescence images along the two axes indicated in red. b) When cells were scratched from the agar plate and imaged directly, some cells showed foci which were most often located at the septum between the cocci. When cells were treated with DNase for 30min and subsequently grown for three generations, the foci disappeared almost completely. Image adapted from [245].

In the next step, we incubated the *comE-mcherry* $\Delta pilV$ cells with 3 kbp Cy5-DNA for 15 min. The distribution of mCherry fluorescence became spotty, often revealing distinct foci (Figure 3.10b, c), reminiscent of the fluorescence pattern generated by imported Cy5-DNA. The patterns of Cy5-DNA and ComE-mCherry were highly correlated, indicating co-localization between ComE and imported DNA (Figure 3.10b, c). Most cells that had little or no Cy5-DNA signal retained their ring-like ComE-mCherry fluorescence (e.g. Figure 3.10b inset).

In summary, ComE-mCherry is homogenously distributed in the periplasm in the absence of transforming DNA. Imported DNA forms foci in the periplasm and co-localization of ComE indicates that the periplasmic DNA interacts with ComE

Concerted spatio-temporal dynamics of imported DNA and ComE DNA uptake protein during gonococcal transformation

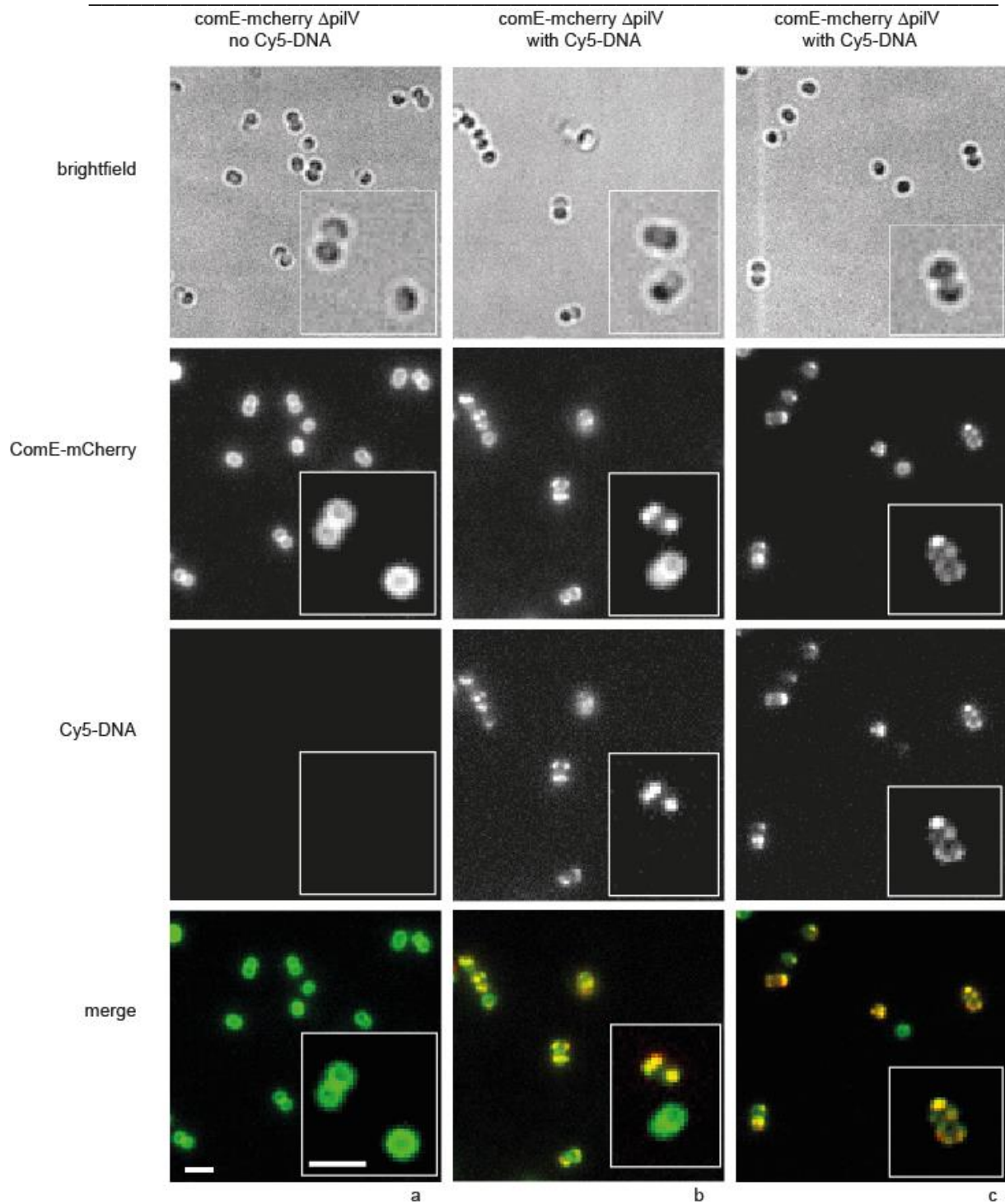


Figure 3.10 ComE-mCherry colocalizes with the spotty pattern of Cy5-DNA. *comE-mcherry* cells were incubated with a) no DNA, b, c) 10 kbp Cy5-DNA fragments for 15min and visualized. Scale bars: 2.5 μ m, insets: 2x magnification. Image adapted from [245].

3.1.6 Spatio-temporal dynamics of Cy3-DNA foci and ComE-mCherry in the periplasm.

We investigated the spatio-temporal dynamics of the foci/ spotty pattern of Cy3-DNA in the periplasm. To determine the initial location of Cy3-DNA after import, we acquired a time lapse of 10 kbp Cy3-DNA import. Individual 10 kbp Cy3-fragments are clearly visible (Fig. 3.3). Indeed, we observed the successive appearance of well-defined fluorescent spots correlated with a step-wise increase of fluorescence intensity (Figure 3.11a-d). These foci showed little movement over a time scale of 60 min. To investigate whether there was a preferred location of DNA import (as reported for *B. subtilis*), we projected the location of initial occurrence to the major axis of a diplococcus and normalized this distance to the cell length (1min time resolution). Only diplococci were analysed in order to find the location relative to the septum. We found no preferred location of DNA uptake (Figure 3.11e).

Concerted spatio-temporal dynamics of imported DNA and ComE DNA uptake protein during gonococcal transformation

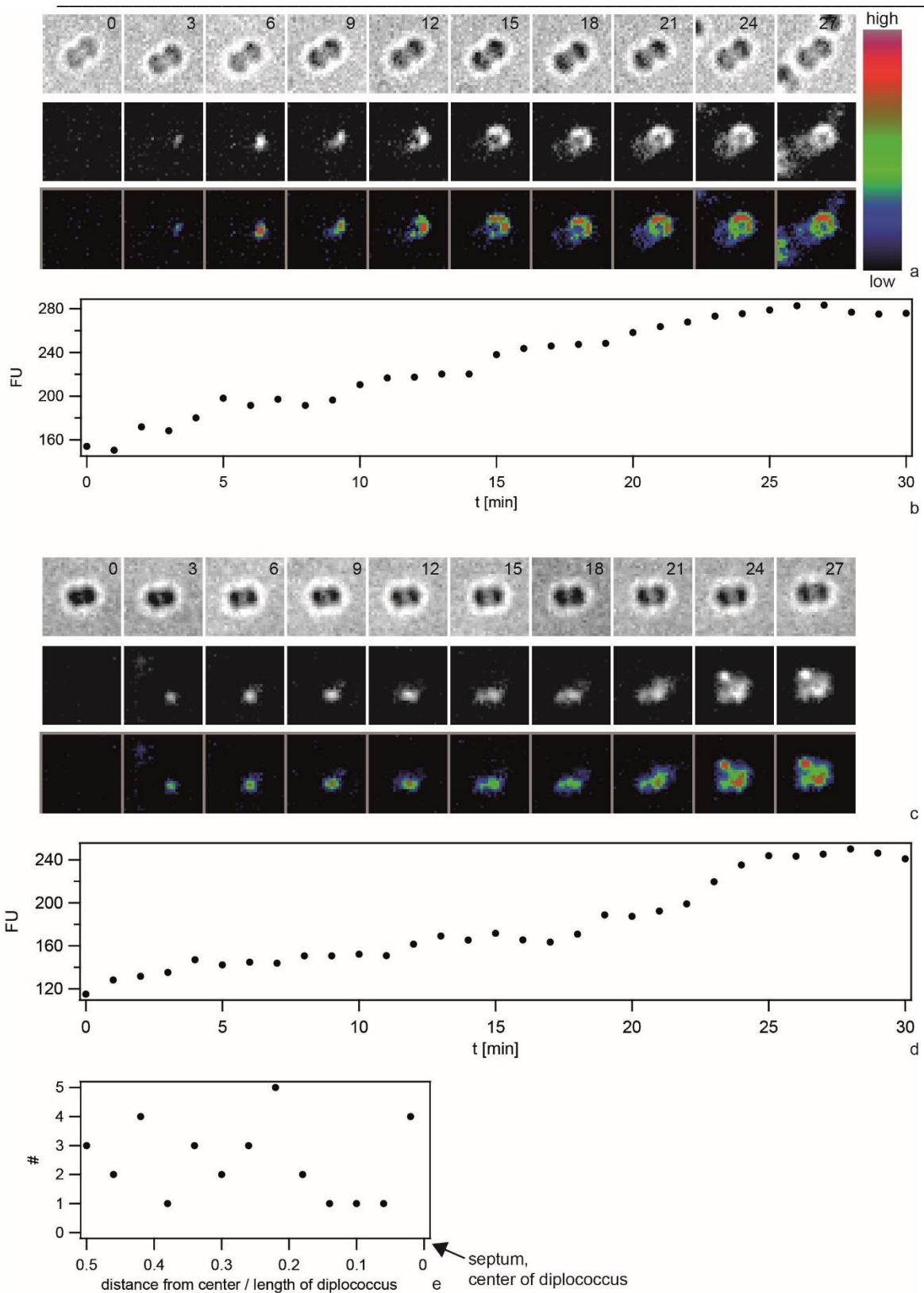


Figure 3.11 Dynamics of focus formation ($\Delta pilV$) with 10 kbp fragments of Cy3-DNA. a, c) Examples for time lapse of binding and import. Upper line: brightfield image, middle line: fluorescence image, lower line: pseudocolored intensity image. $\Delta t = 3$ min b, d) Fluorescence intensities of cells shown in a, c). e) Distribution of initial location of Cy3-DNA foci normalized to length of diplococcus. Image adapted from [245].

Next, we investigated the spatio-temporal dynamics of ComE-mCherry during exposure to unlabeled 10 kbp transforming DNA. These experiments were performed at 37°C and therefore the image quality was not comparable to Figure 3.10. Initially, the fluorescence intensity was homogeneous or ring-like (Figure 3.12). Spontaneously, the fluorescence accumulated to form a focus whereas the fluorescence in the remainder of the cell decayed. The intensity of the focus increased for ~ 10 min and was then stable. At 18 min, a second focus appeared again taking ~ 15 min to reach its maximum intensity. This second focus was stable for another 30 min. Monococci also formed stable multiple foci (data not shown). This experiment indicates that the formation of stable foci is not caused by fluorescence labeling of DNA.

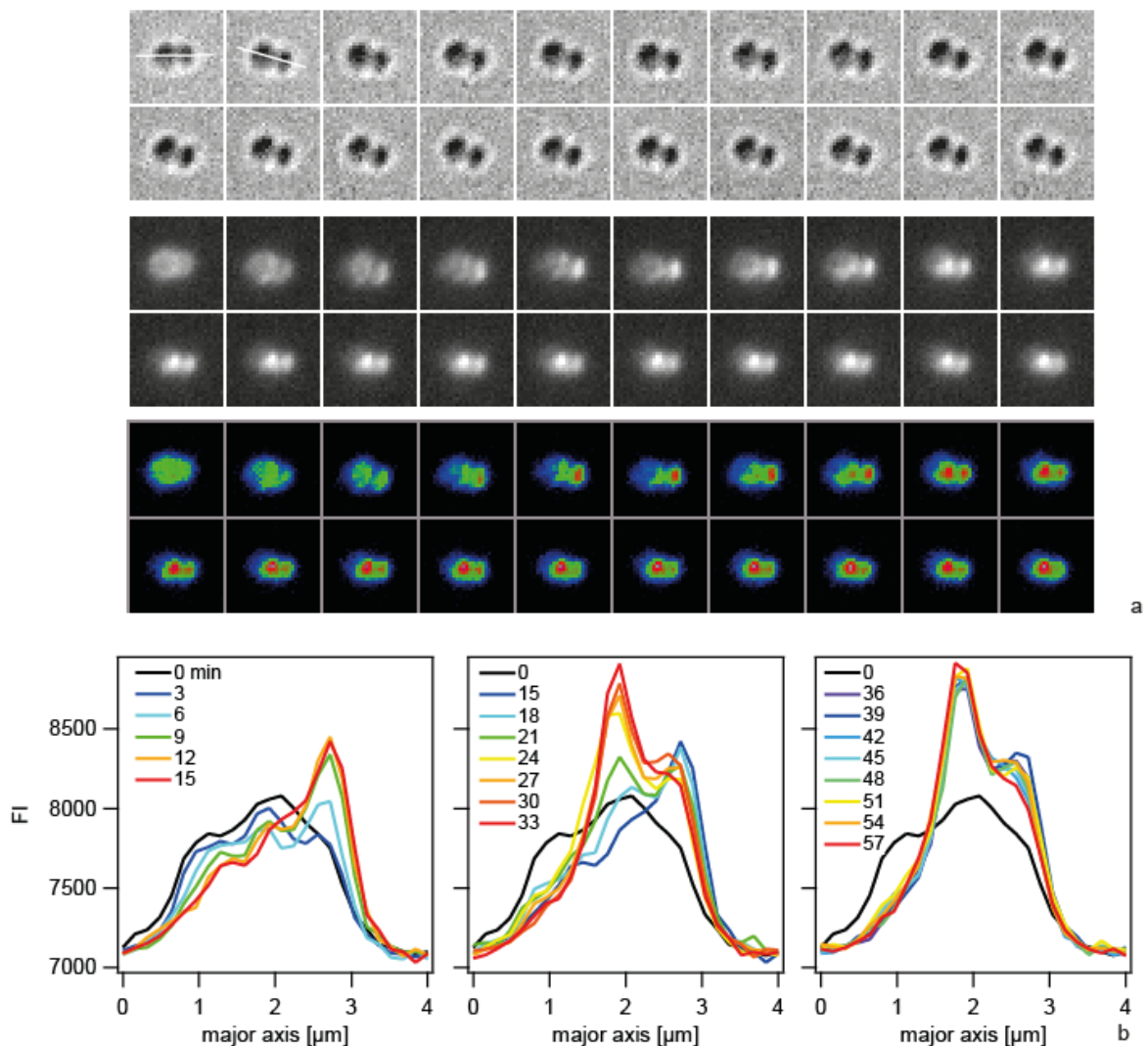


Figure 3.12 Spatio-temporal dynamics of ComE-mCherry upon addition of 10 kbp transforming DNA. a) Time-lapse of ComE-mCherry dynamics. Upper line: brightfield image, middle line: fluorescence image, lower line: pseudocolored intensity image. The line denotes the major axis. $\Delta t = 3$ min. b) Intensity profiles through the major axis at different time points. Image adapted from [245].

Additional experiments by Heike Gangel and Enno Oldewurtel demonstrated a redistribution of DNA towards the septa of diplococci, the duration of which depended on fragment length [245].

In summary, our data strongly suggests the following spatio-temporal dynamics. Transforming DNA is imported at random locations. DNA fragments form foci with associated ComE that are recruited at the septa. The time scale of recruitment depends on DNA length.

3.2 The kinetics of DNA uptake during transformation provide evidence for a translocation ratchet mechanism

In section 3.1, we have shown that DNA uptake over the outer membrane and its storage in the periplasm requires the type IV pilus machinery including the retraction ATPase and the periplasmic DNA binding protein ComE [245]. However, the mechanism generating the force to transport DNA over the outer membrane remains to be elucidated. We aim to solve this long-standing question by comparing the kinetics of DNA uptake with those of processes possibly involved its powering. To this end, we seek to measure the force-velocity relationship of DNA uptake by an optical tweezers assay and test whether it is influenced by the ComE concentration. We compare our experimental results to the force-velocity curve predicted by the theoretical model for a translocation ratchet [149]. Moreover, we compare our data with the experimentally determined force-velocity relationship of pilus retraction [251, 252]. The results presented in this section have been published in the following study:

Hepp, C. and B. Maier, Kinetics of DNA uptake during transformation provide evidence for a translocation ratchet mechanism. Proceedings of the National Academy of Sciences, 2016. [253]

3.2.1 DNA binding and uptake in the optical tweezers assay

We aimed at quantifying the velocity of DNA uptake at the single molecule level. To this end, we generated 10 kbp DNA fragments that contained the 12 bp DNA uptake sequence (DUS) [20] at one extremity and multiple biotin tags at the other end (2.11). Streptavidin-coated beads were incubated with the modified DNA as described (2.12). In the first step, we determined the binding probability of DNA to gonococci. To this end, a DNA-coated bead was

trapped in the optical trap and placed in close proximity to a diplococcus. After about 30 s, the trapped bead was moved away from the cell in 100 nm steps to test for deflection of the bead and thus binding (Figure 3.13a). A binding event was defined as a deflection of the bead from the center of the trap exceeding 20 pN. Roughly half of the attempts with wt cells resulted in DNA binding (Figure 3.13b). In all of our strains *recA* expression is repressed to inhibit gene conversion in the pilin locus [46]. Using uncoated beads that were treated like DNA-coated beads but without adding DNA, only 7 % of the attempts resulted in binding, indicating that binding was mostly specific to DNA. Next, we tested whether the presence of the minor pilin ComP affected the probability of binding. ComP was shown to bind specifically to the DUS [114] but its abundance within the pilus is low compared to the major pilin Pile. With our assay we found no significant difference in binding probability between a *comP* deletion strain and the wt (Figure 3.13b), in agreement with mostly unspecific binding of DNA to either T4P or the cell surface in general [254]. Finally, we investigated the binding probability to gonococci that had the gene for the minor pilin *pilV* deleted. *pilV* deletion is known to increase the binding and uptake probability [255]. With this strain, the binding probability was significantly higher than for wt (Figure 3.13b), suggesting that specific binding occurs more frequently.

The kinetics of DNA uptake during transformation provide evidence for a translocation ratchet mechanism

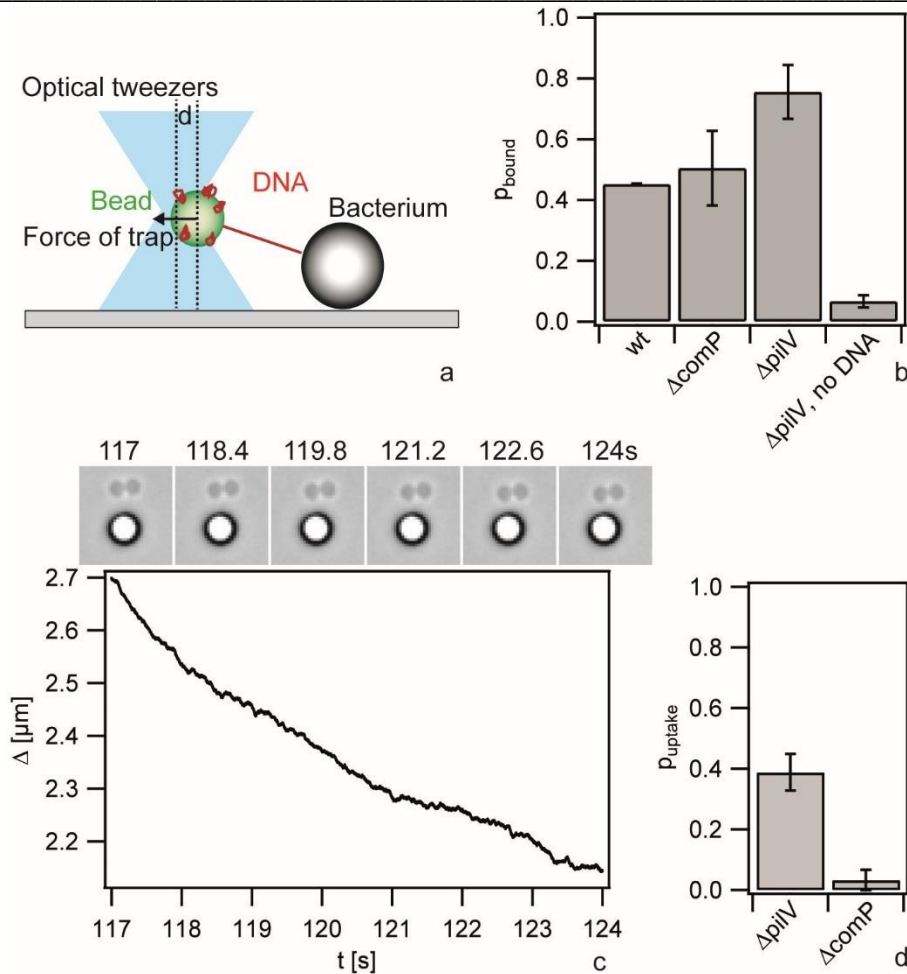


Figure 3.13 Probability of DNA binding and uptake. a) Scheme of the experimental setup. A bead coated with DNA is trapped in an optical trap and placed close to a bacterium. b) A binding event is defined as a deflection of the bead from the center of the trap exceeding 20 pN while the bead was moved away from the bacterium. Binding probability of wt (Ng003), ΔcomP (Ng031), ΔpilV (Ng005), and ΔpilV (Ng005) with plain beads. c) Typical DNA uptake event at $F = 4 \text{ pN}$. Upper image: Time lapse, lower image: distance Δ between bacterium and bead as a function of time. d) Probability of DNA uptake subsequent to binding with ΔpilV and ΔcomP . Image adapted from [253].

For the following reasons, the ΔpilV strain (Table 2.1, Ng005) was used to study DNA uptake. First, the binding probability is higher than for the wt, which did not show *comP* dependent binding in our tests. Second, it is known that the DNA uptake efficiency is drastically enhanced [255] and therefore the success rate of the single molecule experiment is much higher. Third, *pilV* deletion strongly inhibits surface motility compared to wt, which substantially benefits the assay. Finally, the binding and retraction probabilities of T4P to the beads are strongly reduced. Wt gonococci would bind to and retract beads at a frequency of $\sim 1 \text{ s}^{-1}$ [252] interfering with the quantification of DNA uptake.

We detected DNA uptake as follows. A DNA-coated bead was trapped in the laser trap. Subsequently, binding was tested as described above. If the deflected bead was at a distance sufficient for observing DNA uptake, the measurement was started at a force of 10 pN as determined by QPD detection. If necessary, the force was reduced to trigger DNA uptake. If DNA uptake could not be directly started, attempts to extract DNA possibly already imported into the cell, were made by applying higher forces (DNA extraction will be described in detail in Figure 3.16). If extraction was successful, the force was decreased once more to allow for re-uptake of the extracted DNA. A typical DNA uptake event at an external force of $F = 4\text{pN}$ is shown in Figure 3.13c. While DNA is imported, the length of the tether between the bead and the bacterium, Δ , shortens continuously. DNA uptake can be clearly distinguished from T4P retraction events because the speed is significantly lower. The speed of wt T4P retraction $v_{\Delta pilV}$ (8 pN) = (2050 ± 30) nm/s (Figure 3.14a) [252, 256]. To ensure that deletion of *pilV* did not affect the speed of T4P retraction, we characterized T4P retraction in the $\Delta pilV$ strain and found $v_{\Delta pilV}$ (8 pN) = (2010 ± 30) nm/s (Figure 3.14b) in agreement with the wt data.

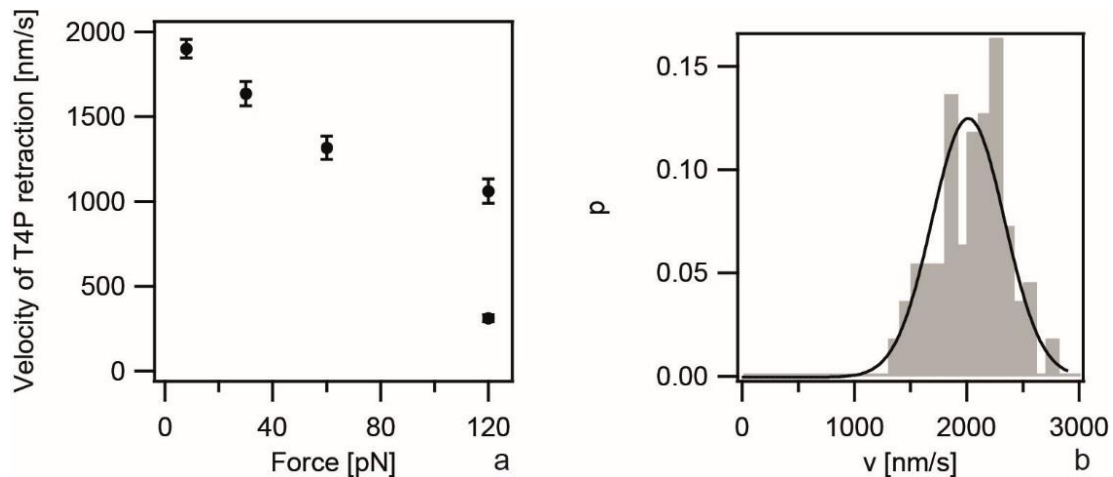


Figure 3.14 Velocity versus force relationship of T4P retraction. The speed of T4P retraction was determined by placing uncoated beads close to a bacterium at a force clamped to different values. Pili bound to the bead and the speed was measured during retraction as described in [251]. a) Average speed of T4P retraction at different forces of wt gonococci Data taken from [252]. b) Distribution of T4P retraction speeds at $F = 8\text{ pN}$ for $\Delta pilV$ (Ng005). Image adapted from [253].

As a control showing that the DNA uptake events observed were specific to the gonococcal DNA uptake system, we attempted to observe DNA tether shortening in a $\Delta comP$ strain. Deletion of *comP* has been shown to inhibit DNA uptake [254]. To this end, a DNA-

coated bead was trapped in the optical trap and placed adjacent to a diplococcus, followed by the procedure to establish DNA uptake described above. For each change of force, the bead was monitored for a sufficient amount of time to decide whether or not DNA uptake might have been started. While the probability that DNA binding resulted in uptake was $p_{\Delta pilV} = (0.39 \pm 0.06)$ for the $\Delta pilV$ strain (Figure 3.13d), the probability for the $\Delta comP$ strain was $p_{\Delta pilV} = (0.03 \pm 0.03)$, i.e. in agreement with full inhibition of DNA uptake.

The beads were coated with multiple DNA molecules to increase the probability of detecting a DNA-uptake event. Even so, only a fraction of $p_{DNAup} = 0.39$ of the binding events resulted in DNA uptake. The probability that two DNA molecules were taken up simultaneously would be $(p_{DNAup} \cdot p_{DNAbind})^2 = 0.09$. Here, the binding probability is most likely overestimated, because transient binding events were included in Figure 3.13b, but were not quantified for determining the DNA uptake probability (Figure 3.13d). Even if two uptake events had started within a short period of time, it would have been very unlikely that both uptake events were detected, because the DNA tethers would have different length and only the shortest tether would register. We conclude that less than 10 % of the analyzed DNA uptake events were caused by the import of more than one DNA molecule and that these events were very unlikely to impact on our data analysis in a significant way.

In summary, we were able to characterize the kinetics of gonococcal DNA uptake during transformation as a function of force at the level of single DNA molecules.

3.2.2 The velocity of DNA uptake depends on ComE

The periplasmic DNA-binding protein ComE is necessary for DNA import into the periplasm [257]. If ComE acted as a chaperone, biasing diffusion of DNA by binding, then its concentration would be expected to affect the translocation time and speed [258]. We tested whether the concentration of ComE affected the speed of DNA import by deleting three of the four identical copies of *comE* generating $\Delta pilV \Delta comE_{234}$ (Table 2.1, Ng052). In bulk experiments, the $\Delta comE_{234}$ strain showed severe reduction of DNA uptake and transformation efficiencies, and of ComE concentration, but their levels were above background levels [257]. We found that the speed at $F = 4 \text{ pN}$ was reduced from $v = (194 \pm 47) \text{ nm/s}$ in the $\Delta pilV$ strain

to $v = (71 \pm 26) \text{ nm/s}$ in the $\Delta pilV \Delta comE_{234}$ strain (Figure 3.15). We conclude that the concentration of ComE affects the speed of DNA import.

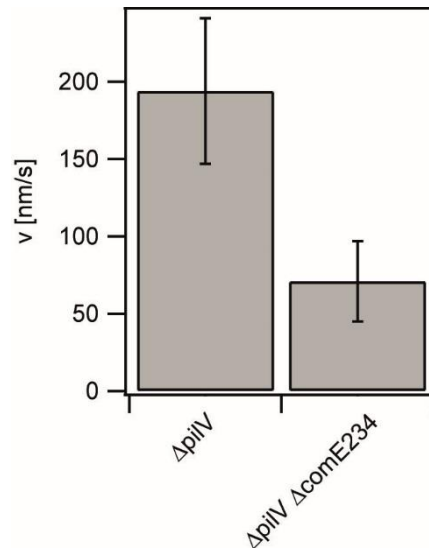


Figure 3.15 The uptake velocity depends on the concentration of ComE. Average speed of DNA uptake for $\Delta pilV$ (Ng005, $N = 22$) and $\Delta pilV \Delta comE_{234}$ (Ng052, $N = 10$) at $F = 4 \text{ pN}$. Image adapted from [253].

3.2.3 Gonococcal DNA uptake is reversible at high forces

DNA uptake by the gram-positive *B. subtilis* using the T4P system is irreversible up to high forces exceeding $F = 50 \text{ pN}$ [259]. On the other hand, DNA uptake by gram-negative *H. pylori* using the T4S system is reversible at $F = 23 \text{ pN}$ [260]. Here, we tested whether DNA uptake in gram-negative *N. gonorrhoeae* using the T4P system is reversible. To this end, we used the force-clamp mode for changing the external force during a DNA uptake event (Figure 3.16). We found that DNA previously imported at low force could be extracted by increasing the force. Figure 3.16a shows a typical trace of the length change Δ of the DNA tether between the bacterium and the bead. While the force was kept constant, there was little variation in the speed of DNA uptake or extraction. Upon changing the force, jumps in the tether length were observed; these rapid length changes can be assigned to the elastic properties of DNA (Figure 3.16b). Multiple rounds of import and extractions were observed.

We note that we observed rare events of continuous reduction of DNA uptake speed (Figure 3.16a, $t \approx 30$ s) or abrupt stalling of DNA uptake (Figure 3.16a, $t \approx 70$ s). There are various explanations for this behavior. When the distance fell below $\Delta < 1.3 \mu\text{m}$, then bead and bacterium were in close contact and the data was dismissed from further analysis. We have shown previously that the periplasm is saturable with 40 kbp DNA and that ComK governs the carrying capacity in a gene-dosage dependent fashion (3.1.4) [261]. With our 10 kbp DNA substrate, we do not expect to saturate the periplasm. However, we cannot rule out that free DNA (whose concentration we reduced to a minimal level by extensive washing) is taken up and causes saturation occasionally.

In conclusion, DNA uptake in *N. gonorrhoeae* is reversible under application of external force.

The kinetics of DNA uptake during transformation provide evidence for a translocation ratchet mechanism

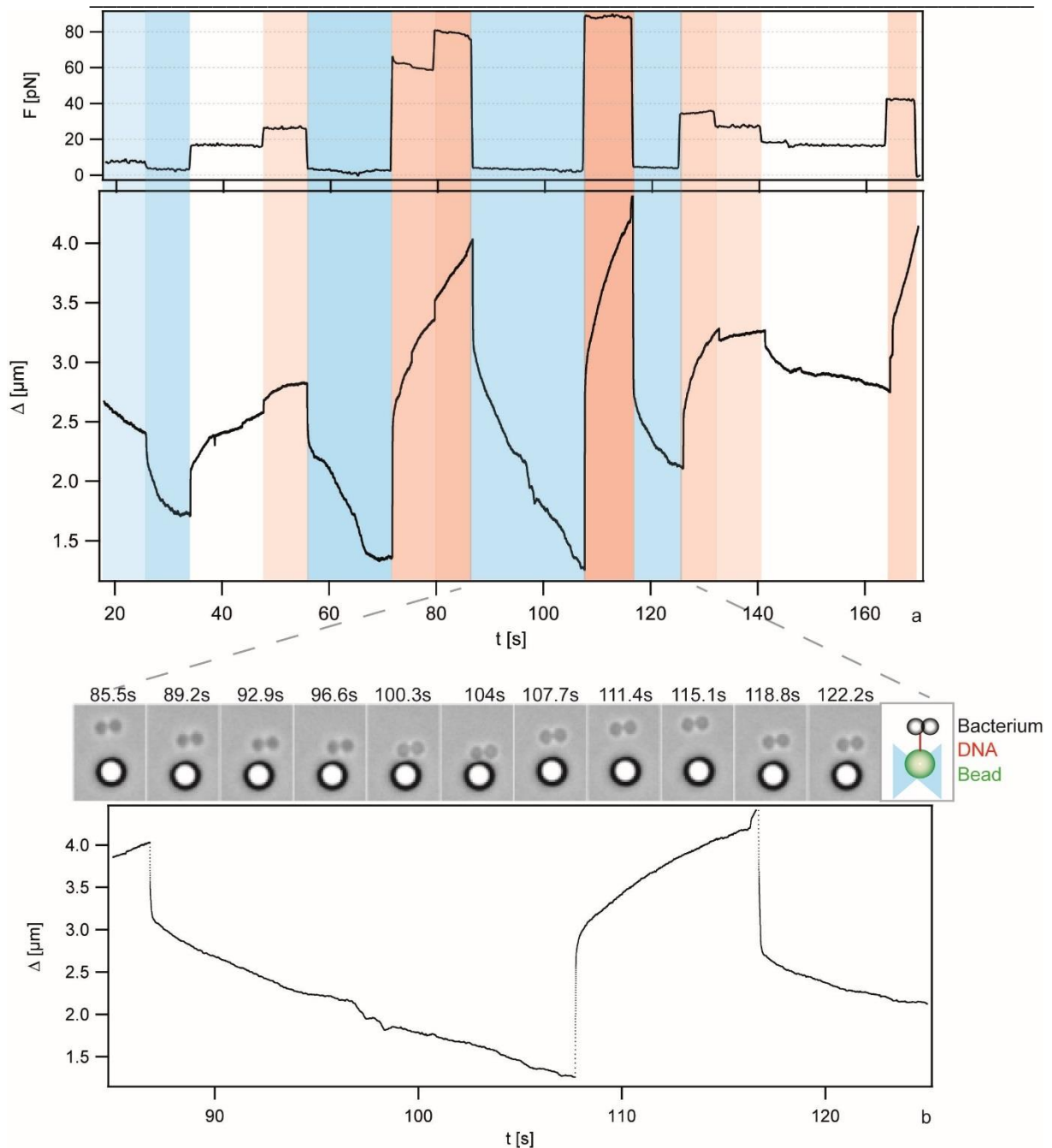


Figure 3.16 DNA uptake is reversible upon application of force. Typical time series of DNA uptake and extractions (Ng005). a) Upper graph: force, lower graph: distance between bead and bacterium Δ as a function of time. For presentation, the data was down-sampled to 1 Hz. Colors guide the eye. Events marked in blue are retraction, red are elongation. More opaque colors signify stronger forces. At $\Delta < 1.3 \mu\text{m}$, tracking was not reliable because bacterium and bead were in contact. b) Lower graph: zoom into the distance between bead and bacterium. Upper graph: corresponding time lapse microscopic images. Image adapted from [253].

3.2.4 The velocity versus force relationship is in agreement with a translocation ratchet model

Conceptually, the simplest mechanism for translocation of a DNA molecule through a pore is the translocation ratchet (Figure 1.3). The idea behind this model is that DNA diffuses through the pore in the outer membrane [150]. The diffusion process is rectified by binding of proteins (chaperones) that are present in the periplasm but not within the extracellular space. In this scenario, the movement is generated by Brownian motion and the energy required for biasing the direction is provided by the binding energy of the chaperones. In the imperfect translocation ratchet model proposed by Peskin et al [149], a rod diffusing in the pore is considered with a diffusion coefficient D . The rod carries ratchet sites with a spacing a between two sites for chaperones. A ratchet site can freely cross the origin from the extracellular side to the periplasm, but it is reflected when it attempts to cross the origin from the periplasm to the extracellular space provided that a chaperone is bound, with a probability p . This probability is related to the dissociation constant $K = k_{\text{off}}/k_{\text{on}} = (1 - p)/p$. For $K > 0$, the direction of DNA translocation is reversible when the extracellular force is sufficiently high. With increasing K , the directional bias (and thus the DNA uptake speed) is expected to decrease. The model describes the velocity-force relation of polymer translocation [149].

$$v(F) = \frac{2D}{a} \frac{1/2 \omega^2}{\left(\frac{e^\omega - 1}{1 - K(e^\omega - 1)} \right) - \omega} \quad (\text{eq. 1})$$

where $\omega = Fa/k_B T$, a is the distance between two binding sites, D is the diffusion constant of DNA within the pore, and $K = k_{\text{off}}/k_{\text{on}}$.

We tested this velocity versus force relation by plotting velocity data (obtained from data as shown in Figure 3.16) as a function of the external force (Figure 3.17). The fit to eq. 1 was restricted to the region $F < 65$ pN, because we expect the transition of the secondary structure of DNA around $F \approx 65$ pN [262]. Eq. 1 described the velocity-force relation of DNA uptake in *N. gonorrhoeae* well with $a = (1.6 \pm 0.3)$ nm, $D = (250 \pm 100)$ nm² s⁻¹, $K = 0.0012 \pm 0.0008$.

Using these fit parameters, we can estimate the speed v_0 at which the DNA would be taken up in the absence of external force applied by the laser tweezers, i.e. $F = 0$ [149]. Without external force, $v_0 = 2Da^{-1}(1 + 2K)^{-1} = (310 \pm 180)$ nm s⁻¹ = (900 ± 500) bp s⁻¹.

Moreover, we obtain the reversal force F_r , where, on average, the system switches from uptake to extraction $F_r = k_B T a^{-1} \ln(1 + K^{-1}) = (17 \pm 2) \text{ pN}$.

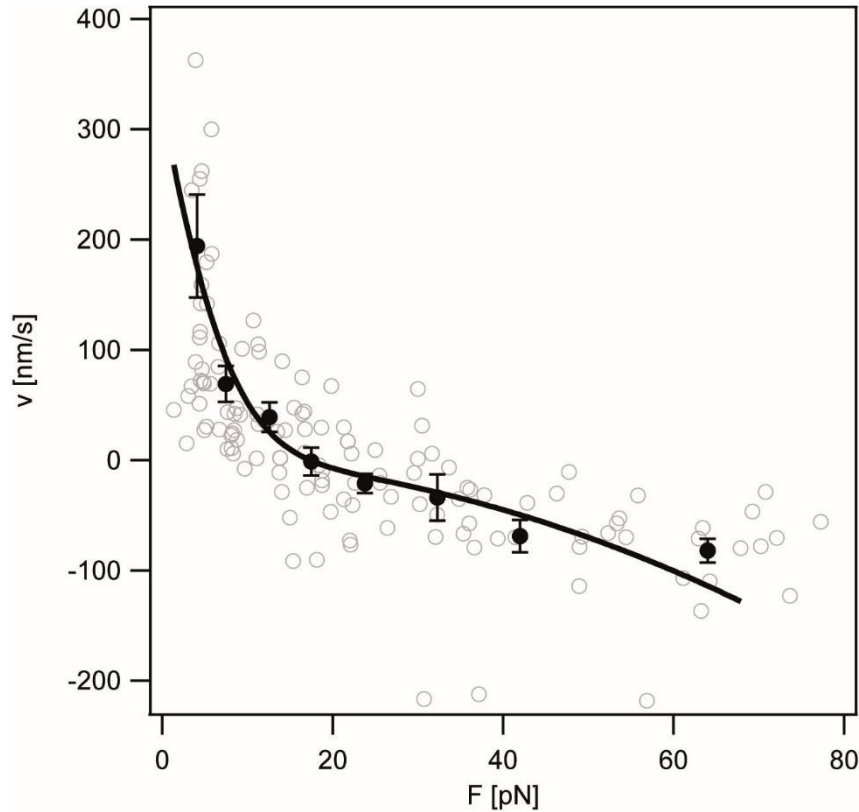


Figure 3.17 Velocity versus force relationship of DNA uptake. (Ng005) Grey open circles: Raw data. Black closed circles: Data binned over 6 – 25 data points. Error bars: standard error of the mean. Full line: fit to equation 1 with $a = (1.6 \pm 0.3) \text{ nm}$, $D = (250 \pm 100) \text{ nm}^2 \text{ s}^{-1}$, $K = 0.0012 \pm 0.0008$. Image adapted from [253]

To confirm that the kinetics of DNA uptake observed in this study was independent of transport through the cytoplasmic membrane, we repeated the experiment using a *comA* deletion strain. ComA is essential for transport of DNA through the cytoplasmic membrane but does not affect DNA uptake into the periplasm [263]. We found that the force-dependent velocity was independent of *comA* (Figure 3.18), indicating that we observed transport of DNA through the outer membrane with our assay.

To summarize, the velocity versus force relation of DNA is in very good agreement with the model of the translocation ratchet.

The kinetics of DNA uptake during transformation provide evidence for a translocation ratchet mechanism

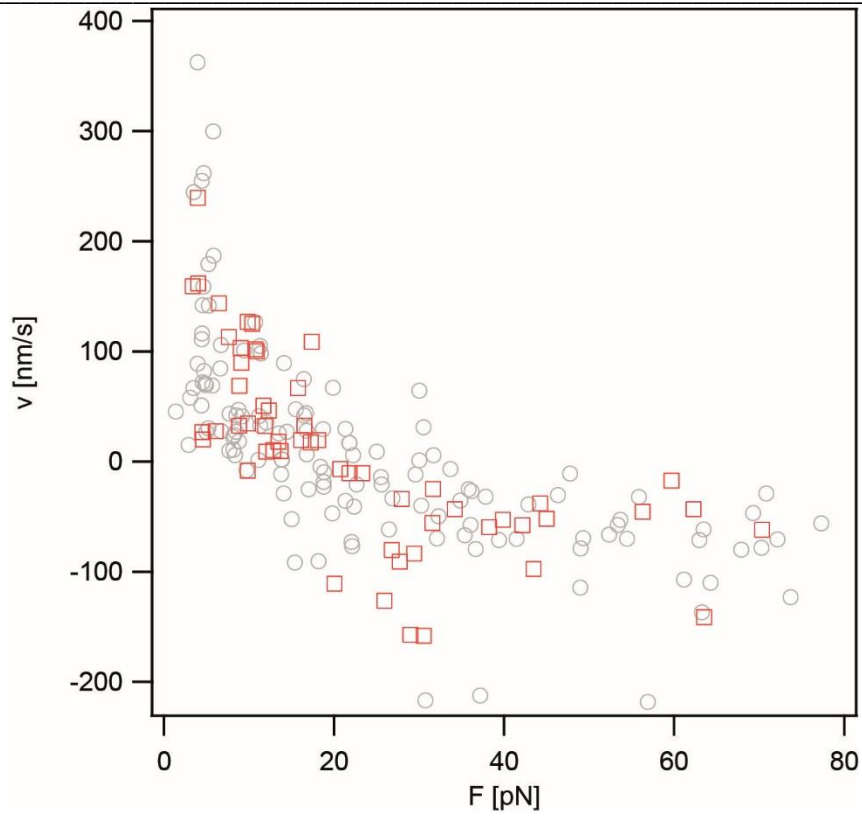


Figure 3.18 Velocity versus force relationship of DNA uptake for $\Delta comA$. Grey open circles: $\Delta pilV$ $recA_{ind}$ (Ng005), red open squares: $\Delta comA$ $\Delta pilV$ $recA_{ind}$ (Ng054).

3.3 Single-stranded DNA uptake during gonococcal transformation

Previous studies demonstrated that ssDNA is a substrate for transformation in *N. gonorrhoeae* [111]. Interestingly, chromosomal DNA of *N. gonorrhoeae* is actively secreted in the form of ssDNA by a type IV secretion system encoded on a gene region called the gonococcal genetic island (GGI) and enhances horizontal gene transfer [25, 29, 30]. Single-stranded DNA has been shown to transform less efficiently than dsDNA to a varying extent. Further, transformation by ssDNA shows a preference for the Crick-strand with respect to the specific DNA uptake sequence (DUS) of *N. gonorrhoeae* [264]. We aimed to test whether the difference in transformation efficiencies for dsDNA and ssDNA is caused by differences in DNA uptake efficiencies. As dsDNA and ssDNA are very different with regards to their secondary structure, we expected to gain information on the mechanism of DNA uptake over the outer membrane by comparing the kinetics. Hence, we measured uptake efficiencies of and capacities for fluorescently labeled dsDNA and ssDNA. As we expected DUS recognition and DNA transport to be mediated by different receptors, we also tested for uptake of ssDNA containing a dsDUS. The results presented in this section describe my contributions to the following publication.

Hepp, C., et al., Single-Stranded DNA Uptake during Gonococcal Transformation. J Bacteriol, 2016. 198(18): p. 2515-23. [265]

The contribution of Heike Gangel and Katja Henseler was the construction of the *nuc* strain. The project was initiated by Niklas Günther as a BSc thesis project under my supervision.

3.3.1 Double-stranded DNA uptake sequence (DUS) supports uptake of otherwise single-stranded DNA

We set out to compare the DNA uptake efficiency of single-stranded DNA (ssDNA) and double-stranded DNA (dsDNA). To minimize the probability of hairpin formation, short

complementary oligonucleotides with a length of 100 bases were synthesized. The sequence was randomly chosen from λ -phage DNA and contained the 12 bp DNA DUS (Table 2.2, NGCH171). The Crick-strand with the DUS at the 3'-end carried a single Cy5-dye at the 5'-end. The Crick-strand was chosen because it showed the highest transformation rate in previous experiments [264]. The DNA fragments were labeled with a single dye molecule to minimize the effect of labeling on the interaction of DNA with components of the DNA uptake machine. dsDNA was generated by hybridization between the unlabeled and the labeled strand (2.5.2). As in 3.1, all DNA uptake experiments were performed in a $\Delta pilV recA_{ind}$ background.

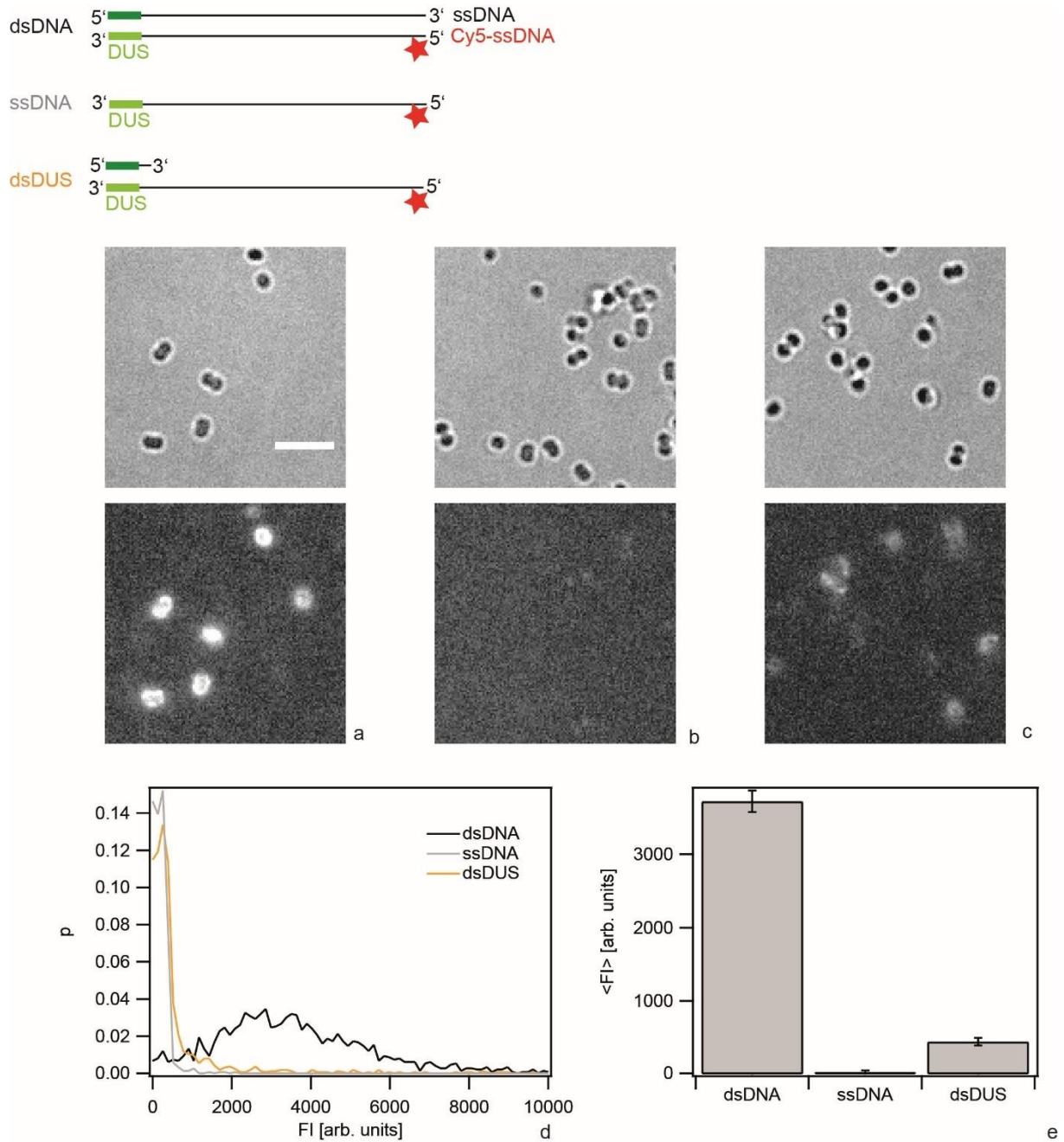


Figure 3.19 dsDUS supports import of ssDNA. Gonococci (*ΔpilV*) were incubated for 1 h with DNA fragments containing a single dye molecule at the 5' end. Subsequently they were treated with DNase I. The fragments consisted of a) dsDNA, b) ssDNA, c) ssDNA with 16 b complementary oligonucleotide containing DUS. Top: Brightfield images, bottom: fluorescence images. d) Probability distribution of the total fluorescence intensity of individual cells incubated with dsDNA (black), ssDNA (grey), 100 b ssDNA with 16 b complementary oligonucleotide containing DUS (orange). e) Average fluorescence intensity of individual cells. Error bar: standard deviation of three independent experiments. Grey bars: fragments with sequence from λ -phage DNA with a single Cy5-dye at the 5' end. (N > 1500 for each condition). Image adapted from [265].

Gonococci were incubated with DNA for 1 h in a gently shaking tube and subsequently treated with DNase. The extended incubation time was chosen to compare our data to previous results (3.1) [261]. Gonococci were imaged (Figure 3.19a, b) and the fluorescence intensities of individual cells were measured using a previously described procedure [261]. From this analysis, the distribution of fluorescence intensities of individual cells was obtained (Figure 3.19c). The distribution of fluorescence intensities after Cy5-dsDNA uptake was broad (Figure 3.19c) and reminiscent of the distribution obtained by the uptake of longer (0.3 – 10 kbp) fragments labeled with multiple dyes per fragment [261]. The amount of imported Cy5-ssDNA was considerably lower than the amount of Cy5-dsDNA (Figure 3.19d, e).

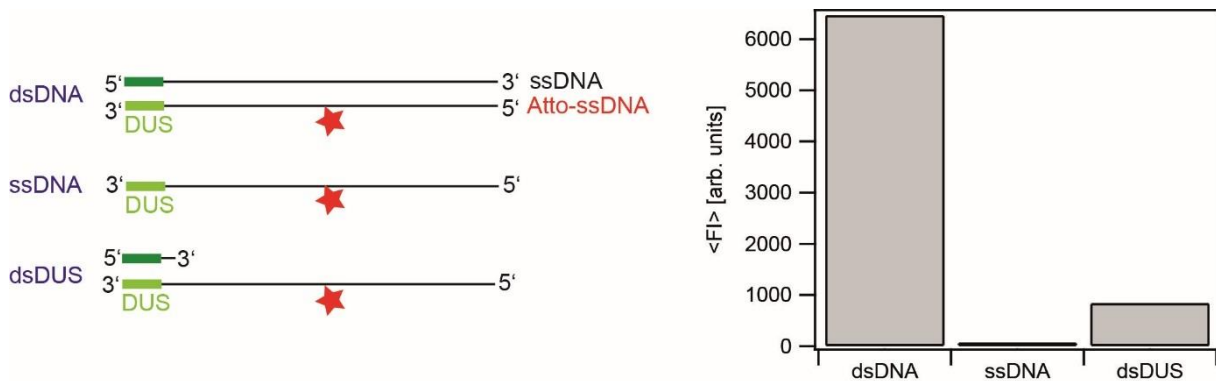


Figure 3.20 Mid-labeling confirms that the import efficiency of ssDNA is increased by dsDUS. Gonococci (*ΔpilV*) were incubated for 1 h with DNA fragments containing a single dye molecule at the center of the fragment. Subsequently they were treated with DNase I. The fragments consisted of dsDNA, ssDNA, or ssDNA with 16 b complementary oligonucleotide containing DUS. Average fluorescence intensity of individual cells. (N > 500 for each condition). Image adapted from [265].

The DNA uptake sequence (DUS) strongly enhances the probability of transformation and DNA uptake. It was conceivable that only double-stranded DUS (dsDUS) was recognized by gonococci. We addressed the question whether a DNA fragment with dsDUS but otherwise ssDNA was taken up. When the complementary strand was added and dsDNA was formed, uptake of dsDNA was detected (Figure 3.19c). To ensure that end-labeling did not introduce an artifact, we repeated the experiment with an Atto 647N-dye attached at position 37 of the DNA-fragment. Mid-labeling produced the same result indicating that the position of the dye did not affect the outcome of the experiment (Figure 3.20). Compared to the experiments using continuously labeled DNA, the background was strongly reduced with individual labels, allowing for a better quantitative comparison between the efficiency of dsDNA, ssDNA, and

dsDUS uptake. Previous work characterizing the binding affinity of the minor pilin ComP to the DUS exclusively used dsDNA [114]. The structure of the DUS-binding protein ComP shows that an electropositive stripe and a DNA-docking platform are consistent with binding of dsDNA.

In conclusion, uptake of single-stranded DNA by gonococci is detectable provided that the DUS is double-stranded.

3.3.2 The thermonuclease Nuc rapidly degrades imported single-stranded DNA

In the next step, the stability of ssDNA within the periplasm was addressed. So far, the time elapsed between the start of DNase treatment and the time point of imaging was variable. In the next step, the onset of imaging was controlled. Again, bacteria were incubated with dsDNA or dsDUS DNA (ssDNA fragment with double-stranded DUS), respectively. Subsequently, extracellular DNA was removed, DNase was added, and the fluorescence intensity was monitored starting directly after addition of DNase. The fluorescence signal associated with dsDNA decayed slowly (Figure 3.21a). The decay kinetics were in agreement with an exponential decay with a characteristic time of $\tau_{\text{dec ds}} = (85 \pm 7)$ min. The decay of dsDUS DNA was considerably faster and occurred at a characteristic time of $\tau_{\text{dec ss}} = (9 \pm 1)$ min. We verified that the decay kinetics did not depend on DNase addition. To this end, the DNase treatment was omitted and imaging started directly after the washing step where DNA was removed. The decay kinetics did not show a significant difference (Figure 3.21c) with $\tau_{\text{dec ds}} = (110 \pm 30)$ min and $\tau_{\text{dec ss}} = (8 \pm 1)$ min. Moreover, the initial fluorescence levels $FI(t=0)$ were comparable between Figure 3.21a and c, indicating that the fluorescence intensity was mainly caused by internalized DNA and that DNA binding to the outside of the cell does not contribute significantly to the fluorescence signal.

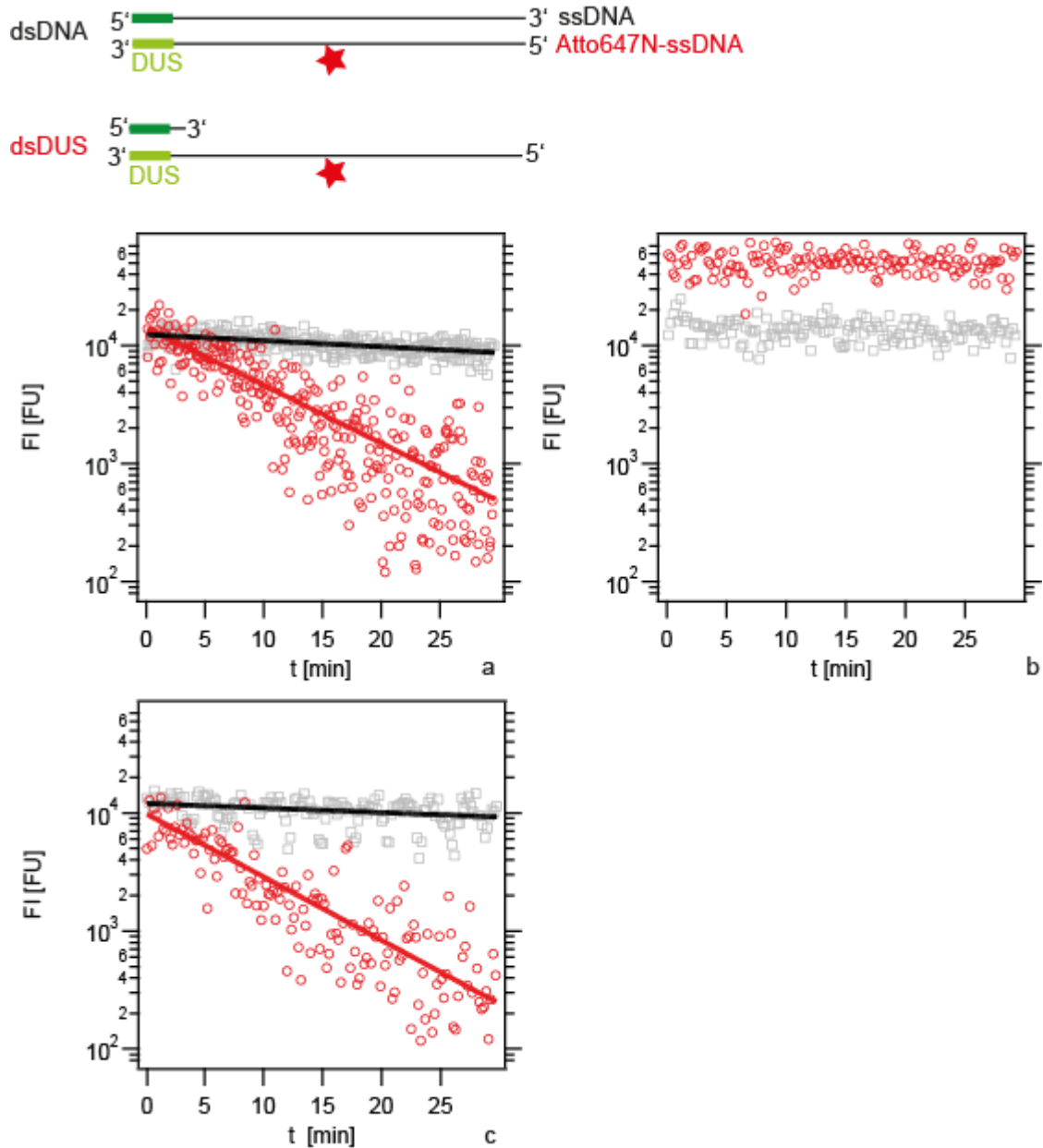


Figure 3.21 Decay of imported dsDNA and dsDUS DNA in nuc deletion strain. a) $\Delta pilV$ and b) $\Delta nuc \Delta pilV$ strains were incubated for 1 h with DNA fragments containing a single dye molecule at the center of the fragment. Single cell fluorescence intensity was monitored starting immediately after DNA removal and addition of DNase I. c) $\Delta pilV$ without addition of DNase I. Grey: dsDNA, red: dsDUS. Full lines are exponential fits to the data. Image adapted from [265].

Recently, the thermonuclease Nuc was speculated to reside within the periplasm [34]. Therefore, we tested whether Nuc was responsible for the decay of imported DNA. To this end, we performed the experiment explained above in a $\Delta nuc \Delta pilV$ strain. Both dsDNA and dsDUS were stable for an extended period of time (Figure 3.21b), indicating that Nuc was responsible for the fast decay observed in Figure 3.21a. Fitting of an exponential decay function was not possible. The fluorescence intensity associated with uptake of dsDUS DNA was significantly ($\sim 3.5 \times$) higher than the signal associated with dsDNA. The observation that in the presence of

Nuc the initial fluorescence intensities are comparable (Figure 3.21a) can be explained by the fact that several minutes elapsed from the removal of extracellular DNA to the start of imaging. Since Nuc causes faster decay of dsDUS than of dsDNA they were present at similar amounts when imaging started.

Since the fluorescence signal associated with imported DNA was stable for 30 min in the *nuc* deletion strain, the fluorescence signal could be used as a measure for the amount of DNA residing within the cell after 1 h exposure to extracellular DNA. First, we verified that DNA uptake was dependent on PilQ, the protein that forms the outer membrane channel required for DNA uptake [16]. *pilQ* deletion caused a ~ 200-fold reduction of the average fluorescence intensity in the presence of dsDNA (Figure 3.22b). This signal can be considered as the basal level, because DNA uptake is inhibited.

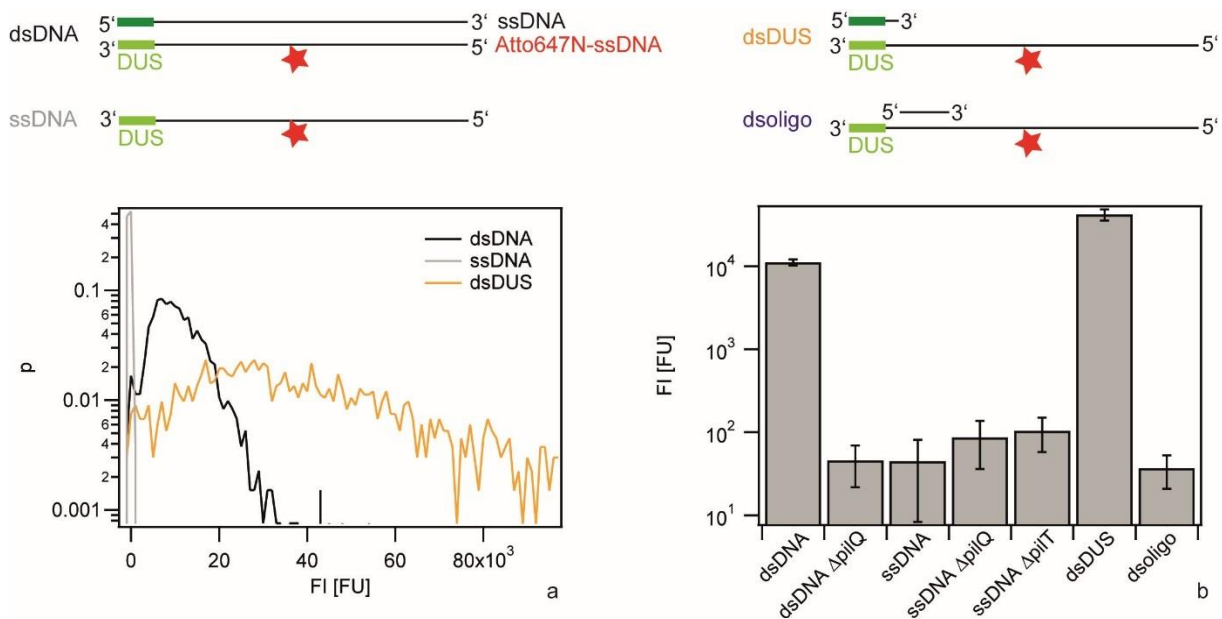


Figure 3.22 Carrying capacities of various DNA fragments in a *nuc* deletion strain. Gonococci were incubated for 1 h with DNA fragments containing a single dye molecule at the center. Subsequently, they were treated with DNase I. a) Probability distribution of the total fluorescence intensity of individual cells. Δ *nuc* Δ *pilV* with dsDNA (black), Δ *nuc* Δ *pilV* with ssDNA (grey), Δ *nuc* Δ *pilV* with dsDUS (orange). b) Average fluorescence intensity of individual cells. dsDNA: Δ *nuc* Δ *pilV* incubated with dsDNA, dsDNA Δ *pilQ*: Δ *pilQ* Δ *nuc* Δ *pilV* incubated with dsDNA, ssDNA: Δ *nuc* Δ *pilV* incubated with ssDNA, ssDNA Δ *pilQ*: Δ *pilQ* Δ *nuc* Δ *pilV* incubated with ssDNA, ssDNA Δ *pilT*: Δ *pilT* Δ *nuc* Δ *pilV* incubated with ssDNA, dsDUS: Δ *nuc* Δ *pilV* incubated with ssDNA with double-stranded DUS, dsoligo: Δ *nuc* Δ *pilV* incubated with ssDNA with 16 bp double-stranded region adjacent to DUS. Error bar: standard deviation of three independent experiments. (N > 1000 for each condition). Image adapted from [265].

The fluorescence associated with ssDNA uptake did not exceed the basal level, indicating the the level of ssDNA uptake was below the detection limit of our setup (Figure 3.22). Deletion of *pilQ* or of gene encoding for the type IV pilus retraction ATPase *pilT* [40] did not change the fluorescence level.

The signal generated by dsDUS DNA exceeded the dsDNA signal in agreement with Figure 3.21b (Figure 3.22a, b). We verified that short stretches of dsDNA other than the DUS did not support uptake of otherwise ssDNA by hybridizing a 16 b fragment adjacent to the DUS motive. The average fluorescence signal was comparable to the signal generated by purely ssDNA (Figure 3.22b), demonstrating the double-stranded DUS was required for generating a significant DNA uptake signal.

We conclude that the thermonuclease Nuc degrades imported ssDNA and dsDNA. In a *nuc* deletion background, the signal associated with uptake of ssDNA was at least 200-fold lower than the dsDNA signal. Double-stranded DUS on otherwise ssDNA was sufficient for exceeding the dsDNA signal.

3.3.3 Uptake kinetics of ssDNA containing double-stranded DUS

We found that gonococci take up single-stranded DNA, but Nuc rapidly degrades ssDNA. Therefore, we used a *nuc* deletion strain for monitoring the kinetics of dsDUS (ssDNA with double-stranded DUS) uptake. Cells were incubated with dsDNA or dsDUS DNA, respectively and images were acquired continuously (Figure 3.23). The fluorescence intensities associated with DNA uptake were determined by quantitative image analysis. Both dsDNA and dsDUS DNA uptake revealed saturation kinetics and were well described by an exponential fit. The characteristic times were $\tau^{\text{up}}_{\text{ds}} = (2.9 \pm 0.3)$ min for dsDNA and $\tau^{\text{up}}_{\text{ss}} = (4.1 \pm 0.4)$ min for dsDUS. The carrying capacities were $\text{FI}^{\text{max}}_{\text{ds}} = (6300 \pm 400)$ FU for dsDNA and $\text{FI}^{\text{max}}_{\text{ss}} = (20000 \pm 800)$ FU for dsDUS, respectively.

In summary, dsDNA and dsDUS DNA uptake showed saturation kinetics with comparable characteristic times.

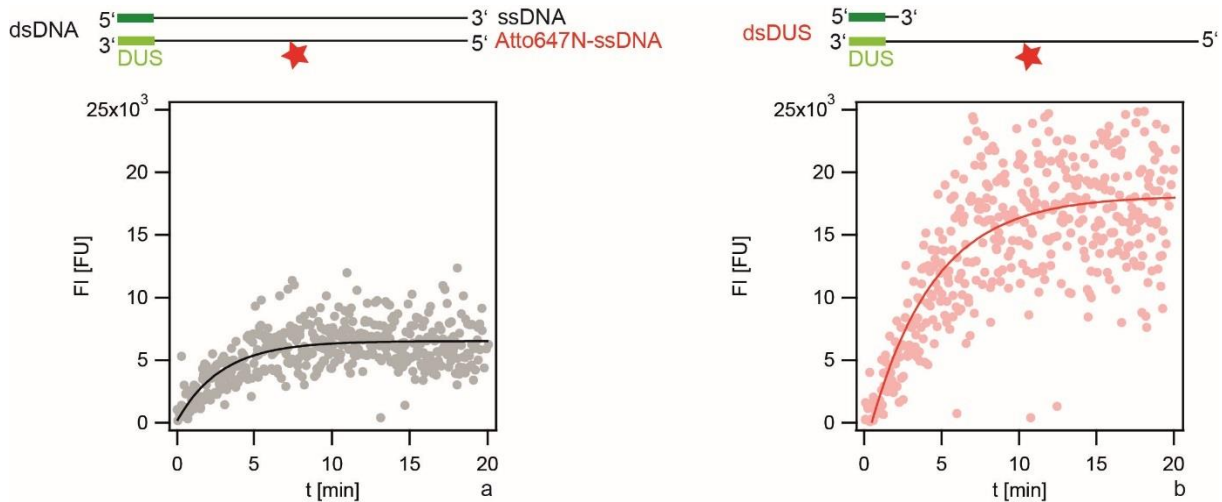


Figure 3.23 Import kinetics of dsDNA and dsDUS DNA. Gonococci (*Δnuc ΔpilV*) were incubated with DNA fragments containing a single dye molecule at the center. The fluorescence intensity of single cells was recorded as a function of time. Each data point depicts the average fluorescence intensity of all cells within one microscopic field of view, averaging ~ 20 individual cells. a) dsDNA, b) dsDUS DNA. Full lines: fits to exponential functions. Image adapted from [265].

3.3.4 Transformation efficiencies of dsDNA, ssDNA and dsDUS

Finally, the question whether the substrate dependence of the transformation efficiency reflected the substrate dependence of DNA uptake was addressed. Unlabeled ssDNA fragments with a length of 300 bp were synthesized (Table 2.2, ngch_L01). The fragments contained part of the sequence of the *gyrB* gene with the point mutation that confers resistance against nalidixic acid and the DUS. dsDNA was generated by PCR using primers kh033 and kh034 (Table 2.2). When these fragments are used as transforming DNA in MS11 wt, they confer antibiotic resistance and enabled us to measure the transformation frequency as described (2.10). In the absence of transforming DNA, the probability did not reach a significant value and was lower than $3 \cdot 10^{-8}$ (Figure 3.24). We attribute these resistant clones to spontaneous mutations. Transformation with the pSY6 plasmid containing the modified *gyrB* gene yielded a transformation probability of $p_{trafo} = 0.13 \pm 0.03$. The transformation probability of the double-stranded 300 bp fragment significantly higher than the background with $p_{trafo} = (3 \pm 2) \cdot 10^{-6}$. Thus, although the probability of transformation is by orders of magnitude lower for the fragment than for the plasmid, transformation is clearly quantifiable. The transformation probability of single-stranded DNA with double-stranded DUS (dsDUS) was $p_{trafo} = (8 \pm 2) \cdot 10^{-8}$, i.e. significantly larger than the background. Using ssDNA fragments, no transformation was detectable. Furthermore, we assessed whether deletion of *nuc* affected the transformation

probabilities by repeating the transformation assay in a Δnuc strain. The transformation probability of dsDNA was ~ 3 times higher as compared to the wt background. *Nuc* deletion did not significantly affect the transformation probability when dsDNA or ssDNA were used as substrates (Figure 3.24).

Taken together, the transformation assays show that short fragments of dsDNA and ssDNA with dsDUS are used as substrates for transformation in our system, but the probability of ssDNA transformation does not exceed the background level most likely caused by spontaneous mutations.

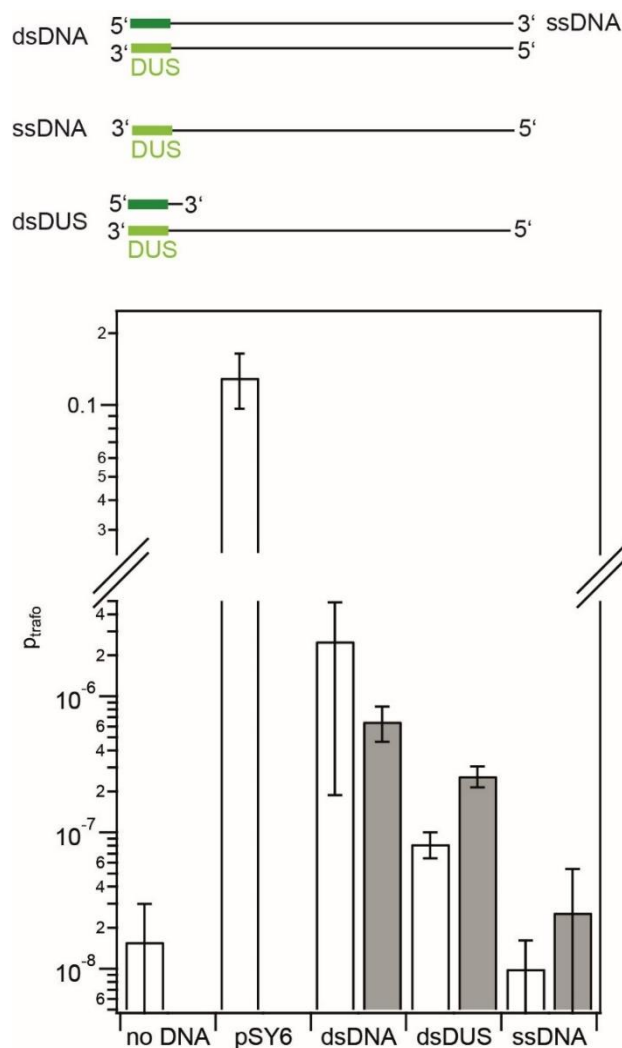


Figure 3.24 Transformation probability with dsDNA, ssDNA, and dsDUS. Transformation assays were performed with unlabeled DNA containing part of the gene encoding for the modified gyrase B that confers resistance against nalidixic acid. pSY6 is a plasmid containing the DUS and the sequence of the modified gyrase B. The fragments consisted of dsDNA, ssDNA, ssDNA with 16 b complementary oligonucleotide containing DUS (dsDUS). White bars: wt, grey bars: Δnuc . Error bars: standard error of the mean obtained from three or more independent experiments. Image adapted from [265].

4 Discussion

4.1 The functional roles of ComE in DNA uptake

We have shown, that the periplasmic DNA binding protein ComE forms stable complexes with imported DNA. Moreover, the ComE governs the DNA carrying capacity of the periplasm in a gene-dosage dependent fashion. The concentration of ComE affects the force-velocity relationship of DNA uptake, implying an active role for ComE in DNA transport. In contrast, the observed DNA uptake kinetics are not consistent with an active role of the type IV pilus in DNA transport. However, the force-velocity curve we obtained for DNA uptake fits the theoretical model of a translocation ratchet.

4.1.1 ComE binds DNA *in vivo* and governs the DNA carrying capacity of the periplasm

In the absence of DNA, ComE is homogeneously distributed in the periplasm. The DNA-free condition was ensured by previous incubation in liquid culture in the presence of DNaseI. When the cells were taken directly from agar plates without DNaseI treatment, some cells carried ComE foci which were mostly found at the septa of diplococci. We assumed these foci were caused by uptake and accumulation of DNA from lysed siblings or secretion. Most importantly, ComE-mCherry colocalized with Cy5-DNA in foci. This observation corresponds to the notion that ComE diffuses freely in the periplasm until it binds to incoming DNA and is

immobilized at the site of DNA entry. This behavior has also been observed in the naturally transformable pathogen *Vibrio cholerae*, where the ComE ortholog ComEA colocalizes with imported YOYO-DNA [266]. Interestingly, *N. gonorrhoeae comE* can restore the function of a *V. cholerae comEA* deletion indicating functional conservation in Gram negative species. Thus, DNA import dependent on ComE binding likely represents a general mechanism in the competence machinery of naturally transformable Gram negative bacteria. In our experiments, ComE-DNA complexes were not transient and remained stable for more than 30 min. In Gram positive *B. subtilis*, the ComE ortholog ComEA is the only protein not readily localized on the cell pole before DNA uptake [231]. Hence, ComEA has been suggested to sequester the DNA anywhere on the cytoplasmic membrane and moves to the site of the rate limiting DNA uptake step [267]. Similarly, ComE in might compact imported DNA in gonococci and thus increase the capacity of the periplasmic DNA reservoir.

As predicted, the ComE concentration was found to determine the DNA capacity of the periplasm. The amount of DNA incorporated by the cells was independent of fragment length, suggesting ComE as a limiting factor to the overall amount of DNA taken up. How much DNA can the cytoplasm hold on its own? With an estimated height of 20 nm and a cell radius of 0.4 μm , the volume of the periplasm is estimated to be $3 \times 10^{-5} \mu\text{m}^3$. The volume of a 10 kbp DNA fragment as a statistical coil with a gyration radius of 235 nm is $5 \times 10^{-2} \mu\text{m}^3$. The periplasm of *N. gonorrhoeae* can hold about 40 kbp of DNA. Obviously, DNA must be compacted to fit into the periplasm (similar to the organization of genomic DNA) and energy must be spent for packaging. To assess whether ComE is solely required for packaging DNA, we incubated DNA with fragments of 300 bp that correspond to the Kuhn segment length of a DNA double helix, which is about 100 nm. The Kuhn segment length is a measure for the stiffness of a polymer in that it specifies the minimum length over which the polymer can be bent by Brownian motion. Hence, the 100 nm DNA fragments cannot form a statistical coil and thus do not have to be compacted. Nevertheless, ComE is essential for uptake of these fragments, indicating it has a different functional role than merely compacting DNA to fit into the cell.

4.1.2 Physical constraints on the molecular mechanism of DNA uptake from the uptake kinetics of ssDNA

Earlier studies demonstrated that bacterial import machines are powered by strong molecular motors, but the mechanism of force generation remains unclear [230, 268]. We found that, while a double-stranded DUS is essential for efficient DNA recognition, the uptake machinery can process both double-stranded and single-stranded DNA. In a *nuc* deletion strain, the rates of uptake for dsDNA and ssDNA are comparable. This observation allows some conclusions on the nature of the motor that imports DNA into the periplasm of Gram negative bacteria. One possible mechanism of driving DNA import is a cyclic molecular motor [269]. Upon binding to DNA, a cyclic molecular motor performs a conformational change resulting in the translocation of a long biomolecule, in this case DNA. Subsequently, the motor releases DNA and performs another conformational change to return to its original position, where it can attach to the next DNA binding site and repeat the cycle. A standard example for such a cyclic molecular motor is myosin which is able to move on actin fibers and thus provides muscle contraction. Due to their physical constraints, cyclic molecular motors depend on the structure of their cargo. For example, the molecular motor the bacteriophage Φ 29 uses to package its DNA into the viral capsid requires contact to backbone phosphates that are 10 bp apart from each other [134]. However, the respective conformations of dsDNA and ssDNA are structurally very different: While dsDNA forms a stable, right handed and relatively rigid helix, ssDNA is much more flexible and can adapt various structures depending on its sequence. Thus, a putative cyclic molecular motor cannot explain why both substrates are translocated with a comparable efficiency.

4.1.3 The force-dependent velocity is consistent with a translocation ratchet driven by ComE

In the periplasm of Gram negative bacteria, no potential energy sources like ATP or electrochemical gradients exist. Thus, DNA uptake is likely powered by other mechanisms like chaperone binding, chain coiling or crosslinking [150]. During our single-molecule DNA uptake experiments, the velocity of DNA length change was influenced by varying the force

and could be reversed to DNA extraction instead of uptake upon increasing the force. This result is in agreement with theoretical predictions for an imperfect translocation ratchet [149]. Our data clearly reveals an effect of the ComE concentration on the DNA translocation velocity. The notion that less chaperones result in a slower translocation speed is supported by Langevin dynamics simulations of chaperone-assisted polymer translocation [270]. Moreover, ComE has been shown to bind DNA and is essential for DNA uptake. As discussed above, ComE is homogeneously distributed within the periplasm in the absence of DNA. Upon the addition of DNA, it relocates to form ComE-DNA complexes (Figure 3.10). The fuel for DNA uptake is most likely provided by the binding energy of ComE to DNA. The similar rates of ssDNA and dsDNA uptake described in 4.1.2 can be explained by the free diffusion of ComE in the periplasm. This enables ComE to bind the DNA in any structural conformation and drive DNA import regardless of the distance and orientation of potential binding sites to one another. The apparently low dissociation constant of this interaction provokes the question, how DNA is separated from DNA to complete the cycle of the DNA uptake motor. Firstly, prior to transport into the cytoplasm, ComE must dissociate from DNA, as it cannot be transported along with DNA by the cytoplasmic channel ComA. Moreover, ComE can possibly be liberated by the cytoplasmic degradation of DNA. After dissociating from DNA, ComE is regenerated and can assist in DNA uptake of more environmental DNA.

The model formulated by Peskin and Oster assumes a constant length between the adjacent binding sites of the biopolymer [149]. As ComE is reported to bind DNA without sequence specificity [203], it can bind anywhere on the DNA, thereby reducing the distance of two possible binding sites to 1 bp, which corresponds to a length of 0.3 nm. Thus, the distance between two binding sites according to the model is likely to be governed by the dimensions of ComE. The 3D structure of the ComE homolog HB8 from *T. thermophilus* has a diameter of roughly 2 nm. The fit of the Peskin model to our data resulted in a distance of 1.6 nm between two binding sites, which agrees nicely with the notion that the distance of ComE binding sites on DNA is limited by ComE's own size. The resulting diffusion constant $K_D = 0.0012$ suggests a high affinity of ComE to DNA which is in agreement with experimental data such as the remarkable stability of focal ComE-DNA complexes within the periplasm (Figure 3.12). The free energy barrier of polymer translocation is expected affected by various other parameters. One example is the change of chain entropy that can play a role during the DNA translocation process. However, more than 70 binding sites of the ratcheting chaperone ComE are located on a single Kuhn segment, thus rendering a possible entropic effect negligible. The fact that our experimental data fits the Peskin model quite well indicates effects due to molecular crowding

are most likely negligible [271]. Beside the model applied in this study other theoretical approaches to describe molecular motors have been developed [272]. The insertion of mutations in the ComE sequence is likely to alter the K_D of the ComE-DNA interaction. Testing mutants would answer the question whether the model used to describe the data in this study applies to a wide range of possible binding energies or whether alternative models for molecular motors must be employed.

4.1.4 Type IV pilus retraction does not directly drive DNA import

Type IV pilus (Tfp) biogenesis is a prerequisite for DNA uptake in *N. gonorrhoeae* and other naturally transformable species [4]. However, the role of Tfp in the process of DNA uptake is yet unclear. It has been suggested that Tfp protruding from the cell are “fishing” for external DNA which is subsequently imported into the periplasm by Tfp depolymerization [273-275]. This finding is supported by the discoveries of extended competence associated Tfps in *S. pneumoniae* and *V. cholerae* [276, 277]. However, extended Tfp have not been found in *B. subtilis*, indicating they are generally not necessary for DNA uptake during natural transformation [278]. Thus, the existence of an alternative Tfp DNA uptake complex has been proposed. As depolymerizing Tfp can exert high forces, pilus retraction constitutes another possible mechanism of DNA uptake.

Based on the comparison of force-dependent DNA uptake kinetics with previous measurement of Tfp retraction, we dismiss Tfp retraction as a mechanism of DNA uptake. We arrive at this evaluation for the following reasons. In case DNA is imported by Tfp retraction, the force-velocity relationship of DNA import and Tfp retraction should be comparable. The speed of *N. gonorrhoeae* Tfp retraction measured in previous studies is 2 $\mu\text{m/s}$ at a force of 8 pN and its reversal force exceeds 100 pN [279]. For Tfp-driven DNA uptake, we would thus expect to see DNA uptake at 2 $\mu\text{m/s}$, followed by pauses during which the retracted pilus needs to extend again to grab the next binding site on the DNA molecule. However, the velocity of DNA uptake at 8 pN is much slower and not interrupted by pauses. Furthermore, DNA uptake is reversed to extraction at 17 pN on average, a force at which pilus retraction is hardly slowed down.

Our data suggests the existence of a specific DNA uptake complex called a competence pilus that is formed by the Tfp machinery. This short pilus permits the binding of the DUS to its receptor ComP on the surface of the cell. Hence, like other naturally transformable bacteria, *N. gonorrhoeae* might not require protruding Tfp to acquire DNA from the environment. This is supported by a recent study demonstrating the transformability of pilin antigenic variants despite their non-piliated phenotypes [228]. Although pilus retraction can be excluded to drive DNA import, the pilus retraction ATPase PilT is still required for DNA uptake. It has been proposed that PilT serves to remodel Tfp to competence pili or allows passage of DNA through the opened PilQ pore left behind by the retracted pilus [163, 280]. Interestingly, the integration of the minor pilin and DNA receptor ComP into the pilus structure is counteracted by PilV, another minor pilin. Deletion of *pilV* results in two apparently unrelated phenotypes: Hypercompetence for natural transformation and a reduced number of extended pili, resulting in reduced motility and host cell interaction [175, 227]. In consideration of a study showing that minor pilins prime assembly of Tfp in *P. aeruginosa* [190], we speculate that PilV supports the formation of a fully extended pilus for motility and host cell interaction, while ComP supports the formation of a competence pilus. Hence, ComP might localize at the pilus tip.

Based on the presented facts and considerations, we propose a model for DNA uptake into the periplasm of *N. gonorrhoeae* (Figure 4.1). The ComP DNA receptor at the tip of a short competence pilus is exposed at the cell surface via pilus elongation. After ComP binding to the DUS of incoming DNA, retraction of the competence pilus contrives the DNA through the PilQ pore into the periplasm. Once DNA arrives in the periplasm, its diffusion is biased by ComP to power translocation of the entire fragment.

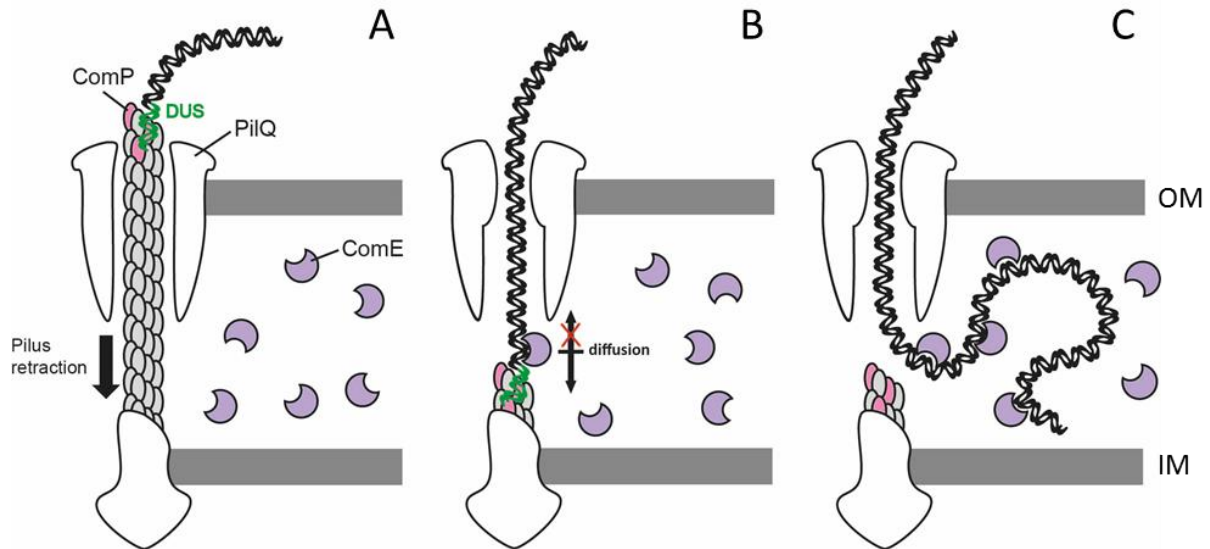


Figure 4.1 Proposed mechanism of DNA uptake into the periplasm of Gram negative bacteria. [A] A competence pseudopilus exposes the DUS receptor ComP to the environment, binding to the DUS of extracellular DNA. [B] Retraction of the competence pilus threads DNA through the PilQ pore into the periplasm, where the chaperone ComE is able to bind and inhibit diffusion back into the extracellular space. [C] By sequential binding of more ComE chaperones, the DNA is ratcheted into the periplasm. OM: outer membrane, IM: inner membrane.

4.1.5 DNA uptake is reversible for Gram negative bacteria

In Gram negative bacteria, the natural transformation process can be dissociated in four steps: DNA binding, transport through the outer membrane, transport through the inner membrane and homologous recombination into the genome [281]. Our results and other studies show that DNA can be massed in the cytoplasm for extended periods of time (3.1) [230, 266]. We found that DNA uptake over the outer membrane into the periplasm of Gram negative *N. gonorrhoeae* is powered by reversible binding of ComE. Thus, the next step of natural transformation, where DNA is translocated over the inner membrane into the cytoplasm, requires work against the force exerted by ComE binding.

The power source of DNA import into the cytoplasm has not been identified in Gram negative bacteria. Upon entry into the cytoplasm as a single strand, DNA is coated by various ssDNA binding proteins that either protect it from degradation and inhibit or mediate recombination [282]. Like ComE, these proteins could form a translocation ratchet and thus bias the diffusion of ssDNA over the cytoplasmic membrane (Figure 4.2A). The DEAD-box helicase ComFA is a cytoplasmic protein in *B. subtilis* that is essential for efficient transformation and controls the rate of DNA uptake [234, 283]. Its role might either be the ATP-

powered translocation of DNA or the conversion of dsDNA to ssDNA. The homolog to ComFA in *N. gonorrhoeae* is the primosome assembly protein PriA [284]. The cellular function of PriA is to restart chromosomal replication in case the progression of a replication fork is disrupted. Moreover, it is essential for homologous recombination in DNA repair and natural transformation [213]. The cytoplasmic DNA translocation channel ComA is conserved in *N. gonorrhoeae*, *B. subtilis* and *H. pylori* and likely universal to naturally transformable bacteria, regardless of fundamental differences in their DNA uptake machinery [284, 285]. Hence, it is tempting to speculate that translocation into the cytoplasm of *N. gonorrhoeae* and *H. pylori* can exert the same forces as in *B. subtilis*. Previously, studies revealed a reversal force of 50 pN for DNA translocation over the cytoplasmic membrane of Gram positive *B. subtilis* [268]. In contrast, the reversal force for both Gram negative systems lies around 20 pN (Figure 4.2B). Under these circumstances, inner membrane transport would be able to overpower ComE-DNA binding and DNA would be translocated into the cytoplasm, resulting in release and recovery of ComE. In comparison to the reversal forces, the velocity of DNA uptake in *N. gonorrhoeae* is about 10 times lower than in *H. pylori*, indicating that while the mechanisms and resulting velocities of uptake are entirely different, the low reversal forces must be conserved for the system to work.

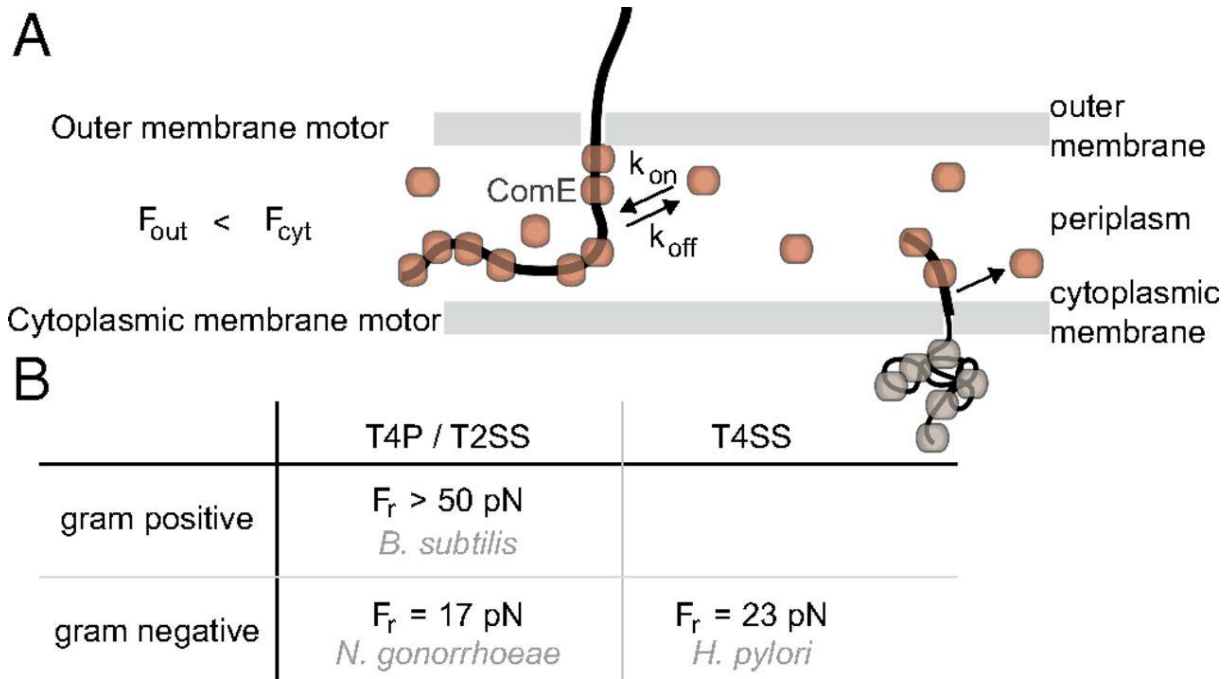


Figure 4.2 Force generation by cytoplasmic and outer membrane motors. (A) Hypothetical model for DNA transport through the Gram-negative cell envelope. A translocation ratchet drives uptake of DNA from the environment into the periplasm by reversible ComE binding. For transport across the inner membrane to occur, ComE must unbind. *B. subtilis* data suggest that in agreement with this prerequisite, the force generated by the cytoplasmic motor is considerably larger. (B) Reversal forces for *B. subtilis* [268], *N. gonorrhoeae*, and *H. pylori* [230]. T4P/T2SS, type 4 pilus/type 2 secretion system; T4SS, type 4 secretion system. Figure adapted from [253].

4.2 Power and limitations of the Cy3-DNA approach

In this work, we covalently labeled DNA with a fluorescent Cyanine-3 dye and observed DNA uptake by light microscopy. This new approach makes it possible to characterize DNA uptake on the single cell level. Previous studies describe DNA uptake on the population level. Moreover, tracking of fluorescent DNA uptake has the power to reveal the spatial distribution of the ingested DNA within a cell. Finally, DNA uptake in cells can be quantified while happening, allowing for uptake kinetics of individual cells.

To test the validity of our approach, we compared the effect of previously characterized mutations on uptake of Cy3-DNA. The properties of DNA uptake agree with previous data on

the outer membrane pore PilQ [226], the inner membrane channel ComA [210], the minor pilins PilV and ComP [226] [175], as well as the periplasmic DNA binding protein ComE [203]. A previous study measured the effect of the covalent Cy3-label on DNA uptake in *Helicobacter pylori* and reported a decrease of DNA uptake speed by a factor of about two [230]. In *N. gonorrhoeae*, the outer membrane pore PilQ has a diameter of 6.5 nm, while a DNA double helix measures 2.4 nm. Due to this discrepancy in size, we do not expect the Cy3 label to have drastic effects on DNA uptake kinetics. A clear limitation of the Cy3 approach is the inability of the labeled DNA to be transported through the inner membrane channel ComA and reach the cytoplasm. This raises the question whether the accumulation of Cy3-DNA observed in the cytoplasm is caused by the modification. However, preincubation with unlabeled DNA decreased the cells' uptake capacity for Cy3-DNA, indicating native DNA also accumulates [261]. A recent study reports cytoplasmic import of and transformation by fluorescent DNA synthesized via PCR, providing a potential tool for future studies of DNA transport into the cytoplasm [286].

To facilitate imaging, we performed most experiments in a *pilV* deletion background that shows a drastic increase in both DUS-mediated DNA uptake and transformation efficiency. In the absence of PilV, the DUS receptor ComP is likely overrepresented in the pilus structure and thus, the probability of DUS binding to the receptor and initiating DNA uptake is elevated compared to a wildtype strain. This raises the question whether DNA uptake in a *pilV* deletion strain can serve as an appropriate model for DNA uptake under native conditions. The observation of an increase in transformation indicates DNA transport over the inner membrane is not the only bottleneck in the transformation process. Nevertheless, it is unclear whether the wildtype strain reaches saturation under natural conditions. Neisserial biofilms are characterized by an overabundance of chromosomal DNA containing a high concentration of DUS [128]. Additionally, cells inside a biofilm display a considerably slower growth rate than if they were dispersed. Taken together, due to slow growth and high DNA concentrations, cells inside a biofilm very likely face a much higher probability of DUS recognition and initiation of DNA uptake during their generation time than cells under experimental conditions. From this point of view, the DNA uptake behavior of wildtype cells in a biofilm might be quite similar to that of a *pilV* deletion strain under experimental conditions. Further, the DNA uptake mechanism in a *pilV* deletion strain appears to be mechanistically identical to a wildtype strain with all key components still required [175]. The spatial distribution of DNA uptake sites is similar that in a wildtype. In consideration of these points, we conclude that Cy3-DNA is a useful tool to study DNA uptake into the periplasm of Gram negative cells.

4.3 Transforming DNA in the periplasm: Stability, relocalization and degradation

The localization of ComE-DNA foci points to DNA uptake at multiple and random locations around the contour of the cell. These ComE-DNA complexes were fairly stable but showed a spatial redistribution towards the septa of diplococci, suggesting a specific location for the subsequent steps of the natural transformation process. In our assays, we detected degradation of periplasmic DNA mediated by the thermonuclease Nuc, suggesting it limits genetic transfer by natural transformation.

4.3.1 Spatio-temporal dynamics and maintenance within the periplasm

When we tracked DNA uptake, 10 kbp fragments of Cy3-DNA were found at random independent locations on the cell. As the time resolution of the experiment was 1 min, we conclude that the localization of Cy3-DNA reflects the locations of outer membrane transport. For DNA fragments of this length, we did not observe a strong mobility within 30 min. The distribution of assumed DNA import sites correlated with the distribution of type IV pili (Tfp) around the cell indicating an interaction of imported DNA with the Tfp complex. As we did not observe pilus fibers coated with DNA, we were not able to provide evidence for an interaction of DNA with extended Tfp fibers and cannot draw further conclusions on their role in DNA uptake. While we observed multiple DNA complexes distributed around the cell contour of gonococci, DNA import complexes localize to the septum and the cell pole in *B. subtilis* and *H. pylori*, respectively [203, 230, 231]. When the cell wall of *B. subtilis* is dissolved, DNA complexes remain stable on the contour of the resulting spherical cell shape [267]. In *V. cholerae*, DNA complexes are marked by the occurrence of one single pilus that is randomly located on the cell contour. We speculate that organisms employing their Tfp merely for natural transformation only require one pilus to do so. In contrast, *N. gonorrhoeae* requires several pili for efficient twitching motility, all of which are possibly utilized for DNA uptake at some point.

If gonococci are further incubated with unlabeled DNA after Cy3-DNA uptake, Cy3-DNA will start to move to the septa of diplococci [261]. For smaller Cy3-DNA fragments of about 300 bp, this redistribution happens within minutes independently of incubation with unlabeled DNA. We interpret this result as the expulsion of previously acquired DNA from the DNA uptake complexes by the arrival of new DNA. Occasionally, the resulting DNA accumulations on the intersection start to move perpendicular to the longitudinal axis of a diplococcus towards the periphery of the cell. These structures are somewhat reminiscent of DNA filled membrane blebs named “transformasomes” in *H. influenzae* [287]. They are 10 times more frequent in competent than non-competent cells and were originally considered to be the sites of DNA import. The protein Tetracpac (Tpc) is a putative murein hydrolase essential for transformation. Moreover, deletion of *tpc* results in a severe defect in cell separation, manifesting in the formation of tetrapacs instead of gonococci [215]. This phenotype is consistent with Tpc acting at the septum, where it could liberate accumulated DNA by degradation of the cell wall and make it available for inner membrane transport. Interestingly, the cell division protein FtsE is reported to both bind DNA and interact with FtsZ, a protein that marks the site of prokaryotic cell division [288]. Moreover, the pneumococcal nuclease EndA that is essential for DNA transport over the cytoplasmic membrane in *S. pneumoniae*, is located midcell upon competence induction [289] (Figure 4.3). Cy3-DNA colocalizes with EndA indicating midcell is the site of active DNA uptake in *S. pneumoniae*. However, this midcell localization is independent of the expression of the inner membrane channel ComEC. Accordingly, we found that the accumulation of imported DNA at the septa is independent of the *N. gonorrhoeae* ortholog ComA [261]. It is currently unclear whether the accumulation DNA at the site of cell division in *N. gonorrhoeae* is connected to import over the cytoplasmic membrane.

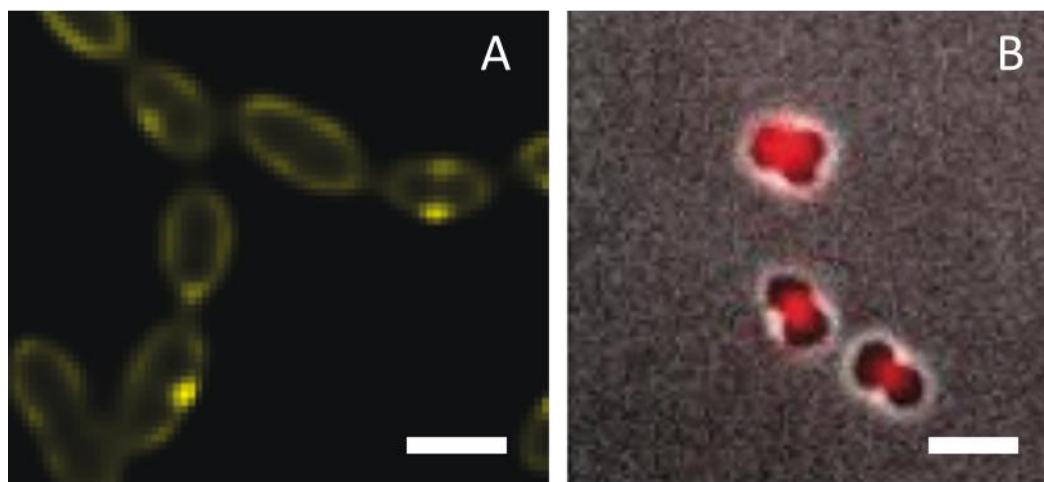


Figure 4.3 The nuclease EndA in *S. pneumoniae* and Cy3- DNA in *N. gonorrhoeae* relocate at the site of cell division. (A) Localization of EndA-GFP in *S. pneumoniae* upon induction of competence. Scale bar: 1 μm . Image adapted from [289]. (B) Localization of Cy3-DNA in *N. gonorrhoeae* after incubation with unlabeled DNA. Scale bar: 2 μm . Image adapted from [245].

4.3.2 Nuc degrades imported DNA

Our measurements on the stability of fluorescently labeled DNA in the periplasm indicate a quick degradation of ssDNA by the thermonuclease Nuc. When ssDNA carrying a dsDUS is used to transform *N. gonorrhoeae*, deletion of Nuc increases the transformation efficiency. This is consistent with the existence of an intermediate reservoir of DNA in the periplasm (3.1.2). Double stranded DNA is also subjected to degradation by Nuc, but the decay is considerably slower than for ssDNA. Thus, degradation by Nuc explains previous results on the stability of 10 kbp fragments that are still detected for hours, although their concentration slowly decreases. Recombinant Nuc has been shown to degrade both dsDNA and ssDNA [128].

Neisseria species contain large quantities of extracellular DNA in their biofilms. Nuc has been shown to regulate biofilm architecture due to its DNA-degrading activity. Hence, it has been proposed to be secreted into the extracellular environment [128]. Despite this hypothesis, Nuc could not be detected in the supernatant of *N. gonorrhoeae* cultures. Moreover, Nuc has been shown to degrade neutrophil extracellular traps (NETs) [129]. Being a vital part of the immune response to pathogens, NETs consist of chromosomal DNA from neutrophilic granulocytes and can severely inhibit the motility of intruders, making them susceptible to phagocytosis. In this context, there is clear evidence of extracellular Nuc activity [129], albeit it is unclear whether Nuc is liberated from within the cell through active secretion or through cell lysis. Nuc carries an N-terminal signal peptide that is consistent with a localization in the

periplasm. Moreover, a *pilQ* deletion strain exhibits no signal upon incubation with fluorescent DNA, ensuring DNA degradation takes place within the cell. Further, as discussed previously, covalently labeled DNA is unlikely to enter the cytoplasm. Hence, we conclude that degradation of imported DNA by Nuc takes place in the periplasm.

Previously, recombinant Nuc was shown to degrade both ssDNA and dsDNA, but the rate of degradation of the two substrates has not been compared [128]. In our study, we found that the fluorescence signal of ssDNA decreases much faster upon Nuc activity than the signal of dsDNA. Assuming that there is no signal decrease due to DNA being transported out of the cell before degradation, this discrepancy can be caused by two main reasons: 1. ssDNA is degraded faster than dsDNA. 2. Degraded ssDNA diffuses out of the cell at a higher rate than degraded dsDNA, either due to the smaller size of the nucleotides or the shorter persistence length of its degradation products. In this study, we used entirely unmethylated synthetic DNA fragments. In vitro, Nuc treatment of *N. gonorrhoeae* chromosomal DNA specifically reveals a certain resistance towards degradation, which might be caused by extensive methylation [128]. Thus, periplasmic degradation of *N. gonorrhoeae* chromosomal DNA might proceed considerably slower.

Although both ssDNA and dsDNA are substrates for natural transformation, the inner membrane channel ComA exclusively translocates ssDNA into the periplasm [120]. This implies that dsDNA must be converted to ssDNA within the periplasm at some point and consequently, ssDNA should be detectable inside the periplasm in succession of dsDNA uptake. Although ssDNA has been reported to transiently form in the periplasm [110], it has been found to be elusive and hardly reproducible in *N. gonorrhoeae*. Rapid degradation of transient ssDNA by Nuc could explain, why the detection of ssDNA is so difficult and thus close an important knowledge gap in the mechanism of *N. gonorrhoeae* natural transformation. However, a very recent in-silico study on the structure and sequence of ComA revealed a putative zinc binding motif that might enable ComA to degrade the non-translocated ssDNA strand all by itself [214].

4.4 Single stranded DNA as a substrate for natural transformation.

In contrast to other organisms, where the induction of competence depends on various factors like nutritional status and cell density, *N. gonorrhoeae* is constitutively competent. However, transformation in *Neisseria* is regulated by a preference to take up DNA from their own species. This trait is mediated by the 12-bp DNA uptake sequence (DUS) that is accumulated in the genome of *N. gonorrhoeae*.

The main source of transforming DNA in *N. gonorrhoeae* is currently unclear. DNA of lysed cells is generally assumed to be the substrate of transformation. However, most *N. gonorrhoeae* strains possess a mobile genetic element, the gonococcal genetic island (GGI), which enables them to secrete ssDNA into the environment. In early biofilms, the probability of gene transfer is reportedly elevated [290]. Moreover, early biofilms seem to contain a rather large fraction of ssDNA compared to late biofilms indicating secreted ssDNA plays a significant role in gene transfer [291]. To further assess the contribution of ssDNA-mediated transformation, assessing its efficiency is important.

Previous studies support the notion that *N. gonorrhoeae* can be efficiently transformed by ssDNA. Duffin and Seifert reported that ssDNA transformation efficiency was dependent on the DNA strain respective to the DUS. The Crick-DUS was found to transform more efficiently, resulting in transformation levels similar to dsDNA in strain MS11, and a 24× reduction compared to dsDNA in strain FA1090 [264]. Earlier reports characterized transformation levels of ssDNA and dsDNA as similar [111]. In our DNA uptake experiments, ssDNA was not taken up efficiently compared to dsDNA and was below the detection limit of our assay. Moreover, transformation of ssDNA did not exceed the background level caused by spontaneous mutation. If ssDNA fragments carried a dsDUS, transformation and DNA uptake could be detected. It has been proposed earlier that different lengths and preparation methods of the transforming DNA can account for discrepancies between studies on transformation efficiencies [264]. In this study, we employed short synthetic fragments to prevent dimerization and hairpin formation of ssDNA. Additionally, the chemical synthesis of ssDNA rules out any possible contamination with double-stranded DNA. While transformation efficiency decreases with the length of homologous regions in the substrate, transformation of our 300-bp synthetic

fragment was still quantifiable. Previously, 7 kbp fragments of phage DNA had been used [264, 292]. The absence of dsDNA contaminations was verified by Southern Blotting. Nevertheless, hairpin formation or partial dimerization in the DUS regions of these long fragments can cause secondary structures. If they resemble dsDUS, these structures might be targets for the DUS receptor, causing efficient transformation of ssDNA. Similarly, DUS hairpins might cause transformation of secreted ssDNA in the natural situation [292]. Interestingly, a significant fraction of DUSs in the chromosome of *N. gonorrhoeae* are arranged as inverted repeats which promote hairpin formation. These inverted repeats do not enhance the transformation efficiency of dsDNA plasmids compared to two consecutive DUSs [6]. It remains to be assessed whether the transformation of single-stranded DNA might be enhanced by inverted repeats.

5 Outlook

5.1 Fluorescence microscopy approaches to understand the mechanism of transport through the cytoplasmic membrane

After elucidating the mechanism of DNA transport through the outer membrane, we currently focus on mechanistic characterization of transport through the cytoplasmic membrane of *N. gonorrhoeae*. Initially, we seek to ascertain whether transport through the cytoplasmic membrane is spatially and temporally uncoupled from transport through the outer membrane and whether it occurs at specific sites.

In this work, we have shown that DNA uptake over the outer membrane is powered by ComE from within the periplasm and can thus be uncoupled from transport over the inner membrane. As DNA-ComE complexes in the periplasm are usually stable for more than 30 min, we expect DNA transport through the inner membrane to be temporally separated from outer membrane transport. Rearrangement of DNA within the periplasm leads to an accumulation of DNA at the septum of a diplococcus, which marks the current or former site of cell division in *N. gonorrhoeae*. In some rod-like bacteria like *B. subtilis*, cytoplasmic import happens at the cell poles [231, 293]. Similarly, it is conceivable that cocci import DNA at the septum. In *S. pneumoniae*, the competence-associated nuclease EndA locates at the septum upon competence induction [294]. Moreover, the involvement of the cell division and peptidoglycan binding proteins Tpc and ComL in *N. gonorrhoeae* suggests a possible functional connection of transformation and the cell cycle [216, 217]. Indeed, genome maintenance might require a coordination of the two processes.

To test the hypothesis of temporal and spatial separation, we aim to track DNA uptake over the inner membrane. For this purpose, we set out to create fluorescent fusion proteins from two key players of cytoplasmic DNA import, the inner membrane channel ComA and the cytoplasmic ssDNA binding protein DprA. By observing intracellular localization and spatial rearrangements of these proteins, we expect to either find static DNA import complexes at specific sites in the cell or to be able to observe DNA uptake by colocalization of proteins with parts of the DNA uptake machinery, ComE-mCherry or labeled DNA.

5.2 Localization and quantification of ComA

ComA is a polytopic transmembrane protein that is essential for transformation and highly conserved in all studied naturally transformable species [4, 233]. It is essential for translocation of ssDNA into the cytoplasm. The C-terminal β -lactamase-like domain has recently been shown to carry a putative zinc binding motif and has been proposed to have a nucleolytic function [214]. ComA is expected to form homodimers analogous to the related family of ABC transporters. In *B. subtilis*, the ComEC ortholog is considered to work in conjunction with the DEAD -box ATPase ComFA that controls the rate of DNA uptake into the cytoplasm [283].

In order to study whether ComA occupies a specific position within the cell, we replaced the ComA ORF by a C-terminal ComA-mCherry protein fusion. The transformation efficiency of the *comE-mcherry* fusion strain was comparable to the wild type, while a deletion of ComA abrogates transformation, thus indicating the functionality of the protein fusion.

Strikingly, the level of fluorescent ComA-mCherry was very low and required detection by a camera equipped with an amplifier for single molecule sensitivity. To assess the total number of fluorescent molecules per cell, we performed quantification of fluorescent molecules by photobleaching [295]. First, the fluorescence intensity of single molecules was determined by the mean value of several individual bleaching events. Subsequently, the intensity of single molecules was compared to whole-cell fluorescence. Our preliminary results show that on average, a cell only contains ~6 fluorescent molecules. Under the assumption that ComA forms homodimers, this means each cell would contain only three functional ComA channels on

average. However, not all mCherry domains might be matured at the time of acquisition. Thus, the average maturation time of the ComA-mCherry protein fusion should be assessed to introduce a correction factor for the determination. In agreement with the low expression level, ComA subunits or complexes were detected as foci around the cell contour of gonococci (Figure 5.1a). No specific location of ComA with respect to the septum could be observed in diplococci. Hence, a specific position of cytoplasmic DNA import could not be inferred from the localization of ComA alone. Subsequently, we tested the alternative hypothesis that ComA is localized at the site of uptake over the outer membrane, possibly by interaction with the type IV pilus machinery. Colocalization experiments of Cy5-DNA foci and ComA-mCherry revealed no good match the two signals, indicating either DNA and or ComA generally have to rearrange for efficient translocation (Figure 5.1).

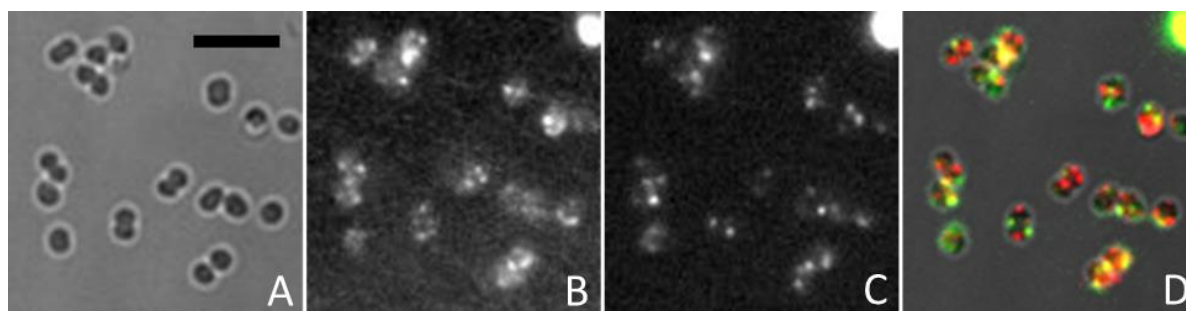


Figure 5.1 Localization of ComA-mCherry in comparison to imported Cy5-DNA. (A) Brightfield image. (B) ComA-mCherry fluorescence image. (C) Cy5-DNA fluorescence image (D) Overlay of A, B (red) and C (green). Scale bar: 4 μm .

5.3 Tracking DNA uptake by accumulation of DprA

DprA is a cytoplasmatic ssDNA binding protein that is either essential for natural transformation or required for full efficiency thereof in various transformable species [224]. Moreover, it has been found to be absolutely required for natural transformation in *N. gonorrhoeae* [296]. In *B. subtilis*, DprA is located to the cell pole together with other components of the transformation machinery [293]. Experiments with DprA in *B. subtilis*

indicate, that it protects DNA from degradation and initiates the loading of RecA onto the translocated fragment [225]. Due to this function, we expect DprA to colocalize with DNA right after import into the cytoplasm, indicating the location of DNA entry. Hence, accumulation of a fluorescent DprA fusion protein upon DNA incubation might enable us to mark the site of DNA import into the cytoplasm. Coating by RecA subsequently initiates homologous recombination of the fragment into the genome. In *V. cholerae*, RecA-GFP has been previously employed to detect DNA translocation into the periplasm [297]. Upon DNA addition, the frequency of fluorescent RecA foci increased and colocalized with fluorescent ComE foci, indicating DNA import through the outer and inner membrane is spatially coupled in *V. cholerae*. However, RecA foci were present in the absence of transforming DNA [297].

As DprA binding should be more specific and is supposed to precede RecA binding, we chose to track a fluorescent DprA-YFP fusion protein, replacing DprA in its native locus. Like *comA-mcherry*, *dprA-yfp* shows transformation efficiencies comparable with the wildtype *dprA* strain. In contrast, and consistent with recent reports [296], a *dprA* deletion was non-transformable.

In the majority of cells, the YFP signal was homogenously distributed in the periplasm (Figure 5.2). Preliminary results indicate that in about 10 % of the cells DprA-YFP foci manifested with a tendency towards the periphery of the cell (Figure 5.2). However, in preliminary experiments formation of these foci was observed in the presence and absence of external DNA alike. Thus, we hypothesized that DprA might readily accumulate at the future site of cytoplasmic DNA import by interaction with other components of the DNA import machinery. We tested *pilQ*, *pilT* and *comA* deletion strains, none of which showed a striking reduction in DprA-YFP foci in preliminary experiments, indicating neither the type IV pilus nor the inner membrane channel ComA recruits DprA.

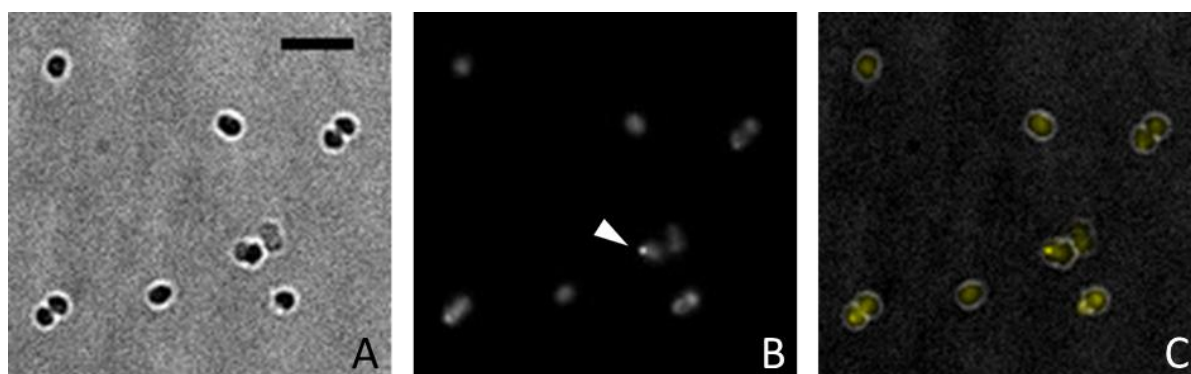


Figure 5.2 The cellular distribution of DprA-YFP in *N. gonorrhoeae*. (A) Brightfield image. (B) DprA-YFP fluorescence image. The white arrow denotes a peripheral DprA-YFP focus, as seen in roughly 10% of the cells. (C) Overlay of A, B. Scale bar: 4 μ m

5.4 Discussion of preliminary results

Preliminary experiments showed remarkably low expression levels and no site-specific localization of ComA in diplococci. Predominantly, *N. gonorrhoeae* cells remain associated after cell division, which results in their diplococcal morphology. As a consequence, the septum of a diplococcus might no longer be the active site of cell division. If the site of cell division cannot be known with certainty, the localization of ComA with respect to it cannot be correctly assessed. To allow a more precise determination of the division site, structural proteins associated with cell division can be fluorescently tagged and tracked. In our group, a fluorescent fusion of FtsZ with mCherry has recently been generated, allowing determination of the active cell division axis. It will be very interesting to assess whether the DprA foci colocalize with the FtsZ ring. As both FtsZ and ComA are tagged with mCherry, new fluorescent protein fusions have to be designed for colocalization experiments of the two proteins.

At first glance, DprA foci could neither be associated with DNA import events nor with the DNA import machinery. One possible explanation for this is the relative rarity of cytoplasmic DNA import in comparison to periplasmic DNA import. Moreover, DprA has been shown to modulate pilin antigenic variation independently of transformation [296]. Thus, the majority of the observed DprA-YFP foci might arise from cellular events not associated with transformation. However, the tendency for foci to occur near the periphery of the cell suggests otherwise. DprA foci arising from DNA import might actually be so transient they are

underrepresented in snapshots of a cell population compared to transformation-independent DprA foci. To detect them anyway, time-lapse microscopy at a high temporal resolution might be required. Alternatively, DprA might readily be recruited to the periphery of the cell by an unknown interaction partner, before DNA import into the cytoplasm even begins. This unknown protein might in turn recruit ComA and thus determine the site of cytoplasmic DNA import. Protein interaction studies can contribute to the identification of a putative cytoplasmic DNA import complex.

6 Abstract

Competence for natural transformation is widespread among bacterial species. In the case of Gram-negative systems, a key step to transformation is the import of DNA across the outer membrane. Although the proteins essential for transformation have been identified, the mechanism of DNA uptake remains to be elucidated. In this work, we combine fluorescence microscopy, nanomanipulation by optical tweezers and molecular biological techniques. Employing these methods, we reveal the mechanistic role of the periplasmic DNA binding protein ComE in DNA uptake over the outer membrane and compare the uptake efficiency of double-stranded DNA (dsDNA) and single-stranded DNA (ssDNA).

We have shown that the periplasmic DNA binding protein ComE forms complexes with imported DNA at the site of DNA uptake in *Neisseria gonorrhoeae*. These relatively stable complexes support the accumulation of ample amounts of DNA within the gonococcal periplasm in a gene-dosage dependent fashion.

Further, we provided evidence that ComE powers DNA uptake over the outer membrane of Gram negative bacteria via a translocation ratchet mechanism. In this type of active transport, the diffusion of a biopolymer inside a membrane pore is rectified by the binding of chaperones inside the target compartment. Our evidence can be divided into three parts: 1. The force-velocity relationship of DNA uptake is in very good agreement with a theoretical description of a translocation ratchet mechanism. 2. The velocity of DNA uptake depends on the concentration of ComE. 3. The force-velocity relationship of type IV pilus retraction excludes it as a power source for DNA uptake.

Finally, we characterized DNA uptake and transformation of dsDNA and ssDNA in *N. gonorrhoeae*. For successful DNA uptake as a prerequisite for transformation, DNA has to bind to the cell surface in a first step in order to be transported across the outer membrane in a second step. We found that a double-stranded DNA uptake sequence (DUS) is required for species-

specific DNA recognition and binding in the first step. In contrast, the kinetics of DNA transport in the second step are comparable for dsDNA and ssDNA, which is consistent with a ComE-dependent translocation ratchet mechanism.

Based on our findings, we propose a more precise mechanistic model for the DNA uptake process into the periplasm of Gram negative bacteria. Initially, a type IV competence pilus binds DNA at the surface of the cell and threads it into the periplasm by pilus retraction. In a second step, ComE binds to periplasmic DNA and powers transport via a translocation ratchet mechanism. While the secondary structure of DNA is important for initial, species-specific DNA binding, it is irrelevant for DNA transport. A second, stronger molecular motor transports the transforming DNA from the periplasm to the cytoplasm.

7 Zusammenfassung

Die Kompetenz für die natürliche Transformation ist in Bakterien weit verbreitet. In gramnegativen Systemen stellt der DNA-Import über die äußere Membran einen entscheidenden Schritt für die Transformation dar. Obwohl die für die Transformation notwendigen Proteine identifiziert sind, musste der Mechanismus der DNA-Aufnahme noch geklärt werden. In dieser Arbeit kombinieren wir Fluoreszenzmikroskopie, Nanomanipulation durch eine optische Pinzette und molekularbiologische Techniken. Mithilfe dieser Methoden klärten wir die mechanistische Rolle des periplasmatischen DNA-Bindeproteins ComE in der DNA-Aufnahme über die äußere Membran und vergleichen die Aufnahmeeffizienz doppelsträngiger und einzelsträngiger DNA (dsDNA und ssDNA).

Wir zeigten, dass das periplasmatische DNA-Bindeprotein ComE in *N. gonorrhoeae* mit importierter DNA an der Stelle der DNA-Aufnahme Komplexe bildet. Diese recht stabilen Komplexe erlauben die Ansammlung beachtlicher DNA-Mengen im Periplasma der Gonokokken in Abhängigkeit von der ComE-Konzentration

Außerdem wiesen wir nach, dass ComE die DNA-Aufnahme über die äußere Membran gramnegativer Bakterien durch einen Translokationsratschen-Mechanismus antreibt. Bei dieser Art des aktiven Transports wird die Diffusion eines Biopolymers innerhalb einer Membranpore durch die Bindung von Chaperonen im Zielkompartiment ausgerichtet. Unser Nachweis gliedert sich in drei Teile: 1. Die kraftabhängige DNA-Aufnahmegeschwindigkeit stimmt sehr gut mit der theoretischen Beschreibung einer Translokationsratsche überein. 2. Die DNA-Aufnahmegeschwindigkeit hängt von der ComE-Konzentration ab. 3. Die kraftabhängige Geschwindigkeit der Typ-IV-Pilusretraktion schließt selbige als einen Antrieb für die DNA-Aufnahme aus.

Schließlich charakterisierten wir DNA-Aufnahme und Transformation von dsDNA und ssDNA in *N. gonorrhoeae*. Erfolgreiche DNA-Aufnahme ist eine Voraussetzung für die

Transformation. Dafür muss DNA in einem ersten Schritt an die Zelle binden, um in einem zweiten Schritt über die Membran transportiert zu werden. Wir fanden heraus, dass eine doppelsträngige DNA-Aufnahmesequenz (DUS) für die spezifische DNA-Erkennung und Bindung notwendig ist. Demgegenüber ist die Kinetik des DNA-Transports im zweiten Schritt für dsDNA und ssDNA vergleichbar, was mit einem ComE-abhängigen Translokationsratschen-Mechanismus übereinstimmt.

Aufgrund unserer Erkenntnisse schlagen wir ein genaueres mechanistisches Model für den DNA-Aufnahmemechanismus ins Periplasma gramnegativer Bakterien vor. Zuerst bindet ein Typ-IV-Kompetenzpilus DNA an der Zelloberfläche und fädelt sie durch Pilusretraktion ins Periplasma ein. In einem zweiten Schritt bindet dann ComE an die periplasmatische DNA und treibt den Transport durch einen Translokationsratschen-Mechanismus an. Ein zweiter, stärkerer Motor transportiert die transformierende DNA daraufhin ins Cytoplasma.

8 References

1. Garcia-Vallve, S., et al., *HGT-DB: a database of putative horizontally transferred genes in prokaryotic complete genomes*. Nucleic Acids Res, 2003. **31**(1): p. 187-9.
2. Lorenz, M.G. and W. Wackernagel, *Bacterial gene transfer by natural genetic transformation in the environment*. Microbiol Rev, 1994. **58**(3): p. 563-602.
3. Luo, Y. and A. Wasserfallen, *Gene transfer systems and their applications in Archaea*. Syst Appl Microbiol, 2001. **24**(1): p. 15-25.
4. Chen, I. and D. Dubnau, *DNA uptake during bacterial transformation*. Nat Rev Microbiol, 2004. **2**(3): p. 241-9.
5. Johnsborg, O., V. Eldholm, and L.S. Havarstein, *Natural genetic transformation: prevalence, mechanisms and function*. Res Microbiol, 2007. **158**(10): p. 767-78.
6. Ambur, O.H., S.A. Frye, and T. Tonjum, *New functional identity for the DNA uptake sequence in transformation and its presence in transcriptional terminators*. J Bacteriol, 2007. **189**(5): p. 2077-85.
7. Davidsen, T., et al., *Biased distribution of DNA uptake sequences towards genome maintenance genes*. Nucleic Acids Res, 2004. **32**(3): p. 1050-8.
8. Smith, H.O., M.L. Gwinn, and S.L. Salzberg, *DNA uptake signal sequences in naturally transformable bacteria*. Res Microbiol, 1999. **150**(9-10): p. 603-16.
9. Palmen, R. and K.J. Hellingwerf, *Uptake and processing of DNA by Acinetobacter calcoaceticus--a review*. Gene, 1997. **192**(1): p. 179-90.
10. Saunders, N.J., J.F. Peden, and E.R. Moxon, *Absence in Helicobacter pylori of an uptake sequence for enhancing uptake of homospecific DNA during transformation*. Microbiology, 1999. **145** (Pt 12): p. 3523-8.
11. Claverys, J.P. and L.S. Havarstein, *Cannibalism and fratricide: mechanisms and raisons d'etre*. Nat Rev Microbiol, 2007. **5**(3): p. 219-29.
12. Hamilton, H.L. and J.P. Dillard, *Natural transformation of Neisseria gonorrhoeae: from DNA donation to homologous recombination*. Mol Microbiol, 2006. **59**(2): p. 376-85.
13. Hamoen, L.W., G. Venema, and O.P. Kuipers, *Controlling competence in Bacillus subtilis: shared use of regulators*. Microbiology, 2003. **149**(Pt 1): p. 9-17.
14. Redfield, R.J., et al., *A novel CRP-dependent regulon controls expression of competence genes in Haemophilus influenzae*. J Mol Biol, 2005. **347**(4): p. 735-47.
15. Claverys, J.-P., M. Prudhomme, and B. Martin, *Induction of Competence Regulons as a General Response to Stress in Gram-Positive Bacteria*. Annual Review of Microbiology, 2006. **60**(1): p. 451-475.
16. Redfield, R.J., *Evolution of bacterial transformation: is sex with dead cells ever better than no sex at all?* Genetics, 1988. **119**(1): p. 213-221.
17. Redfield, R.J., *Do bacteria have sex?* Nat Rev Genet, 2001. **2**(8): p. 634-639.

18. Szollosi, G.J., I. Derenyi, and T. Vellai, *The maintenance of sex in bacteria is ensured by its potential to reload genes*. Genetics, 2006. **174**(4): p. 2173-80.
19. Baltrus, D.A., *Exploring the costs of horizontal gene transfer*. Trends in ecology & evolution, 2013. **28**(8): p. 489-95.
20. Frye, S.A., et al., *Dialects of the DNA uptake sequence in Neisseriaceae*. PLoS genetics, 2013. **9**(4): p. e1003458.
21. Ambur, O.H., et al., *Steady at the wheel: conservative sex and the benefits of bacterial transformation*. Philos Trans R Soc Lond B Biol Sci, 2016. **371**(1706).
22. Finkel, S.E. and R. Kolter, *DNA as a nutrient: novel role for bacterial competence gene homologs*. J Bacteriol, 2001. **183**(21): p. 6288-93.
23. Palmen, R., P. Buijsman, and K.J. Hellingwerf, *Physiological regulation of competence induction for natural transformation in Acinetobacter calcoaceticus*. Archives of Microbiology, 1994. **162**(5): p. 344-351.
24. Blomqvist, T., H. Steinmoen, and L.S. Havarstein, *Natural genetic transformation: A novel tool for efficient genetic engineering of the dairy bacterium Streptococcus thermophilus*. Appl Environ Microbiol, 2006. **72**(10): p. 6751-6.
25. Dillard, J.P. and H.S. Seifert, *A variable genetic island specific for Neisseria gonorrhoeae is involved in providing DNA for natural transformation and is found more often in disseminated infection isolates*. Mol Microbiol, 2001. **41**(1): p. 263-77.
26. Baron, C., *VirB8: a conserved type IV secretion system assembly factor and drug target*. Biochem Cell Biol, 2006. **84**(6): p. 890-9.
27. Cascales, E. and P.J. Christie, *The versatile bacterial type IV secretion systems*. Nat Rev Microbiol, 2003. **1**(2): p. 137-49.
28. Voth, D.E., L.J. Broderdorf, and J.G. Graham, *Bacterial Type IV secretion systems: versatile virulence machines*. Future Microbiol, 2012. **7**(2): p. 241-57.
29. Hamilton, H.L., K.J. Schwartz, and J.P. Dillard, *Insertion-duplication mutagenesis of neisseria: use in characterization of DNA transfer genes in the gonococcal genetic island*. J Bacteriol, 2001. **183**(16): p. 4718-26.
30. Hamilton, H.L., et al., *Neisseria gonorrhoeae secretes chromosomal DNA via a novel type IV secretion system*. Mol Microbiol, 2005. **55**(6): p. 1704-21.
31. Guiral, S., et al., *Competence-programmed predation of noncompetent cells in the human pathogen Streptococcus pneumoniae: genetic requirements*. Proc Natl Acad Sci U S A, 2005. **102**(24): p. 8710-5.
32. Moscoso, M. and J.-P. Claverys, *Release of DNA into the medium by competent Streptococcus pneumoniae: kinetics, mechanism and stability of the liberated DNA*. Molecular Microbiology, 2004. **54**(3): p. 783-794.
33. Steinmoen, H., E. Knutsen, and L.S. Havarstein, *Induction of natural competence in Streptococcus pneumoniae triggers lysis and DNA release from a subfraction of the cell population*. Proc Natl Acad Sci U S A, 2002. **99**(11): p. 7681-6.
34. Steinmoen, H., A. Teigen, and L.S. Havarstein, *Competence-induced cells of Streptococcus pneumoniae lyse competence-deficient cells of the same strain during cocultivation*. J Bacteriol, 2003. **185**(24): p. 7176-83.
35. Claverys, J.P., B. Martin, and L.S. Havarstein, *Competence-induced fratricide in streptococci*. Mol Microbiol, 2007. **64**(6): p. 1423-33.
36. Borgeaud, S., et al., *The type VI secretion system of Vibrio cholerae fosters horizontal gene transfer*. Science, 2015. **347**(6217): p. 63-7.
37. Mejean, V. and J.P. Claverys, *DNA processing during entry in transformation of Streptococcus pneumoniae*. J Biol Chem, 1993. **268**(8): p. 5594-9.
38. Morrison, D.A., *Transformation in pneumococcus: protein content of eclipse complex*. J Bacteriol, 1978. **136**(2): p. 548-57.

39. Grove, D.E., et al., *Differential single-stranded DNA binding properties of the paralogous SsbA and SsbB proteins from Streptococcus pneumoniae*. J Biol Chem, 2005. **280**(12): p. 11067-73.
40. Berge, M., et al., *Transformation of Streptococcus pneumoniae relies on DprA- and RecA-dependent protection of incoming DNA single strands*. Mol Microbiol, 2003. **50**(2): p. 527-36.
41. Chi, F., et al., *Crossing the barrier: evolution and spread of a major class of mosaic pbp2x in Streptococcus pneumoniae, S. mitis and S. oralis*. Int J Med Microbiol, 2007. **297**(7-8): p. 503-12.
42. *Global incidence and prevalence of selected curable sexually transmitted infections: 2008*. Reproductive Health Matters, 2012. **20**(40): p. 207-209.
43. Criss, A.K. and H.S. Seifert, *A bacterial siren song: intimate interactions between Neisseria and neutrophils*. Nat Rev Microbiol, 2012. **10**(3): p. 178-90.
44. Shafer, W.M. and R.F. Rest, *Interactions of gonococci with phagocytic cells*. Annu Rev Microbiol, 1989. **43**: p. 121-45.
45. Workowski, K.A., et al., *Sexually transmitted diseases treatment guidelines, 2010*. MMWR Recomm Rep, 2010. **59**(RR-12): p. 1-110.
46. Rotman, E. and H.S. Seifert, *The genetics of Neisseria species*. Annual review of genetics, 2014. **48**: p. 405-31.
47. Smith, J.M., et al., *How clonal are bacteria?* Proc Natl Acad Sci U S A, 1993. **90**(10): p. 4384-8.
48. Haubold, B., et al., *Detecting linkage disequilibrium in bacterial populations*. Genetics, 1998. **150**(4): p. 1341-8.
49. Allen, V.G., et al., *Neisseria gonorrhoeae treatment failure and susceptibility to cefixime in Toronto, Canada*. JAMA, 2013. **309**(2): p. 163-70.
50. Lahra, M.M., W.H.O.W. Pacific, and P. South East Asian Gonococcal Antimicrobial Surveillance, *Surveillance of antibiotic resistance in Neisseria gonorrhoeae in the WHO Western Pacific and South East Asian Regions, 2010*. Commun Dis Intell Q Rep, 2012. **36**(1): p. 95-100.
51. Workowski, K.A., S.M. Berman, and J.M. Douglas, Jr., *Emerging antimicrobial resistance in Neisseria gonorrhoeae: urgent need to strengthen prevention strategies*. Ann Intern Med, 2008. **148**(8): p. 606-13.
52. Tobiason, D.M. and H.S. Seifert, *The obligate human pathogen, Neisseria gonorrhoeae, is polyploid*. PLoS Biol, 2006. **4**(6): p. e185.
53. Tobiason, D.M. and H.S. Seifert, *Genomic content of Neisseria species*. J Bacteriol, 2010. **192**(8): p. 2160-8.
54. Marri, P.R., et al., *Genome sequencing reveals widespread virulence gene exchange among human Neisseria species*. PLoS One, 2010. **5**(7): p. e11835.
55. Parkhill, J., et al., *Complete DNA sequence of a serogroup A strain of Neisseria meningitidis Z2491*. Nature, 2000. **404**(6777): p. 502-6.
56. Buisine, N., C.M. Tang, and R. Chalmers, *Transposon-like Correia elements: structure, distribution and genetic exchange between pathogenic Neisseria sp.* FEBS Lett, 2002. **522**(1-3): p. 52-8.
57. Correia, F.F., S. Inouye, and M. Inouye, *A 26-base-pair repetitive sequence specific for Neisseria gonorrhoeae and Neisseria meningitidis genomic DNA*. J Bacteriol, 1986. **167**(3): p. 1009-15.
58. Correia, F.F., S. Inouye, and M. Inouye, *A family of small repeated elements with some transposon-like properties in the genome of Neisseria gonorrhoeae*. J Biol Chem, 1988. **263**(25): p. 12194-8.

59. Liu, S.V., et al., *Genome analysis and strain comparison of correia repeats and correia repeat-enclosed elements in pathogenic Neisseria*. J Bacteriol, 2002. **184**(22): p. 6163-73.
60. Saunders, N.J. and L.A. Snyder, *The minimal mobile element*. Microbiology, 2002. **148**(Pt 12): p. 3756-60.
61. Snyder, L.A., et al., *The repertoire of minimal mobile elements in the Neisseria species and evidence that these are involved in horizontal gene transfer in other bacteria*. Mol Biol Evol, 2007. **24**(12): p. 2802-15.
62. Spencer-Smith, R., et al., *Sequence features contributing to chromosomal rearrangements in Neisseria gonorrhoeae*. PLoS One, 2012. **7**(9): p. e46023.
63. Schoen, C., et al., *Whole-genome comparison of disease and carriage strains provides insights into virulence evolution in Neisseria meningitidis*. Proc Natl Acad Sci U S A, 2008. **105**(9): p. 3473-8.
64. Francis, F., et al., *Organization and transcription of the division cell wall (dcw) cluster in Neisseria gonorrhoeae*. Gene, 2000. **251**(2): p. 141-51.
65. Siddique, A., N. Buisine, and R. Chalmers, *The transposon-like Correia elements encode numerous strong promoters and provide a potential new mechanism for phase variation in the meningococcus*. PLoS Genet, 2011. **7**(1): p. e1001277.
66. Snyder, L.A., J.A. Cole, and M.J. Pallen, *Comparative analysis of two Neisseria gonorrhoeae genome sequences reveals evidence of mobilization of Correia Repeat Enclosed Elements and their role in regulation*. BMC Genomics, 2009. **10**: p. 70.
67. Snyder, L.A., W.M. Shafer, and N.J. Saunders, *Divergence and transcriptional analysis of the division cell wall (dcw) gene cluster in Neisseria spp*. Mol Microbiol, 2003. **47**(2): p. 431-42.
68. Woodhams, K.L., et al., *Prevalence and detailed mapping of the gonococcal genetic island in Neisseria meningitidis*. J Bacteriol, 2012. **194**(9): p. 2275-85.
69. Snyder, L.A., S.A. Jarvis, and N.J. Saunders, *Complete and variant forms of the 'gonococcal genetic island' in Neisseria meningitidis*. Microbiology, 2005. **151**(Pt 12): p. 4005-13.
70. Dominguez, N.M., K.T. Hackett, and J.P. Dillard, *XerCD-mediated site-specific recombination leads to loss of the 57-kilobase gonococcal genetic island*. J Bacteriol, 2011. **193**(2): p. 377-88.
71. Jain, S., et al., *Characterization of the single stranded DNA binding protein SsbB encoded in the Gonococcal Genetic Island*. PLoS One, 2012. **7**(4): p. e35285.
72. Moxon, R., C. Bayliss, and D. Hood, *Bacterial contingency loci: the role of simple sequence DNA repeats in bacterial adaptation*. Annu Rev Genet, 2006. **40**: p. 307-33.
73. Jordan, P.W., L.A. Snyder, and N.J. Saunders, *Strain-specific differences in Neisseria gonorrhoeae associated with the phase variable gene repertoire*. BMC Microbiol, 2005. **5**: p. 21.
74. Saunders, N.J., et al., *Repeat-associated phase variable genes in the complete genome sequence of Neisseria meningitidis strain MC58*. Mol Microbiol, 2000. **37**(1): p. 207-15.
75. Snyder, L.A., S.A. Butcher, and N.J. Saunders, *Comparative whole-genome analyses reveal over 100 putative phase-variable genes in the pathogenic Neisseria spp*. Microbiology, 2001. **147**(Pt 8): p. 2321-32.
76. Bayliss, C.D., et al., *Neisseria meningitidis escape from the bactericidal activity of a monoclonal antibody is mediated by phase variation of lgtG and enhanced by a mutator phenotype*. Infect Immun, 2008. **76**(11): p. 5038-48.
77. Tauseef, I., Y.M. Ali, and C.D. Bayliss, *Phase variation of PorA, a major outer membrane protein, mediates escape of bactericidal antibodies by Neisseria meningitidis*. Infect Immun, 2013. **81**(4): p. 1374-80.

78. Levinson, G. and G.A. Gutman, *Slipped-strand mispairing: a major mechanism for DNA sequence evolution*. Mol Biol Evol, 1987. **4**(3): p. 203-21.
79. Murphy, G.L., et al., *Phase variation of gonococcal protein II: regulation of gene expression by slipped-strand mispairing of a repetitive DNA sequence*. Cell, 1989. **56**(4): p. 539-47.
80. De Bolle, X., et al., *The length of a tetranucleotide repeat tract in Haemophilus influenzae determines the phase variation rate of a gene with homology to type III DNA methyltransferases*. Mol Microbiol, 2000. **35**(1): p. 211-22.
81. Richardson, A.R., et al., *Mutator clones of Neisseria meningitidis in epidemic serogroup A disease*. Proc Natl Acad Sci U S A, 2002. **99**(9): p. 6103-7.
82. Jennings, M.P., et al., *The genetic basis of the phase variation repertoire of lipopolysaccharide immunotypes in Neisseria meningitidis*. Microbiology, 1999. **145** (Pt 11): p. 3013-21.
83. Martin, P., et al., *Microsatellite instability regulates transcription factor binding and gene expression*. Proc Natl Acad Sci U S A, 2005. **102**(10): p. 3800-4.
84. Metruccio, M.M., et al., *A novel phase variation mechanism in the meningococcus driven by a ligand-responsive repressor and differential spacing of distal promoter elements*. PLoS Pathog, 2009. **5**(12): p. e1000710.
85. Jordan, P., L.A. Snyder, and N.J. Saunders, *Diversity in coding tandem repeats in related Neisseria spp.* BMC Microbiol, 2003. **3**: p. 23.
86. Hall, L.M. and S.K. Henderson-Begg, *Hypermutable bacteria isolated from humans--a critical analysis*. Microbiology, 2006. **152**(Pt 9): p. 2505-14.
87. Levinson, G. and G.A. Gutman, *High frequencies of short frameshifts in poly-CA/TG tandem repeats borne by bacteriophage M13 in Escherichia coli K-12*. Nucleic Acids Res, 1987. **15**(13): p. 5323-38.
88. Sparling, P.F., *Genetic transformation of Neisseria gonorrhoeae to streptomycin resistance*. J Bacteriol, 1966. **92**(5): p. 1364-71.
89. Swanson, J., *Studies on gonococcus infection. IV. Pili: their role in attachment of gonococci to tissue culture cells*. J Exp Med, 1973. **137**(3): p. 571-89.
90. Wolfgang, M., et al., *PilT mutations lead to simultaneous defects in competence for natural transformation and twitching motility in piliated Neisseria gonorrhoeae*. Molecular microbiology, 1998. **29**(1): p. 321-30.
91. Hamrick, T.S., et al., *Antigenic variation of gonococcal pilin expression in vivo: analysis of the strain FA1090 pilin repertoire and identification of the pilS gene copies recombining with pilE during experimental human infection*. Microbiology, 2001. **147**(Pt 4): p. 839-49.
92. Haas, R. and T.F. Meyer, *The repertoire of silent pilus genes in Neisseria gonorrhoeae: evidence for gene conversion*. Cell, 1986. **44**(1): p. 107-15.
93. Forest, K.T., et al., *Assembly and antigenicity of the Neisseria gonorrhoeae pilus mapped with antibodies*. Infect Immun, 1996. **64**(2): p. 644-52.
94. Aho, E.L., A.M. Keating, and S.M. McGillivray, *A comparative analysis of pilin genes from pathogenic and nonpathogenic Neisseria species*. Microb Pathog, 2000. **28**(2): p. 81-8.
95. Aho, E.L., et al., *Characterization of a class II pilin expression locus from Neisseria meningitidis: evidence for increased diversity among pilin genes in pathogenic Neisseria species*. Infect Immun, 1997. **65**(7): p. 2613-20.
96. Helm, R.A. and H.S. Seifert, *Frequency and rate of pilin antigenic variation of Neisseria meningitidis*. J Bacteriol, 2010. **192**(14): p. 3822-3.
97. Seifert, H.S., et al., *Multiple gonococcal pilin antigenic variants are produced during experimental human infections*. J Clin Invest, 1994. **93**(6): p. 2744-9.

98. Hill, S.A. and C.C. Grant, *Recombinational error and deletion formation in Neisseria gonorrhoeae: a role for RecJ in the production of pilE (L) deletions*. Mol Genet Genomics, 2002. **266**(6): p. 962-72.
99. Koomey, M., et al., *Effects of recA mutations on pilus antigenic variation and phase transitions in Neisseria gonorrhoeae*. Genetics, 1987. **117**(3): p. 391-8.
100. Mehr, I.J. and H.S. Seifert, *Differential roles of homologous recombination pathways in Neisseria gonorrhoeae pilin antigenic variation, DNA transformation and DNA repair*. Mol Microbiol, 1998. **30**(4): p. 697-710.
101. Sechman, E.V., K.A. Kline, and H.S. Seifert, *Loss of both Holliday junction processing pathways is synthetically lethal in the presence of gonococcal pilin antigenic variation*. Mol Microbiol, 2006. **61**(1): p. 185-93.
102. Sechman, E.V., M.S. Rohrer, and H.S. Seifert, *A genetic screen identifies genes and sites involved in pilin antigenic variation in Neisseria gonorrhoeae*. Mol Microbiol, 2005. **57**(2): p. 468-83.
103. Skaar, E.P., M.P. Lazio, and H.S. Seifert, *Roles of the recJ and recN genes in homologous recombination and DNA repair pathways of Neisseria gonorrhoeae*. J Bacteriol, 2002. **184**(4): p. 919-27.
104. Stohl, E.A. and H.S. Seifert, *The recX gene potentiates homologous recombination in Neisseria gonorrhoeae*. Mol Microbiol, 2001. **40**(6): p. 1301-10.
105. Serkin, C.D. and H.S. Seifert, *Iron availability regulates DNA recombination in Neisseria gonorrhoeae*. Mol Microbiol, 2000. **37**(5): p. 1075-86.
106. Cahoon, L.A. and H.S. Seifert, *An alternative DNA structure is necessary for pilin antigenic variation in Neisseria gonorrhoeae*. Science, 2009. **325**(5941): p. 764-7.
107. Cahoon, L.A. and H.S. Seifert, *Transcription of a cis-acting, noncoding, small RNA is required for pilin antigenic variation in Neisseria gonorrhoeae*. PLoS Pathog, 2013. **9**(1): p. e1003074.
108. Biswas, G.D., et al., *Factors affecting genetic transformation of Neisseria gonorrhoeae*. J Bacteriol, 1977. **129**(2): p. 983-92.
109. Solomon, J.M., B.A. Lazazzera, and A.D. Grossman, *Purification and characterization of an extracellular peptide factor that affects two different developmental pathways in Bacillus subtilis*. Genes Dev, 1996. **10**(16): p. 2014-24.
110. Chaussee, M.S. and S.A. Hill, *Formation of single-stranded DNA during DNA transformation of Neisseria gonorrhoeae*. Journal of bacteriology, 1998. **180**(19): p. 5117-22.
111. Stein, D.C., *Transformation of Neisseria gonorrhoeae: physical requirements of the transforming DNA*. Can J Microbiol, 1991. **37**(5): p. 345-9.
112. Duffin, P.M. and H.S. Seifert, *DNA uptake sequence-mediated enhancement of transformation in Neisseria gonorrhoeae is strain dependent*. J Bacteriol, 2010. **192**(17): p. 4436-44.
113. Boyle-Vavra, S. and H.S. Seifert, *Uptake-sequence-independent DNA transformation exists in Neisseria gonorrhoeae*. Microbiology, 1996. **142** (Pt 10): p. 2839-45.
114. Cehovin, A., et al., *Specific DNA recognition mediated by a type IV pilin*. Proceedings of the National Academy of Sciences of the United States of America, 2013. **110**(8): p. 3065-70.
115. Ambur, O.H., et al., *Restriction and sequence alterations affect DNA uptake sequence-dependent transformation in Neisseria meningitidis*. PLoS One, 2012. **7**(7): p. e39742.
116. Goodman, S.D. and J.J. Scocca, *Identification and arrangement of the DNA sequence recognized in specific transformation of Neisseria gonorrhoeae*. Proc Natl Acad Sci U S A, 1988. **85**(18): p. 6982-6.

117. Sadarangani, M., et al., *Construction of Opa-positive and Opa-negative strains of Neisseria meningitidis to evaluate a novel meningococcal vaccine*. PLoS One, 2012. **7**(12): p. e51045.
118. Dillard, J.P., *Genetic Manipulation of Neisseria gonorrhoeae*. Curr Protoc Microbiol, 2011. **Chapter 4**: p. Unit4A 2.
119. Carrasco, B., et al., *Chromosomal transformation in Bacillus subtilis is a non-polar recombination reaction*. Nucleic Acids Res, 2016. **44**(6): p. 2754-68.
120. Facius, D. and T.F. Meyer, *A novel determinant (comA) essential for natural transformation competence in Neisseria gonorrhoeae and the effect of a comA defect on pilin variation*. Mol Microbiol, 1993. **10**(4): p. 699-712.
121. Roberts, R.J., et al., *REBASE--a database for DNA restriction and modification: enzymes, genes and genomes*. Nucleic Acids Res, 2015. **43**(Database issue): p. D298-9.
122. Stein, D.C., et al., *Restriction and modification systems of Neisseria gonorrhoeae*. Gene, 1995. **157**(1-2): p. 19-22.
123. Budroni, S., et al., *Neisseria meningitidis is structured in clades associated with restriction modification systems that modulate homologous recombination*. Proc Natl Acad Sci U S A, 2011. **108**(11): p. 4494-9.
124. Kobayashi, I., *Behavior of restriction-modification systems as selfish mobile elements and their impact on genome evolution*. Nucleic Acids Res, 2001. **29**(18): p. 3742-56.
125. Jansen, R., et al., *Identification of genes that are associated with DNA repeats in prokaryotes*. Mol Microbiol, 2002. **43**(6): p. 1565-75.
126. Grissa, I., G. Vergnaud, and C. Pourcel, *The CRISPRdb database and tools to display CRISPRs and to generate dictionaries of spacers and repeats*. BMC Bioinformatics, 2007. **8**: p. 172.
127. Zhang, Y., et al., *Processing-independent CRISPR RNAs limit natural transformation in Neisseria meningitidis*. Mol Cell, 2013. **50**(4): p. 488-503.
128. Steichen, C.T., et al., *The Neisseria gonorrhoeae biofilm matrix contains DNA, and an endogenous nuclease controls its incorporation*. Infection and immunity, 2011. **79**(4): p. 1504-11.
129. Juneau, R.A., et al., *A Thermonuclease of Neisseria gonorrhoeae Enhances Bacterial Escape From Killing by Neutrophil Extracellular Traps*. The Journal of infectious diseases, 2015. **212**(2): p. 316-24.
130. Gunn, J.S., et al., *Cloning and linkage analysis of Neisseria gonorrhoeae DNA methyltransferases*. J Bacteriol, 1992. **174**(17): p. 5654-60.
131. Fuchs, G., *Allgemeine Mikrobiologie*. 2014: Thieme.
132. Simon, S.M. and G. Blobel, *A protein-conducting channel in the endoplasmic reticulum*. Cell, 1991. **65**(3): p. 371-80.
133. Chemla, Y.R., et al., *Mechanism of force generation of a viral DNA packaging motor*. Cell, 2005. **122**(5): p. 683-92.
134. Aathavan, K., et al., *Substrate interactions and promiscuity in a viral DNA packaging motor*. Nature, 2009. **461**(7264): p. 669-73.
135. Smith, D.E., et al., *The bacteriophage straight phi29 portal motor can package DNA against a large internal force*. Nature, 2001. **413**(6857): p. 748-52.
136. Gonzalez-Huici, V., M. Salas, and J.M. Hermoso, *The push-pull mechanism of bacteriophage O29 DNA injection*. Mol Microbiol, 2004. **52**(2): p. 529-40.
137. Evilevitch, A., et al., *Osmotic pressure inhibition of DNA ejection from phage*. Proc Natl Acad Sci U S A, 2003. **100**(16): p. 9292-5.
138. Simpson, A.A., et al., *Structure of the bacteriophage [phis]29 DNA packaging motor*. Nature, 2000. **408**(6813): p. 745-750.

139. Guasch, A., et al., *Detailed architecture of a DNA translocating machine: The high-resolution structure of the bacteriophage phi 29 connector particle*. Journal of Molecular Biology, 2002. **315**(4): p. 663-676.
140. Morais, M.C., et al., *Cryoelectron-microscopy image reconstruction of symmetry mismatches in bacteriophage phi 29*. Journal of Structural Biology, 2001. **135**(1): p. 38-46.
141. Zhang, F., et al., *Function of hexameric RNA in packaging of bacteriophage phi 29 DNA in vitro*. Mol Cell, 1998. **2**(1): p. 141-7.
142. Guo, P.X., S. Erickson, and D. Anderson, *A small viral RNA is required for in vitro packaging of bacteriophage phi 29 DNA*. Science, 1987. **236**(4802): p. 690-4.
143. Guo, P., et al., *Inter-RNA interaction of phage phi29 pRNA to form a hexameric complex for viral DNA transportation*. Mol Cell, 1998. **2**(1): p. 149-55.
144. Grimes, S., P.J. Jardine, and D. Anderson, *Bacteriophage phi 29 DNA packaging*. Adv Virus Res, 2002. **58**: p. 255-94.
145. Grimes, S. and D. Anderson, *RNA dependence of the bacteriophage phi 29 DNA packaging ATPase*. J Mol Biol, 1990. **215**(4): p. 559-66.
146. Shu, D. and P. Guo, *Only one pRNA hexamer but multiple copies of the DNA-packaging protein gp16 are needed for the motor to package bacterial virus phi29 genomic DNA*. Virology, 2003. **309**(1): p. 108-13.
147. Meister, M., S.R. Caplan, and H.C. Berg, *Dynamics of a tightly coupled mechanism for flagellar rotation. Bacterial motility, chemiosmotic coupling, protonmotive force*. Biophys J, 1989. **55**(5): p. 905-14.
148. Khan, S. and H.C. Berg, *Isotope and thermal effects in chemiosmotic coupling to the flagellar motor of Streptococcus*. Cell, 1983. **32**(3): p. 913-9.
149. Peskin, C.S., G.M. Odell, and G.F. Oster, *Cellular motions and thermal fluctuations: the Brownian ratchet*. Biophysical journal, 1993. **65**(1): p. 316-24.
150. Simon, S.M., C.S. Peskin, and G.F. Oster, *What drives the translocation of proteins?* Proceedings of the National Academy of Sciences of the United States of America, 1992. **89**(9): p. 3770-4.
151. Cheng, M.Y., et al., *Mitochondrial heat-shock protein hsp60 is essential for assembly of proteins imported into yeast mitochondria*. Nature, 1989. **337**(6208): p. 620-5.
152. Ostermann, J., et al., *Protein folding in mitochondria requires complex formation with hsp60 and ATP hydrolysis*. Nature, 1989. **341**(6238): p. 125-30.
153. Kagan, B.L., A. Finkelstein, and M. Colombini, *Diphtheria toxin fragment forms large pores in phospholipid bilayer membranes*. Proc Natl Acad Sci U S A, 1981. **78**(8): p. 4950-4.
154. Pelicic, V., *Type IV pili: e pluribus unum?* Mol Microbiol, 2008. **68**(4): p. 827-37.
155. Merz, A.J., M. So, and M.P. Sheetz, *Pilus retraction powers bacterial twitching motility*. Nature, 2000. **407**(6800): p. 98-102.
156. Skerker, J.M. and H.C. Berg, *Direct observation of extension and retraction of type IV pili*. Proc Natl Acad Sci U S A, 2001. **98**(12): p. 6901-4.
157. Maier, B., et al., *Single pilus motor forces exceed 100 pN*. Proc Natl Acad Sci U S A, 2002. **99**(25): p. 16012-7.
158. Clausen, M., et al., *High-force generation is a conserved property of type IV pilus systems*. J Bacteriol, 2009. **191**(14): p. 4633-8.
159. Berry, J.L., et al., *Structure and assembly of a trans-periplasmic channel for type IV pili in Neisseria meningitidis*. PLoS Pathog, 2012. **8**(9): p. e1002923.
160. Reichow, S.L., et al., *Structure of the cholera toxin secretion channel in its closed state*. Nat Struct Mol Biol, 2010. **17**(10): p. 1226-32.
161. Chami, M., et al., *Structural insights into the secretin PulD and its trypsin-resistant core*. J Biol Chem, 2005. **280**(45): p. 37732-41.

162. Hofreuter, D., S. Odenbreit, and R. Haas, *Natural transformation competence in Helicobacter pylori is mediated by the basic components of a type IV secretion system*. Molecular microbiology, 2001. **41**(2): p. 379-91.
163. Chang, Y.W., et al., *Architecture of the type IVa pilus machine*. Science, 2016. **351**(6278): p. aad2001.
164. Siewering, K., et al., *Peptidoglycan-binding protein TsaP functions in surface assembly of type IV pili*. Proc Natl Acad Sci U S A, 2014. **111**(10): p. E953-61.
165. Craig, L., et al., *Type IV pilus structure by cryo-electron microscopy and crystallography: implications for pilus assembly and functions*. Mol Cell, 2006. **23**(5): p. 651-62.
166. Friedrich, C., I. Bulyha, and L. Sogaard-Andersen, *Outside-in assembly pathway of the type IV pilus system in Myxococcus xanthus*. J Bacteriol, 2014. **196**(2): p. 378-90.
167. Bulyha, I., et al., *Regulation of the type IV pili molecular machine by dynamic localization of two motor proteins*. Mol Microbiol, 2009. **74**(3): p. 691-706.
168. Georgiadou, M., et al., *Large-scale study of the interactions between proteins involved in type IV pilus biology in Neisseria meningitidis: characterization of a subcomplex involved in pilus assembly*. Mol Microbiol, 2012. **84**(5): p. 857-73.
169. Li, C., et al., *Type IV pilus proteins form an integrated structure extending from the cytoplasm to the outer membrane*. PLoS One, 2013. **8**(7): p. e70144.
170. Tammam, S., et al., *PilMNO PQ from the Pseudomonas aeruginosa type IV pilus system form a transenvelope protein interaction network that interacts with Pila*. J Bacteriol, 2013. **195**(10): p. 2126-35.
171. Balasingham, S.V., et al., *Interactions between the lipoprotein PilP and the secretin PilQ in Neisseria meningitidis*. J Bacteriol, 2007. **189**(15): p. 5716-27.
172. Ayers, M., et al., *PilM/N/O/P proteins form an inner membrane complex that affects the stability of the Pseudomonas aeruginosa type IV pilus secretin*. J Mol Biol, 2009. **394**(1): p. 128-42.
173. Tammam, S., et al., *Characterization of the PilN, PilO and PilP type IVa pilus subcomplex*. Mol Microbiol, 2011. **82**(6): p. 1496-514.
174. Gu, S., et al., *Solution structure of homology region (HR) domain of type II secretion system*. J Biol Chem, 2012. **287**(12): p. 9072-80.
175. Aas, F.E., C. Lovold, and M. Koomey, *An inhibitor of DNA binding and uptake events dictates the proficiency of genetic transformation in Neisseria gonorrhoeae: mechanism of action and links to Type IV pilus expression*. Mol Microbiol, 2002. **46**(5): p. 1441-50.
176. Karuppiyah, V. and J.P. Derrick, *Structure of the PilM-PilN inner membrane type IV pilus biogenesis complex from Thermus thermophilus*. J Biol Chem, 2011. **286**(27): p. 24434-42.
177. Korotkov, K.V., et al., *Structural and functional studies on the interaction of GspC and GspD in the type II secretion system*. PLoS Pathog, 2011. **7**(9): p. e1002228.
178. Karuppiyah, V., et al., *Structure and assembly of an inner membrane platform for initiation of type IV pilus biogenesis*. Proc Natl Acad Sci U S A, 2013. **110**(48): p. E4638-47.
179. Karuppiyah, V., et al., *Structure and oligomerization of the PilC type IV pilus biogenesis protein from Thermus thermophilus*. Proteins, 2010. **78**(9): p. 2049-57.
180. Abendroth, J., et al., *The three-dimensional structure of the cytoplasmic domains of EpsF from the type 2 secretion system of Vibrio cholerae*. J Struct Biol, 2009. **166**(3): p. 303-15.
181. Abendroth, J., et al., *The X-ray structure of the type II secretion system complex formed by the N-terminal domain of EpsE and the cytoplasmic domain of EpsL of Vibrio cholerae*. J Mol Biol, 2005. **348**(4): p. 845-55.

182. Yamagata, A. and J.A. Tainer, *Hexameric structures of the archaeal secretion ATPase GspE and implications for a universal secretion mechanism*. EMBO J, 2007. **26**(3): p. 878-90.
183. Mistic, A.M., K.A. Satyshur, and K.T. Forest, *P. aeruginosa PilT structures with and without nucleotide reveal a dynamic type IV pilus retraction motor*. J Mol Biol, 2010. **400**(5): p. 1011-21.
184. Satyshur, K.A., et al., *Crystal structures of the pilus retraction motor PilT suggest large domain movements and subunit cooperation drive motility*. Structure, 2007. **15**(3): p. 363-76.
185. Lu, C., et al., *Hexamers of the type II secretion ATPase GspE from Vibrio cholerae with increased ATPase activity*. Structure, 2013. **21**(9): p. 1707-17.
186. Parge, H.E., et al., *Structure of the fibre-forming protein pilin at 2.6 Å resolution*. Nature, 1995. **378**(6552): p. 32-8.
187. Keizer, D.W., et al., *Structure of a pilin monomer from Pseudomonas aeruginosa: implications for the assembly of pili*. J Biol Chem, 2001. **276**(26): p. 24186-93.
188. LaPointe, C.F. and R.K. Taylor, *The type 4 prepilin peptidases comprise a novel family of aspartic acid proteases*. J Biol Chem, 2000. **275**(2): p. 1502-10.
189. Nunn, D., *Bacterial type II protein export and pilus biogenesis: more than just homologies?* Trends Cell Biol, 1999. **9**(10): p. 402-8.
190. Nguyen, Y., et al., *Pseudomonas aeruginosa minor pilins prime type IVa pilus assembly and promote surface display of the PilY1 adhesin*. J Biol Chem, 2015. **290**(1): p. 601-11.
191. Sauvonnet, N., et al., *Pilus formation and protein secretion by the same machinery in Escherichia coli*. EMBO J, 2000. **19**(10): p. 2221-8.
192. Cisneros, D.A., et al., *Minor pseudopilin self-assembly primes type II secretion pseudopilus elongation*. EMBO J, 2012. **31**(4): p. 1041-53.
193. Berry, J.L., et al., *Functional analysis of the interdependence between DNA uptake sequence and its cognate ComP receptor during natural transformation in Neisseria species*. PLoS genetics, 2013. **9**(12): p. e1004014.
194. Drake, S.L. and M. Koomey, *The product of the pilQ gene is essential for the biogenesis of type IV pili in Neisseria gonorrhoeae*. Molecular microbiology, 1995. **18**(5): p. 975-86.
195. Nouwen, N., et al., *Domain structure of secretin PulD revealed by limited proteolysis and electron microscopy*. EMBO J, 2000. **19**(10): p. 2229-36.
196. Collins, R.F., et al., *Analysis of the PilQ secretin from Neisseria meningitidis by transmission electron microscopy reveals a dodecameric quaternary structure*. J Bacteriol, 2001. **183**(13): p. 3825-32.
197. Opalka, N., et al., *Structure of the filamentous phage pIV multimer by cryo-electron microscopy*. J Mol Biol, 2003. **325**(3): p. 461-70.
198. Py, B., L. Loiseau, and F. Barras, *An inner membrane platform in the type II secretion machinery of Gram-negative bacteria*. EMBO Rep, 2001. **2**(3): p. 244-8.
199. Clausen, M., M. Koomey, and B. Maier, *Dynamics of type IV pili is controlled by switching between multiple states*. Biophys J, 2009. **96**(3): p. 1169-77.
200. Li, Y., et al., *Extracellular polysaccharides mediate pilus retraction during social motility of Myxococcus xanthus*. Proc Natl Acad Sci U S A, 2003. **100**(9): p. 5443-8.
201. Biais, N., et al., *Force-dependent polymorphism in type IV pili reveals hidden epitopes*. Proc Natl Acad Sci U S A, 2010. **107**(25): p. 11358-63.
202. Leighton, T.L., et al., *Novel Role for PilNO in Type IV Pilus Retraction Revealed by Alignment Subcomplex Mutations*. J Bacteriol, 2015. **197**(13): p. 2229-38.
203. Chen, I. and E.C. Gotschlich, *ComE, a competence protein from Neisseria gonorrhoeae with DNA-binding activity*. J Bacteriol, 2001. **183**(10): p. 3160-8.

204. Inamine, G.S. and D. Dubnau, *ComEA, a Bacillus subtilis integral membrane protein required for genetic transformation, is needed for both DNA binding and transport*. J Bacteriol, 1995. **177**(11): p. 3045-51.
205. Dubnau, D., *DNA uptake in bacteria*. Annu Rev Microbiol, 1999. **53**: p. 217-44.
206. Berge, M., et al., *Uptake of transforming DNA in Gram-positive bacteria: a view from Streptococcus pneumoniae*. Mol Microbiol, 2002. **45**(2): p. 411-21.
207. Friedrich, A., T. Hartsch, and B. Averhoff, *Natural transformation in mesophilic and thermophilic bacteria: identification and characterization of novel, closely related competence genes in Acinetobacter sp. strain BD413 and Thermus thermophilus HB27*. Appl Environ Microbiol, 2001. **67**(7): p. 3140-8.
208. Graupner, S., et al., *Type IV pilus genes pilA and pilC of Pseudomonas stutzeri are required for natural genetic transformation, and pilA can be replaced by corresponding genes from nontransformable species*. J Bacteriol, 2000. **182**(8): p. 2184-90.
209. Yeh, Y.C., et al., *Characterization of a ComE3 homologue essential for DNA transformation in Helicobacter pylori*. Infect Immun, 2003. **71**(9): p. 5427-31.
210. Facius, D., M. Fussenegger, and T.F. Meyer, *Sequential action of factors involved in natural competence for transformation of Neisseria gonorrhoeae*. FEMS Microbiol Lett, 1996. **137**(2-3): p. 159-64.
211. Saier, M.H., Jr., *A functional-phylogenetic classification system for transmembrane solute transporters*. Microbiol Mol Biol Rev, 2000. **64**(2): p. 354-411.
212. van der Heide, T. and B. Poolman, *ABC transporters: one, two or four extracytoplasmic substrate-binding sites?* EMBO Rep, 2002. **3**(10): p. 938-43.
213. Kline, K.A. and H.S. Seifert, *Mutation of the priA gene of Neisseria gonorrhoeae affects DNA transformation and DNA repair*. J Bacteriol, 2005. **187**(15): p. 5347-55.
214. Baker, J.A., et al., *Potential DNA binding and nuclease functions of ComEC domains characterized in silico*. Proteins, 2016. **84**(10): p. 1431-42.
215. Fussenegger, M., et al., *Tetrapac (tpc), a novel genotype of Neisseria gonorrhoeae affecting epithelial cell invasion, natural transformation competence and cell separation*. Molecular microbiology, 1996. **19**(6): p. 1357-72.
216. Fussenegger, M., et al., *Tetrapac (tpc), a novel genotype of Neisseria gonorrhoeae affecting epithelial cell invasion, natural transformation competence and cell separation*. Mol Microbiol, 1996. **19**(6): p. 1357-72.
217. Fussenegger, M., et al., *A novel peptidoglycan-linked lipoprotein (ComL) that functions in natural transformation competence of Neisseria gonorrhoeae*. Mol Microbiol, 1996. **19**(5): p. 1095-105.
218. Kidane, D., et al., *The cell pole: the site of cross talk between the DNA uptake and genetic recombination machinery*. Critical reviews in biochemistry and molecular biology, 2012. **47**(6): p. 531-55.
219. Cox, M.M., *Regulation of bacterial RecA protein function*. Crit Rev Biochem Mol Biol, 2007. **42**(1): p. 41-63.
220. San Filippo, J., P. Sung, and H. Klein, *Mechanism of eukaryotic homologous recombination*. Annu Rev Biochem, 2008. **77**: p. 229-57.
221. Kidane, D. and P.L. Graumann, *Intracellular protein and DNA dynamics in competent Bacillus subtilis cells*. Cell, 2005. **122**(1): p. 73-84.
222. Aguilera, A.s. and R. Rothstein, *Molecular genetics of recombination*. Topics in current genetics,. 2007, Berlin ; New York: Springer. xxiv, 524 p.
223. Beernink, H.T. and S.W. Morrical, *RMPs: recombination/replication mediator proteins*. Trends Biochem Sci, 1999. **24**(10): p. 385-9.
224. Duffin, P.M. and D.A. Barber, *DprA is required for natural transformation and affects pilin variation in Neisseria gonorrhoeae*. Microbiology, 2016. **162**(9): p. 1620-1628.

225. Mortier-Barriere, I., et al., *A key presynaptic role in transformation for a widespread bacterial protein: DprA conveys incoming ssDNA to RecA*. Cell, 2007. **130**(5): p. 824-36.
226. Aas, F.E., et al., *Competence for natural transformation in Neisseria gonorrhoeae: components of DNA binding and uptake linked to type IV pilus expression*. Mol Microbiol, 2002. **46**(3): p. 749-60.
227. Imhaus, A.F. and G. Dumenil, *The number of Neisseria meningitidis type IV pili determines host cell interaction*. EMBO J, 2014. **33**(16): p. 1767-83.
228. Obergfell, K.P. and H.S. Seifert, *The Pilin N-terminal Domain Maintains Neisseria gonorrhoeae Transformation Competence during Pilus Phase Variation*. PLoS Genet, 2016. **12**(5): p. e1006069.
229. Aas, F.E., et al., *Substitutions in the N-terminal alpha helical spine of Neisseria gonorrhoeae pilin affect Type IV pilus assembly, dynamics and associated functions*. Mol Microbiol, 2007. **63**(1): p. 69-85.
230. Stingl, K., et al., *Composite system mediates two-step DNA uptake into Helicobacter pylori*. Proc Natl Acad Sci U S A, 2010. **107**(3): p. 1184-9.
231. Hahn, J., et al., *Transformation proteins and DNA uptake localize to the cell poles in Bacillus subtilis*. Cell, 2005. **122**(1): p. 59-71.
232. Provvedi, R. and D. Dubnau, *ComEA is a DNA receptor for transformation of competent Bacillus subtilis*. Molecular microbiology, 1999. **31**(1): p. 271-80.
233. Draskovic, I. and D. Dubnau, *Biogenesis of a putative channel protein, ComEC, required for DNA uptake: membrane topology, oligomerization and formation of disulphide bonds*. Mol Microbiol, 2005. **55**(3): p. 881-96.
234. Londono-Vallejo, J.A. and D. Dubnau, *Mutation of the putative nucleotide binding site of the Bacillus subtilis membrane protein ComFA abolishes the uptake of DNA during transformation*. J Bacteriol, 1994. **176**(15): p. 4642-5.
235. Russel, M., *Macromolecular assembly and secretion across the bacterial cell envelope: type II protein secretion systems*. J Mol Biol, 1998. **279**(3): p. 485-99.
236. Kibbe, W.A., *OligoCalc: an online oligonucleotide properties calculator*. Nucleic Acids Res, 2007. **35**(Web Server issue): p. W43-6.
237. Vingataramin, L. and E.H. Frost, *A single protocol for extraction of gDNA from bacteria and yeast*. Biotechniques, 2015. **58**(3): p. 120-5.
238. Tonjum, T., et al., *Identification and characterization of pilG, a highly conserved pilus-assembly gene in pathogenic Neisseria*. Molecular microbiology, 1995. **16**(3): p. 451-64.
239. Freitag, N.E., H.S. Seifert, and M. Koomey, *Characterization of the pilF-pilD pilus-assembly locus of Neisseria gonorrhoeae*. Molecular microbiology, 1995. **16**(3): p. 575-86.
240. Winther-Larsen, H.C., et al., *Neisseria gonorrhoeae PilV, a type IV pilus-associated protein essential to human epithelial cell adherence*. Proceedings of the National Academy of Sciences of the United States of America, 2001. **98**(26): p. 15276-81.
241. Wolfgang, M., et al., *Components and dynamics of fiber formation define a ubiquitous biogenesis pathway for bacterial pili*. EMBO J, 2000. **19**(23): p. 6408-18.
242. Aas, F.E., et al., *Substitutions in the N-terminal alpha helical spine of Neisseria gonorrhoeae pilin affect Type IV pilus assembly, dynamics and associated functions*. Molecular microbiology, 2007. **63**(1): p. 69-85.
243. Winther-Larsen, H.C., et al., *Neisseria gonorrhoeae PilV, a type IV pilus-associated protein essential to human epithelial cell adherence*. Proc Natl Acad Sci U S A, 2001. **98**(26): p. 15276-81.
244. Reese, M.G., *Application of a time-delay neural network to promoter annotation in the Drosophila melanogaster genome*. Comput Chem, 2001. **26**(1): p. 51-6.

245. Gangel, H., et al., *Concerted spatio-temporal dynamics of imported DNA and ComE DNA uptake protein during gonococcal transformation*. PLoS Pathog, 2014. **10**(4): p. e1004043.
246. Hough V, P.C., *Method and means for recognizing complex patterns*. 1962, Hough V, Paul C.: United States.
247. Kawaguchi, T., M. Rizon, and D. Hidaka, *Detection of eyes from human faces by hough transform and separability filter*. Electronics and Communications in Japan Part II-Electronics, 2005. **88**(5): p. 29-39.
248. Maier, B. and J.O. Radler, *DNA on fluid membranes: A model polymer in two dimensions*. Macromolecules, 2000. **33**(19): p. 7185-7194.
249. Hwang, H., H. Kim, and S. Myong, *Protein induced fluorescence enhancement as a single molecule assay with short distance sensitivity*. Proceedings of the National Academy of Sciences of the United States of America, 2011. **108**(18): p. 7414-8.
250. Suckow, G., P. Seitz, and M. Blokesch, *Quorum sensing contributes to natural transformation of Vibrio cholerae in a species-specific manner*. Journal of bacteriology, 2011. **193**(18): p. 4914-24.
251. Clausen, M., M. Koomey, and B. Maier, *Dynamics of type IV pili is controlled by switching between multiple states*. Biophysical journal, 2009. **96**(3): p. 1169-77.
252. Marathe, R., et al., *Bacterial twitching motility is coordinated by a two-dimensional tug-of-war with directional memory*. Nature communications, 2014. **5**: p. 3759.
253. Hepp, C. and B. Maier, *Kinetics of DNA uptake during transformation provide evidence for a translocation ratchet mechanism*. Proceedings of the National Academy of Sciences, 2016.
254. Aas, F.E., et al., *Competence for natural transformation in Neisseria gonorrhoeae: components of DNA binding and uptake linked to type IV pilus expression*. Molecular microbiology, 2002. **46**(3): p. 749-60.
255. Aas, F.E., C. Lovold, and M. Koomey, *An inhibitor of DNA binding and uptake events dictates the proficiency of genetic transformation in Neisseria gonorrhoeae: mechanism of action and links to Type IV pilus expression*. Molecular microbiology, 2002. **46**(5): p. 1441-50.
256. Kurre, R. and B. Maier, *Oxygen depletion triggers switching between discrete speed modes of gonococcal type IV pili*. Biophysical journal, 2012. **102**(11): p. 2556-63.
257. Chen, I. and E.C. Gotschlich, *ComE, a competence protein from Neisseria gonorrhoeae with DNA-binding activity*. Journal of bacteriology, 2001. **183**(10): p. 3160-8.
258. Yu, W. and K. Luo, *Chaperone-assisted translocation of a polymer through a nanopore*. Journal of the American Chemical Society, 2011. **133**(34): p. 13565-70.
259. Maier, B., et al., *DNA transport into Bacillus subtilis requires proton motive force to generate large molecular forces*. Nature structural & molecular biology, 2004. **11**(7): p. 643-9.
260. Stingl, K., et al., *Composite system mediates two-step DNA uptake into Helicobacter pylori*. Proceedings of the National Academy of Sciences of the United States of America, 2010. **107**(3): p. 1184-9.
261. Gangel, H., et al., *Concerted spatio-temporal dynamics of imported DNA and ComE DNA uptake protein during gonococcal transformation*. PLoS pathogens, 2014. **10**(4): p. e1004043.
262. van Mameren, J., et al., *Unraveling the structure of DNA during overstretching by using multicolor, single-molecule fluorescence imaging*. Proceedings of the National Academy of Sciences of the United States of America, 2009. **106**(43): p. 18231-6.
263. Facius, D. and T.F. Meyer, *A novel determinant (comA) essential for natural transformation competence in Neisseria gonorrhoeae and the effect of a comA defect on pilin variation*. Molecular microbiology, 1993. **10**(4): p. 699-712.

264. Duffin, P.M. and H.S. Seifert, *Genetic transformation of Neisseria gonorrhoeae shows a strand preference*. FEMS microbiology letters, 2012. **334**(1): p. 44-8.
265. Hepp, C., et al., *Single-Stranded DNA Uptake during Gonococcal Transformation*. J Bacteriol, 2016. **198**(18): p. 2515-23.
266. Seitz, P., et al., *ComEA is essential for the transfer of external DNA into the periplasm in naturally transformable Vibrio cholerae cells*. PLoS genetics, 2014. **10**(1): p. e1004066.
267. Kaufenstein, M., M. van der Laan, and P.L. Graumann, *The three-layered DNA uptake machinery at the cell pole in competent Bacillus subtilis cells is a stable complex*. Journal of bacteriology, 2011. **193**(7): p. 1633-42.
268. Maier, B., et al., *DNA transport into Bacillus subtilis requires proton motive force to generate large molecular forces*. Nat Struct Mol Biol, 2004. **11**(7): p. 643-9.
269. Overballe-Petersen, S., et al., *Bacterial natural transformation by highly fragmented and damaged DNA*. Proc Natl Acad Sci U S A, 2013. **110**(49): p. 19860-5.
270. Yu, W. and K. Luo, *Chaperone-assisted translocation of a polymer through a nanopore*. J Am Chem Soc, 2011. **133**(34): p. 13565-70.
271. Gopinathan, A. and Y.W. Kim, *Polymer translocation in crowded environments*. Phys Rev Lett, 2007. **99**(22): p. 228106.
272. Bressloff, P.C. and J.M. Newby, *Stochastic models of intracellular transport*. Reviews of Modern Physics, 2013. **85**(1): p. 135-196.
273. Allemand, J.F. and B. Maier, *Bacterial translocation motors investigated by single molecule techniques*. FEMS Microbiol Rev, 2009. **33**(3): p. 593-610.
274. Burton, B. and D. Dubnau, *Membrane-associated DNA transport machines*. Cold Spring Harbor perspectives in biology, 2010. **2**(7): p. a000406.
275. Matthey, N. and M. Blokesch, *The DNA-Uptake Process of Naturally Competent Vibrio cholerae*. Trends Microbiol, 2016. **24**(2): p. 98-110.
276. Seitz, P. and M. Blokesch, *DNA-uptake machinery of naturally competent Vibrio cholerae*. Proceedings of the National Academy of Sciences of the United States of America, 2013. **110**(44): p. 17987-92.
277. Laurenceau, R., et al., *A type IV pilus mediates DNA binding during natural transformation in Streptococcus pneumoniae*. PLoS pathogens, 2013. **9**(6): p. e1003473.
278. Chen, I., R. Provvedi, and D. Dubnau, *A macromolecular complex formed by a pilin-like protein in competent Bacillus subtilis*. J Biol Chem, 2006. **281**(31): p. 21720-7.
279. Holz, C., et al., *Multiple pilus motors cooperate for persistent bacterial movement in two dimensions*. Phys Rev Lett, 2010. **104**(17): p. 178104.
280. Gold, V.A., et al., *Structure of a type IV pilus machinery in the open and closed state*. Elife, 2015. **4**.
281. Chen, I. and D. Dubnau, *DNA transport during transformation*. Front Biosci, 2003. **8**: p. s544-56.
282. Claverys, J.P., B. Martin, and P. Polard, *The genetic transformation machinery: composition, localization, and mechanism*. FEMS microbiology reviews, 2009. **33**(3): p. 643-56.
283. Takeno, M., H. Taguchi, and T. Akamatsu, *Role of ComFA in controlling the DNA uptake rate during transformation of competent Bacillus subtilis*. J Biosci Bioeng, 2011. **111**(6): p. 618-23.
284. Kruger, N.J. and K. Stingl, *Two steps away from novelty--principles of bacterial DNA uptake*. Molecular microbiology, 2011. **80**(4): p. 860-7.
285. Johnston, C., et al., *Bacterial transformation: distribution, shared mechanisms and divergent control*. Nat Rev Microbiol, 2014. **12**(3): p. 181-96.

-
286. Corbinais, C., et al., *Following transforming DNA in Helicobacter pylori from uptake to expression*. Mol Microbiol, 2016. **101**(6): p. 1039-53.
287. Kahn, M.E., F. Barany, and H.O. Smith, *Transformasomes: specialized membranous structures that protect DNA during Haemophilus transformation*. Proc Natl Acad Sci U S A, 1983. **80**(22): p. 6927-31.
288. Lang, E., et al., *Identification of neisserial DNA binding components*. Microbiology, 2009. **155**(Pt 3): p. 852-62.
289. Berge, M.J., et al., *Midcell Recruitment of the DNA Uptake and Virulence Nuclease, EndA, for Pneumococcal Transformation*. PLoS pathogens, 2013. **9**(9): p. e1003596.
290. Kouzel, N., E.R. Oldewurtel, and B. Maier, *Gene Transfer Efficiency in Gonococcal Biofilms: Role of Biofilm Age, Architecture, and Pilin Antigenic Variation*. J Bacteriol, 2015. **197**(14): p. 2422-31.
291. Zweig, M., et al., *Secreted single-stranded DNA is involved in the initial phase of biofilm formation by Neisseria gonorrhoeae*. Environ Microbiol, 2014. **16**(4): p. 1040-52.
292. Salgado-Pabon, W., et al., *A novel relaxase homologue is involved in chromosomal DNA processing for type IV secretion in Neisseria gonorrhoeae*. Molecular microbiology, 2007. **66**(4): p. 930-47.
293. Kidane, D., et al., *The cell pole: the site of cross talk between the DNA uptake and genetic recombination machinery*. Crit Rev Biochem Mol Biol, 2012. **47**(6): p. 531-55.
294. Berge, M.J., et al., *Midcell recruitment of the DNA uptake and virulence nuclease, EndA, for pneumococcal transformation*. PLoS Pathog, 2013. **9**(9): p. e1003596.
295. Leake, M.C., et al., *Stoichiometry and turnover in single, functioning membrane protein complexes*. Nature, 2006. **443**(7109): p. 355-8.
296. Duffin, P.M. and D.A. Barber, *DprA is required for natural transformation and affects pilin variation in Neisseria gonorrhoeae*. Microbiology, 2016.
297. Seitz, P. and M. Blokesch, *DNA transport across the outer and inner membranes of naturally transformable Vibrio cholerae is spatially but not temporally coupled*. MBio, 2014. **5**(4).

9 List of Abbreviations

ATP	adenosine triphosphate
Av	antigenic variation
BSA	bovine serum albumine
CRISPR	clustered interspaced short palindromic repeats
Cas	CRISPR associated protein
CREE	Correia repeat encoded elements
Cy3	cyanine-3
Cy5	cyanine-5
DMEM	Dulbecco's modified Eagle medium
DMSO	dimethyl sulphoxide
dsDNA	double-stranded DNA
DUS	DNA uptake sequence
EDTA	ethylenediaminetetraacetic acid
G4	guanine tetraplex
GC	gonococcal growth medium
GFP	green fluorescent protein
GGI	gonococcal genetic island
HEPES	4-(2-hydroxyethyl)-1-piperazineethanesulfonic acid
HGT	horizontal gene transfer
IM	inner membrane
IPTG	isopropyl β -D-1-thiogalactopyranoside
MME	minimal mobile elements
NIME	neisserial intergenic mosaic element
OD₆₀₀	optical density at 600 nm
OM	outer membrane
ORF	open reading frame
PBS	phosphate buffered saline
PCR	polymerase chain reaction
R-M	restriction-modification
sRNA	small RNA
ssDNA	single-stranded DNA
T2SS	type II secretion system
T4SS	type IV secretion system
Tfp	type IV pili
wt	wild-type

Erklärung

Ich versichere, dass ich die von mir vorgelegte Dissertation selbstständig angefertigt, die benutzten Quellen und Hilfsmittel vollständig angegeben und die Stellen der Arbeit – einschließlich Tabellen, Karten und Abbildungen –, die anderen Werken im Wortlaut oder dem Sinn nach entnommen sind, in jedem Einzelfall als Entlehnung kenntlich gemacht habe; dass diese Dissertation noch keiner anderen Fakultät oder Universität zur Prüfung vorgelegen hat; dass sie – abgesehen von unten angegebenen Teilpublikationen – noch nicht veröffentlicht worden ist, sowie, dass ich eine solche Veröffentlichung vor Abschluss des Promotionsverfahrens nicht vornehmen werde. Die Bestimmungen der Promotionsordnung sind mir bekannt. Die von mir vorgelegte Dissertation ist von Prof. Dr. Berenike Maier betreut worden.

Köln, den _____

1. Gangel*, H., Hepp*, C., Müller*, S. et al. *Concerted spatio-temporal dynamics of imported DNA and ComE DNA uptake protein during gonococcal transformation. PLoS Pathogens, 2014. 10(4): p. e1004043. [245].*
2. Hepp, C. and B. Maier, *Kinetics of DNA uptake during transformation provide evidence for a translocation ratchet mechanism. Proceedings of the National Academy of Sciences, 2016. [253]*
3. Hepp, C., et al., *Single-Stranded DNA Uptake during Gonococcal Transformation. J Bacteriol, 2016. 198(18): p. 2515-23. [265]*

Lebenslauf

Geboren: 24.09.1985 in Bad Saulgau

Ausbildung

1992-1996 Grundschule Hohentengen
Grundschule

1996-2005 Gymnasium Mengen
Abitur (29.06.2005)

2005-2007 Eberhard-Karls-Universität, Tübingen
Biochemie
Vordiplom (25.09.2007)

2008-2009 Capital Normal University, Peking, China
DAAD Stipendium (10 Monate)

2007-2011 Eberhard-Karls-Universität, Tübingen
Biochemie
Diplom (August 2011)
Diplomarbeit: "Identifikation potenzieller Interaktionspartner für P_{II} in *Synechococcus elongatus* PCC7942."

Seit 2011 Universität zu Köln
Biophysik
Promotionsstudium